

MOLECULAR ADAPTATIONS IN CADMIUM AND LEAD RESISTANT
ENVIRONMENTAL SPECIES

A THESIS SUBMITTED TO
THE GRADUATE SCHOOL OF NATURAL AND APPLIED SCIENCES
OF
MIDDLE EAST TECHNICAL UNIVERSITY

BY

EDA ŞEYMA KEPENEK

IN PARTIAL FULFILLMENT OF THE REQUIREMENTS
FOR
THE DEGREE OF DOCTOR OF PHILOSOPHY
IN
BIOLOGY

NOVEMBER 2017

Approval of the thesis:

MOLECULAR ADAPTATIONS IN CADMIUM AND LEAD RESISTANT ENVIRONMENTAL SPECIES

submitted by **EDA ŐEYMA KEPENEK** in partial fulfillment of the requirements for the degree of **Doctor of Philosophy in Biology Department, Middle East Technical University** by,

Prof. Dr. Glbin Dural nver
Dean, Graduate school of **Natural and Applied Sciences**

Prof. Dr. Orhan Adalı
Head of Department, **Biology**

Prof. Dr. AyŐe Gl Gzen
Supervisor, **Biological Sciences Dept., METU**

Prof. Dr. Feride Severcan
Co-Supervisor, **Biological Sciences Dept., METU**

Examining Committee Members:

Prof. Dr. Glsn Gkaĝaç Arslan
Chemistry Dept., METU

Prof. Dr. AyŐe Gl Gzen
Biological Sciences Dept., METU

Assoc. Prof. Dr. aĝdaŐ Devrim Son
Biological Sciences Dept., METU

Prof. Dr. İrfan Kandemir
Biology Dept., Ankara University

Assist. Prof. Dr. Aya Doĝan Mollaoĝlu
Physiology Dept., İstanbl Kemerburgaz University

Date: 21.11.2017

I hereby declare that all information in this document has been obtained and presented in accordance with academic rules and ethical conduct. I also declare that, as required by these rules and conduct, I have fully cited and referenced all material and results that are not original to this work.

Name, Last Name: Eda Şeyma Kepenek

Signature:

ABSTRACT

MOLECULAR ADAPTATIONS IN CADMIUM AND LEAD RESISTANT ENVIRONMENTAL SPECIES

Kepenek, Eda Şeyma

Ph.D., Department of Biology

Supervisor: Prof. Dr. Ayşe Gül Gözen

Co-Supervisor: Prof. Dr. Feride Severcan

November 2017, 132 Pages

Environmental pollution caused by heavy metal exposure has detrimental effects on human health. For the reclamation of polluted areas, bacteria have been used in remediation. For those bioremediation attempts, finding the appropriate bacterial strains is an important issue. In their environment, bacteria may exist close to the source of heavy metals. Sudden exposure to high concentrations of the heavy metal may trigger quick response mechanisms to ensure survival. On the other hand, bacteria may live at a distance to the source and thus, experience the gradual increase in the heavy metal concentrations. The gradual increase in the concentration of the heavy metal may cause changes accumulating in time to ensure survival as well. In both, acute or gradual exposure situations, bacteria resist heavy metals by using several resistance mechanisms. In our study, we investigated whether there are differences between molecular profiles of the cells that are acclimated to heavy metals upon either acute or gradual exposure. We measured the changes in molecular profile by using ATR-FTIR spectroscopy and unsupervised chemometric analysis methods (PCA, HCA).

We chose cadmium and lead as heavy metals, and we have studied the molecular profiles of *Brevundimonas*, *Gordonia*, and *Microbacterium* bacterial genera isolated from a freshwater source. In a laboratory environment, after extended exposure bacteria can be acclimated to live and grow in the existence of heavy metals. We allow the bacteria to mimic the situation of being close or away from the source of heavy metal by using two different acclimation procedures (acute vs. gradual). We acclimated bacterial strains to grow at 2 to 4 times higher concentrations than their corresponding minimum inhibitory concentrations. We then measured the molecular alterations caused by the nature of acclimation upon acute or gradual exposure. Results of the IR spectral analysis indicated substantial changes in structure and composition of bacterial macromolecules. Changes in the membrane exhibited itself in decreases of fatty acids amounts and as well as protein to lipid ratios in acclimated groups. The decrease in total protein concentrations that we measured perhaps hints inhibition of several anabolic pathways in all acclimated groups. Furthermore, total protein concentrations in acutely acclimated bacteria were significantly lower than that of gradually acclimated ones. A remarkable increase in exopolymer production was detected in both acutely and gradually heavy metal exposed groups. Exopolymer production, being one of the heavy metal resistance mechanisms in bacteria, appeared to play a central role in survival upon supra lethal exposures. Moreover, bacteria under acute cadmium exposure produced significantly higher exopolysaccharide than under gradual. On the contrary, gradually acclimated strains produced significantly higher exopolysaccharide than those of acutely acclimated ones under lead exposure. Results of PCA and HCA analyzes showed clearcut discriminations between acclimated bacterial strains as acute vs. gradual exposure and control for both of the metals.

This work contributes novel insights into the potential role of IR spectroscopy in the molecular characterization of bacteria acclimated to different stress conditions. Furthermore, our study showed that we may use information about the exopolymer production and amount as background information to find appropriate bacterial strains in bioremediation studies.

Keywords: Heavy metal resistance, *Brevundimonas* sp., *Gordonia* sp., *Microbacterium oxydans*, Cd, Pb, Acclimation, Acute, Gradual, MIC, ATR-FTIR spectroscopy, exopolymer, PCA, HCA

ÖZ

KADMİYUM VE KURŞUNA DİRENÇLİ ÇEVRESEL TÜRLERDE MOLEKÜLER ADAPTASYONLAR

Kepenek, Eda Şeyma
Doktora, Biyoloji Bölümü
Tez Yöneticisi: Prof. Dr. Ayşe Gül Gözen
Ortak Tez Yöneticisi: Prof. Dr. Feride Severcan

Kasım 2017, 132 Sayfa

Ağır metallerden kaynaklanan çevre kirliliğinin insan sağlığı üzerinde çok ciddi zararlı etkileri vardır. Günümüzde, bakteriler ağır metalle kirlenmiş ortamların temizliğinde kullanılmaktadır. Çevre temizliğinde kullanılmak üzere, uygun bakteri suşlarının belirlenmesi önemli husustur.

Bakteriler buldukları ortamda ağır metal kaynağına yakın bulunabilir. Bu durumda yüksek derişimde ağır metale maruz kaldıklarından, hayatta kalmaları hızlı cevap mekanizmasının tetiklenmesi ile sağlanır. Diğer bir yandan, bakteri ağır metal kaynağına belli bir uzaklıkta yaşayıp bu maddenin artışını kademeli olarak hissedebilir. Ağır metal miktarındaki kademeli artış zamanla oluşan değişimlere yol açarak bakterilerin bu şekilde hayatta kalmasını sağlayabilir. Ağır metale akut yada kademeli maruz kalma durumlarının ikisinde de bakteriler hayatta kalmak için çeşitli direnç mekanizmalarını kullanırlar.

Çalışmamızda ATR-FTIR spektroskopisi ve denetlenmemiş analiz metodlarını (PCA, HCA) kullanılarak, ağır metallere akut ya da kademeli olarak maruz bırakılan bakterilerde meydana gelen moleküler değişiklikler arasında fark olup olmadığını araştırdık. İkincil olarak da, bu bakterilerde metal direncinin hangi mekanizmalarla sağlandığı hakkında bilgi edinmeyi amaçladık. Ağır metal olarak kadmiyum ve kurşunu seçtik ve tatlı su kaynağından izole edilen *Brevundimonas*, *Gordonia*, and *Microbacterium* bakteri

cinslerinin moleküler yapılarını çalıştık. Labaratuvar ortamında uzun süre maruziyet sonrasında bakteriler ağır metal varlığında büyümeye ve yaşamaya alışabilmektedir. İki farklı alıştırma prosedürü (akut, kademeli) uygulayarak bakterinin ağır metal kaynağına uzak ya da yakın olma durumunu taklit ettik. Bakteri örneklerini metallerin en düşük öldürücü derişimlerinin 2 ila 4 katı fazla derişimlerde yaşamaya alıştırdık. Ve sonrasında, alıştırma şeklinin farklılığından dolayı meydana moleküler değışiklikleri ölçtük. IR spektral analiz sonuçları, bakteriyel makromoleküllerin yapı ve kompozisyonunda önemli değışikliklerin olduğunu göstermiştir. Bakteriyel membranlardaki değışiklikler kendini yağ asidi miktarlarında ve protein-yağ oranlarındaki azalmalar şeklinden göstermiştir. Bütün alıştırlmış guruplarda protein miktarlarının azaldığı gözlenmiştir. Bu azalmalar bazı anabolik yolların inhibisyonundan kaynaklandığını işaret etmektedir. Buna ek olarak, metale akut olarak alıştırlmış bakterilerdeki protein miktarı, aşamalı olarak alıştırlmışlardan belirgin bir şekilde azdır. Bütün alıştırlmış bakteri guruplarında eekzopolimer üretiminde önemli miktarlarda artışlar gözlenmiştir. Ayrıca, bakterilerin, yüksek oranda ağır metal içeren ortamda hayatta kalmasında ekzopolimer üretiminin ana rolü oynadığı görülmüştür. Kadmiyuma maruz kalma durumunda, akut prosedür kullanılarak alıştırlan bakteriler daha fazla ekzopolimer üretmiştir. Buna karşılık, kurşuna kademeli aşıtırılma durumunda kademeli olarak alıştırlan bakteriler daha fazla ekzopolimer üretmiştir. PCA ve HCA analizleri, kadmiyum ya da kurşun varlığında yaşamaya alıştırlmış gurupların ve kontrol guruplarının çok net bir şekilde birbirinden ayrıldığını göstermiştir.

Çalışmamız IR spektroskopisin farklı stress durumlarına alıştırlmış bakterilerin moleküler karakterizsyonundaki potansiyel rolü konusunda yeni bir bakış açısı getirmektedir. Buna ek olarak, çalışmamız ekzopolimer üretimi konusundaki bilginin biyoremediyasyon çalışmalarında kullanılmaya uygun bakterilerin belirlenmesinde kullanılabileceğini göstermiştir.

Anahtar Kelimeler: Ağır Metal Direnci, *Brevundimonas* sp., *Gordonia* sp., *Microbacterium oxydans*, Cd, Pb, Alıştırma, Akut, Kademeli, MIC, ATR-FTIR spektroskopi, ekzopolimer, PCA, HCA

To my brother Ali Kemal Kepenek

ACKNOWLEDGEMENTS

I would like to my deepest gratitude to my supervisor Prof. Dr. Ayşe Gül Gözen and to my co-supervisor Prof. Dr. Feride Severcan for their guidance, advice, criticism, encouragements, and insight throughout the research.

I would like to thanks to the members of my thesis follow-up committee, Prof. Dr. Gülsün Gökağaç Arslan, and Assoc. Prof. Dr. Çağdaş Son for their constructive contributions during my work.

I would like to extend my thanks to Ph.D. Thesis Committee Members, Prof. Dr. Gülsün Gökağaç Arslan, Prof. Dr. İrfan Kandemir, Assoc. Prof. Dr. Çağdaş Devrim Son, and Assist. Prof. Dr. Ayça Doğan Mollaoğlu.

I would like to thank to my labmates and all members in Severcan's laboratory for their help and friendship.

I would like to give my deepest thanks to my father Nevzi Cihan Kepenek, my mother Zübeyde Kepenek, my brother Hasan Kepenek for their endless patience, support, and understanding. Honestly, I could not have completed this thesis without you. Thanks for being with me.

I would like to thanks to Scientific and Technological Research Council of Turkey (TUBITAK) since this work was supported by the Environment, Atmosphere, Earth and Marine Sciences Research Group (CAYDAG) of the TUBITAK (Project No. 113Y515).

TABLE OF CONTENTS

ABSTRACT.....	V
ÖZ.....	Viii
ACKNOWLEDGEMENTS.....	Xi
TABLE OF CONTENTS.....	Xii
LIST OF TABLES.....	XV
LIST OF FIGURES.....	XVii
LIST OF ABBREVIATIONS.....	XXi
CHAPTERS	
1. INTRODUCTION.....	1
1.1 Heavy Metals and Their Biological Activities.....	1
1.2 Metal Resistance Mechanisms in Bacteria.....	4
1.2.1 Metal exclusion by permeability barrier.....	5
1.2.2 Efflux mechanism.....	5
1.2.3 Intracellular sequestration of heavy metals.....	6
1.2.4 Extracellular sequestration of heavy metals.....	6
1.2.5 Enzymatic detoxification of metal to a less toxic form.....	7
1.2.6 Reduction in metal sensitivity of cellular targets.....	7
1.3 Brief history of Fourier Transform-Infrared (FT-IR) spectroscopy.....	8
1.3.1 Electromagnetic radiation.....	8
1.3.2 IR spectroscopy.....	9
1.3.3 Fourier Transform Infrared spectroscopy (FTIR).....	13
1.3.3.1 Advantages of FTIR spectroscopy.....	14

1.3.4 Attenuated Total Reflection- Fourier Transform Infrared (ATR-FTIR) Spectroscopy.....	15
1.4 Chemometric approaches.....	17
1.4.1 Principal Component Analysis (PCA).....	17
1.4.2 Hierarchical Cluster Analysis (HCA).....	18
1.5 Bacteriological Studies.....	20
1.5.1 Minimum inhibitory concentration (MIC) Determinations.....	20
1.5.2 Broth dilution method.....	20
1.5.3 Bacterial culture passaging.....	21
1.5.4 Acclimation of bacterial strains to heavy metals.....	22
1.6 Aim of the Study.....	22
2. MATERIALS AND METHODS.....	25
2.1 Bacterial strains.....	25
2.2 Growth Conditions.....	25
2.3 Determination of minimum inhibitory concentrations (MIC).....	26
2.4 Acclimation of bacterial strains to cadmium or lead.....	26
2.5 Bacteria Sample preparation for ATR-FTIR spectroscopy.....	27
2.6 ATR-FTIR spectroscopy.....	28
2.7 IR Data Analysis.....	28
2.8 Chemometric approaches.....	28
2.8.1 Principle component analysis (PCA).....	29
2.8.2 Hierarchical cluster analysis (HCA).....	29
2.9 Statistics.....	32
3 RESULTS and DISCUSSION.....	33
3.1 Minimum Inhibitory Concentrations (MIC) for bacterial strains.....	33
3.2 Acclimation of bacterial strains for cadmium or lead.....	34
3.3 ATR-FTIR Spectroscopy.....	37
3.4 Chemometric approaches.....	68

3.4.1 Principle Component Analysis (PCA).....	68
3.4.2 Hierarchical Cluster Analysis (HCA).....	79
4. CONCLUSION.....	89
REFERENCES.....	91
APPENDICES.....	113
A. ATR-FTIR spectra of Cd or Pb-acclimated (acute: A, gradual: G) and control groups of <i>Brevundimonas</i> sp., <i>Gordonia</i> sp., and <i>M. oxydans</i> in the 4000-650 cm ⁻¹ spectral region.....	113
B. PCA loading plots of Cd and Pb exposed (acute or gradual) and control <i>Brevundimonas</i> sp., <i>Gordonia</i> sp., and <i>M. oxydans</i> , in the A- whole spectral region (4000-650 cm ⁻¹), B- lipid region (3200-2800 cm ⁻¹) C- protein region (1800-1500 cm ⁻¹), D- carbohydrate region (1200-900 cm ⁻¹).....	117
CIRRICULUM VITAE.....	129

LIST OF TABLES

TABLES

Table 1. Representations and numbers of samples for acute or gradual exposure procedures.....	27
Table 2. Definitions for sensitivity and specificity for hierarchical cluster analysis based on FTIR data for acute acclimation.....	30
Table 3. Definitions for sensitivity and specificity for hierarchical cluster analysis based on FTIR data for gradual acclimation.....	31
Table 4. Definitions for sensitivity and specificity for hierarchical cluster analysis based on FTIR data for acute and gradual acclimation.....	31
Table 5. Minimum inhibitory Cd and Pb concentrations for environmental strains.....	33
Table 6. Minimum inhibitory Cd and Pb concentrations in the related literature.....	34
Table 7. Gradual acclimation of bacterial strains to Cd or Pb.....	35
Table 8. Acute acclimation of bacterial strains for heavy metals.....	36
Table 9. General band assignments in the spectrum obtained from bacteria.....	38
Table10. The changes in spectral band intensities in Cd or Pb acclimated <i>Brevundimonas</i> sp. with respect to control group.....	45
Table 11. The changes in spectral band intensities in Cd or Pb acclimated <i>Gordonia</i> sp. with respect to the control group.....	46

Table 12. The changes in spectral band intensities in Cd or Pb acclimated *M. oxydans* with respect to the control group.....47

Table 13. The protein-to-lipid ratio (Amide I + Amide II / C=O stretching) of Pb and Pb acclimated bacteria.....51

Table 14. The relative protein concentration (amide I/amide I+ amide II) of acute and gradual and acclimated environmental strains.....55

Table 15. Differences in spectral band intensity change between acutely and gradually Cd or Pb-acclimated *Brevundimonas* sp.....64

Table 16. Differences in spectral band intensity change between acutely and gradually Cd or Pb-acclimated *Gordonia* sp.....65

Table 17. Differences in spectral band intensity change between acutely and gradually Cd or Pb-acclimated *M. oxydans*.....66

LIST OF FIGURES

FIGURES

- Figure 1.** An example of the fast-unspecific uptake system; Cd²⁺ uptake is maintained by the Magnesium (MIT) and/or manganese uptake systems.....2
- Figure 2.** Main transport families involved in heavy metal resistance.....6
- Figure 3.** Simple presentations of some vibrational modes of chemical bonds.....10
- Figure 4.** A typical mid-IR transmission spectrum showing peaks associated with vibrational modes of molecules.....11
- Figure 5.** A) Schematic diagram of a Michelson interferometer configured for FTIR B) The general system flowchart of FTIR.....14
- Figure 6.** The three main sampling modes for FTIR spectroscopy.....15
- Figure 7.** Detection of MIC by using broth dilution method.....21
- Figure 8.** A representative ATR-FTIR spectrum of *Gordonia* sp. showing band assignments in the 4000-650 cm⁻¹ region.....37
- Figure 9.** ATR-FTIR spectra of acclimated (acute: A, gradual: G) and control groups of *Brevundimonas* sp. in the 4000-650 cm⁻¹ spectral region.....39
- Figure 10.** Representative second derivative, vector normalized, average spectra of controls without metal exposure.....41

Figure 11. Representative second derivative, vector-normalized, average spectra of the acclimated (acute: A, gradual: G) and control groups of *Brevundimonas* sp. (A-F) in the presence of Cd or Pb.....42

Figure 12. Representative second derivative, vector-normalized, average spectra of the acclimated (acute: A, gradual: G) and control groups of *M. oxydans* (A-F) in the presence of Cd or Pb.....43

Figure 13. Representative second derivative, vector-normalized, average spectra of the acclimated (acute: A, gradual: G) and control groups of *Gordonia* sp. (A-F) in the presence of Cd or Pb.....44

Figure 14. The CH₃ antisymmetric stretching band intensities of Cd (A, C, E) or Pb (B, D) acclimated and control groups of *Brevundimonas* sp., *Gordonia* sp. and *M. oxydans*.....49

Figure 15. The protein-to-lipid ratio of Cd (A, C, E) or Pb (B, D, F) acclimated and control groups of *Brevundimonas* sp., *Gordonia* sp. and *Microbacterium oxydans*.....52

Figure 16. Changes in spectral band intensities in Cd acclimated (A, C, E), Pb acclimated (B, D, F), and control groups of *Brevundimonas* sp., *Gordonia* sp., and *M. oxydans*.....54

Figure 17. Changes in intensity of C-O stretching of carboxylic acid at 1310 cm⁻¹ in the Cd or Pb-acclimated *Brevundimonas* sp., *Gordonia* sp., and *M. oxydans*; A: acute, G: gradual.....58

Figure 18. Spectral band intensity changes at 1117, 1082, 1056, and 965 cm⁻¹ (carbohydrate region) in Cd or Pb acclimated *Brevundimonas* sp.....61

Figure 19. Spectral band intensity changes at 1117, 1082, 1056, and 965 cm⁻¹ (carbohydrate region) in Cd or Pb acclimated *Gordonia* sp.....62

Figure 20. Spectral band intensity changes at 1117, 1082, 1056, and 965 cm⁻¹ (carbohydrate region) in Cd or Pb acclimated *M. oxydans*.....63

Figure 21. PCA score plots (A) whole spectral region (4000-650 cm⁻¹) (B) lipid region (3200-2800 cm⁻¹) (C) protein region (1800-1500 cm⁻¹) (D) carbohydrate region (1200-900 cm⁻¹) for Cd-acclimated (A: acute, G: gradual) and control groups of *Brevundimonas* sp.....73

Figure 22. PCA score plots (A) whole spectral region (4000-650 cm⁻¹) (B) lipid region (3200-2800 cm⁻¹) (C) protein region (1800-1500 cm⁻¹) (D) carbohydrate region (1200-900 cm⁻¹) for Pb-acclimated (A: acute, G: gradual) and control groups of *Brevundimonas* sp.....74

Figure 23. PCA score plots (A) whole spectral region (4000-650 cm⁻¹) (B) lipid region (3200-2800 cm⁻¹) (C) protein region (1800-1500 cm⁻¹) (D) carbohydrate region (1200-900 cm⁻¹) for Cd-acclimated (A: acute, G: gradual) and control groups of *Gordonia* sp.....75

Figure 24. PCA score plots (A) whole spectral region (4000-650 cm⁻¹) (B) lipid region (3200-2800 cm⁻¹) (C) protein region (1800-1500 cm⁻¹) (D) carbohydrate region (1200-900 cm⁻¹) for Pb-acclimated (A: acute, G: gradual) and control groups of *Gordonia* sp.....76

Figure 25. PCA score plots (A) whole spectral region (4000-650 cm⁻¹) (B) lipid region (3200-2800 cm⁻¹) (C) protein region (1800-1500 cm⁻¹) (D) carbohydrate region (1200-900 cm⁻¹) for Cd-acclimated (A: acute, G: gradual) and control groups of *M. oxydans*.....77

Figure 26. PCA score plots (A) whole spectral region (4000-650 cm⁻¹) (B) lipid region (3200-2800 cm⁻¹) (C) protein region (1800-1500 cm⁻¹) (D) carbohydrate region (1200-900 cm⁻¹) for Pb-acclimated (A: acute, G: gradual) and control groups of *M. oxydans*.....78

Figure 27. HCA; (A) whole, (B) lipid, (C) protein, and (D) carbohydrate region for Cd-acclimated (A: acute, G: gradual) and control *Brevundimonas* sp.....81

Figure 28. HCA; (A) whole, (B) lipid, (C) protein, and (D) carbohydrate region for Pb-acclimated (A: acute, G: gradual) and control *Brevundimonas* sp.....82

Figure 29. HCA; (A) whole, (B) lipid, (C) protein, and (D) carbohydrate region for Cd-acclimated (A: acute, G: gradual) and control *Gordonia* sp.....83

Figure 30. HCA; (A) whole, (B) lipid, (C) protein, and (D) carbohydrate region for Pb-acclimated (A: acute, G: gradual) and control *Gordonia* sp.....84

Figure 31. HCA; (A) whole, (B) lipid, (C) protein, and (D) carbohydrate region for Cd-acclimated (A: acute, G: gradual) and control *M. oxydans*.....85

Figure 32. HCA; (A) whole, (B) lipid, (C) protein, and (D) carbohydrate region for Pb-acclimated (A: acute, G: gradual) and control *M. oxydans*.....86

LIST OF ABBREVIATIONS

ATR	Attenuated Total Reflectance
Cd	Cadmium
CLSI	Clinical and Laboratory Standards Institute
EPS	Extracellular Polysaccharides
EUCAST	European Committee on Antimicrobial Susceptibility Testing
FTIR	Fourier Transform Infrared
HCA	Hierarchical Cluster Analysis
IR	Infrared
LPS	Lipopolysaccharide
MIC	Minimum Inhibitory Concentration
NA	Nutrient Agar
NB	Nutrient Broth
OD	Optical Density
Pb	Lead
PCA	Principle Component Analysis
PHA	Polyhydroxyalkanoate
SEM	Standard Error of Mean

CHAPTER 1

1. INTRODUCTION

1.1 Heavy Metals and Their Biological Activities

Metals are natural constituents of earth crust and have vital roles in life processes of living organisms (Bruins et al., 2000; Nies, 1999). Of the naturally occurring 69 metals, 53 are heavy metals with a density higher than 5 gr/cm³ (Ahemad, 2014; Nies, 1999; Ullah et al., 2015). All of the 53 heavy metals are not biologically active. Heavy metals which are available in adequate amount and solubility shows biological activity (Hassen et al., 1998; Roosa et al., 2014). Several of available heavy metals, such as Cu, Mn, Zn, Ni, Fe, Co are essential for life at low concentrations and required for cell functioning (Ahemad, 2014; Bruins et al., 2000; Maynaud et al., 2014; Nies, 1999; Tchounwou et al., 2012). For example, zinc is involved in the structure of several enzymes and DNA-binding proteins (such as in zinc-finger proteins) and act as a cofactor for several enzymes (dehydrogenases, proteinases, peptidases, and oxidase). Likewise, iron is involved in the composition of several enzymes and iron-sulfur proteins. Also, most heavy metals are transition elements because of their incompletely filled d orbitals and make cations having the ability to form complex compounds which are involved in biochemical reactions. On the other hand, heavy metals such as iron, copper, and nickel are needed for redox reactions (Ahemad, 2014; Bruins et al., 2000; Maynaud et al., 2014; Nies, 1999). Besides their beneficial roles in biological systems, higher concentrations of these heavy metals are toxic to organisms (Xie et al., 2015; Xiong et al., 2015). Other heavy metals, for

example, Cd, Pb, Ag, and Hg are non-essential and do not have any known biological functions. Furthermore, they are toxic at relatively low concentrations (Maynaud et al., 2014; Staley et al., 2015).

Heavy metals enter the cell by using specific or fast-unspecific uptake systems. Specific uptake systems with high substrate specificity use ATP as an energy source and only expressed in times of need or starvation. Fast-unspecific transport systems are driven by the chemiosmotic gradient. Employed by a variety of metal ions, unspecific transport systems are constitutively expressed. Because of constitutive expression, it creates an “open gate”. Since gate cannot be closed in times of metal ion stress; this situation leads to metal ion accumulation which causes toxicity. Example of these systems are magnesium transport systems (CorA: metal inorganic transport, MIT family as MgtA, MgtB), Manganese uptake system (Figure 1), Pit (phosphate inorganic transport) system, and fast sulfate-uptake system (Nies, 1992; Nies & Silver, 1995).

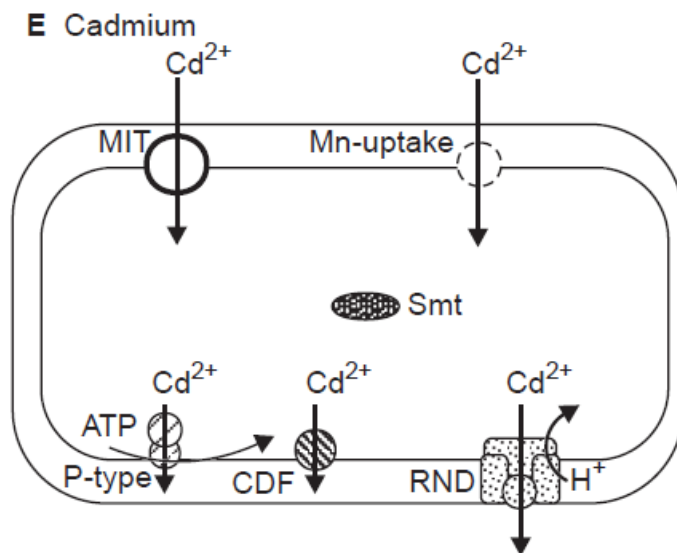


Figure 1. An example of the fast-unspecific uptake system; Cd²⁺ uptake is maintained by the Magnesium (MIT) and/or manganese uptake systems (Nies, 1999).

Cadmium (Cd) and lead (Pb) are also two of the non-essential heavy metals and toxic at low concentrations. They are accumulated in the cell by using magnesium and manganese divalent ion transport systems (Bruins et al., 2000; Nies, 1999; Jarosławiecka & Piotrowska-Seget, 2014). Besides toxicity, their bio-accumulating nature makes them a serious threat to the environment and public health (Guo et al., 2010; Nithiya et al., 2011). Cd is found abundantly in the earth's crust at an average concentration of about 0.1 mg/kg. It is used in the production of alloys, pigments, and batteries which lead to occupational exposure and environmental emission. Non-occupational exposure is caused by digestion of food and tobacco smoking because of the high soil-to-plant transfer rate of Cd. Cd leads to the formation of reactive oxygen species (ROS) which causes enhanced lipid peroxidation, single-strand DNA breaks and disrupts the synthesis of nucleic acids and proteins (Khan et al., 2010; Khan et al., 2015; Tchounwou et al., 2012; Zhai et al., 2015). As a result of Cd exposure, many stress-response systems are expressed involving those for heat shock, oxidative stress, stringent response, cold shock, and SOS. In addition to these, signal transduction pathways which increase free calcium levels or block calcium channels are affected by Cd toxicity. Previous studies have also detected that cadmium binds to proteins, interferes with DNA repair, stimulate protein degradation and induces expression of several genes including metallothioneins, acute-phase reactants, and DNA polymerase β (Tchounwou et al., 2012; Warners et al., 2012).

Similarly, Pb has extensively been used in anthropogenic activities such as fossil fuel burning, mining, and manufacturing. All these activities have caused about a 1000-fold increase in environmental Pb concentration. Pb toxicity affects several organs in the body including the kidneys, liver, central nervous system, endocrine system, and reproductive system. By binding to biological molecules, Pb interferes with their function by a few mechanisms. For instance, it binds to sulfhydryl and amide groups of enzymes, changing their configuration and reducing their activities. Another toxic effect of Pb is to inhibit or mimic the actions of calcium. By mimicking calcium, Pb accumulates in bones of the individuals where it can remain very long time. After a while, it can be released from the bones, enter the bloodstream and affects blood and other organs. Furthermore,

besides disrupting calcium metabolism, Pb can act like magnesium and iron which are found in structures of some enzymes and displaces them. Also, it causes the formation of reactive oxygen species (ROS), disruption of membrane functions, and DNA damage as in the case of Cd. (Jarosławiecka & Piotrowska-Seget, 2014; Naik et al., 2013; Tchounwou et al., 2012).

The environmental concentrations of heavy metals have highly increased in recent years because of anthropogenic activities (Bar et al., 2007; Naik, 2013; Nithiya et al., 2011; Staley et al., 2015; Ullah et al., 2015). Several physicochemical strategies have been developed to remove heavy metals from the polluted environments in the past few decades. Because these methods are expensive and less efficient, bioremediation applying microbes to detoxify and degrade environmental contaminants has become a safe and economical alternative to physicochemical methods (Guo et al., 2010; Mathe et al., 2012). Since bacteria contain several quickly spreading heavy metal resistance mechanisms, they are frequently the choice for bioremediation processes.

1.2 Heavy metal Resistance Mechanisms in Bacteria

The heavy metal ion toxicity related to the “open gate” formations mentioned in section 1.1 has forced bacteria to develop metal-ion homeostasis factors and metal resistance determinants. Heavy metal resistance systems may have developed shortly after the first appearance of prokaryotic life on Earth (Bruins et al., 2000; Nies, 1999; Silver, 1996). In the present era, the environmental pollution caused by anthropogenic activities in the form of elevated heavy metal ion concentrations puts a selective pressure in favor of these resistance mechanisms (Staley et al., 2015). These resistance mechanisms are mostly driven by plasmids enabling horizontal gene transfer causing the quick spread of these resistance elements throughout the bacterial communities (Chudobova et al., 2015; Hoostal et al., 2008). However, chromosomally-encoded resistance functions are also

present (Kardaş et al., 2014; Mergeay et al., 2003; Staley et al., 2015). Because a heavy metal cannot be degraded or modified as toxic organic compounds, only a few resistance mechanisms are present (Nies, 1999).

1.2.1 Metal exclusion by permeability barrier

Metal exclusion with permeability barrier is accomplished by alterations in the cell wall, membrane or envelope of microorganisms. For example, in *E. coli*, exclusion of Cu (II) is achieved by the altered production of outer membrane channel proteins (porins) decreasing the permeability of the membrane to metal ions. Another mechanism is nonspecific binding of metals to the outer membrane. This provides a low-level protection due to saturation of binding sites (Jiménez-Galisteo et al., 2017; Bruins et al., 2000).

1.2.2 Efflux mechanism

Transport of heavy metal ions outside the cell membrane is provided by the three major families of efflux transporters, P_{IB}-type ATPases, cation diffusion facilitator (CDF) transporters and CBA transporters (three- component trans-envelope efflux pump) (Figure 2). These mechanisms provide bacterial heavy metal resistance against highly toxic and reactive metal ions such as Pb (II), Cu (I), Ag (I), Zn (II), and Cd (II) by preventing over accumulation of these ions. P-type ATPases are spanning the inner membrane and transport metal ions from the cytoplasm to periplasm. Similarly, CDF transporters, acting as chemiosmotic ion-proton exchangers, transfer metal ions from cytoplasm to periplasm. CBA on the other hand function also as a chemiosmotic antiporter but extrudes metal ions from the periplasm to outside of the cells (Bruins et al., 2000; Hynninen, 2010; Jarosławiecka & Piotrowska-Seget, 2014; Naik et al., 2013).

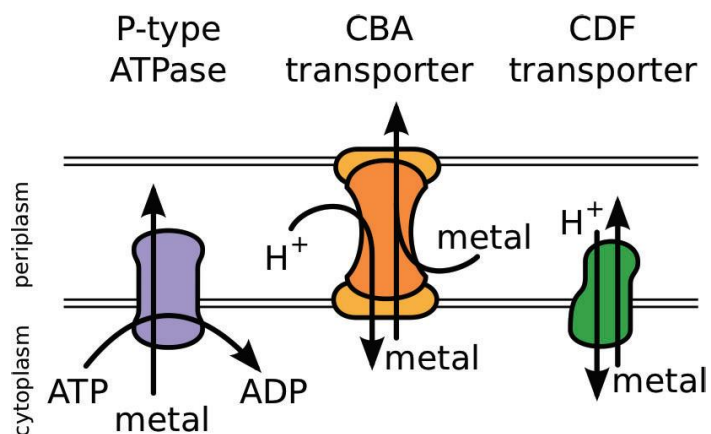


Figure 2. Main transport families involved in heavy metal resistance

1.2.3 Intracellular sequestration of heavy metals

Intracellular sequestration is the accumulation of metals in the cytoplasm via specific metal binding proteins known as metallothioneins. These special metal binding proteins are induced in the presence of heavy metals such as Cd, Pb, Zn, and Cu, and involved in immobilization processes. Metallothioneins are synthesized by several bacterial strains and encoded by *smt* locus containing *smtA* and *smtB* genes (Bruins et al., 2000; Jarosławiecka & Piotrowska-Seget, 2014; Naik et al., 2013).

1.2.4 Extracellular sequestration of heavy metals

Bacterial cells synthesize extracellular biopolymers known as exopolysaccharides (EPS) composed of macromolecules for instance polysaccharides, proteins, nucleic acids, humic substances, lipids and other non-polymeric constituents. Exopolysaccharides (EPS) are mostly acidic heteropolysaccharides with functional groups such as hydroxyl, carboxyl,

amide, and phosphoryl exhibiting high affinity towards heavy metals. EPSs bind metals via their charged moieties leading to metal immobilization within the exopolymeric matrix (Bruins et al., 2000; Jarosławiecka & Piotrowska-Seget, 2014; Naik et al., 2013).

1.2.5 Enzymatic detoxification of metal to a less toxic form

Enzymatic detoxification is mainly a function of the proteins encoded by genes in resistance operons. These genes are responsible for the production of proteins involved in detoxification and transportation of metal ions, and self-regulation of resistance. In the absence of metal ions, the operon codes for a regulatory protein that downregulates the transcription. If metal ion is present in the environment, it stimulates synthesis of a periplasmic binding protein and membrane-associated transport proteins by the same resistance operon. The metal ion is collected by the periplasmic binding protein from surrounding environment and transferred into the cytoplasm by transport proteins for detoxification. The same operon also encodes for the gene producing a reductase responsible for the reduction of the metal ion. Then the reduced metal ion is released to diffuse through the cell membrane and into the surrounding environment (Bruins et al., 2000).

1.2.6 Reduction in metal sensitivity of cellular targets

Some microorganisms overcome the presence of toxic metals by changing the sensitivity of essential cellular components. Mutations that decrease sensitivity but do not alter basic functions or by increasing production of particular cellular components are the ways to combat the heavy metals for this strategy. The microorganisms may also represent resistance to heavy metals by producing metal resistant components or alternate pathways to bypass sensitive components (Bruins et al., 2000). In our study, we have measured the macromolecular profile changes supposed to result from the above mentioned heavy metal resistance mechanisms with infrared red spectroscopy.

1.3 Brief history of Fourier Transform-Infrared (FT-IR) spectroscopy

Discovery of IR dates back to the early 1800s, but the first IR spectra were published only by the end of the century. Later, in the 1940s IR spectrometer was combined with a microscope which obtained a great advantage to extract accurate molecular information from small areas of a sample (Marcelli et al., 2012). In the 1950s and 1960s, although IR spectroscopy was used for identification or differentiation of bacteria, it was laborious and impractical for routine analysis due to instrument limitations and lack of integrated computational analysis (Naumann et al. 1995; Riddle et al., 1956). The use of IR in routine analyses (qualitative, quantitative) has been increasing with the invention of the Fourier Transform Infrared (FT-IR) spectroscopy (Marcelli et al., 2012). After the development of the modern interferometer and multivariate statistical tools, FT-IR spectroscopy was applied for biological systems frequently in the 1980s (Burgula et al., 2007). FT-IR methods for *in-situ* analysis of bacterial cells and complex spectral analysis to identify, differentiate, and classify bacteria reintroduced by Naumann and co-workers in 1991. Since that time, FT-IR spectroscopy has been successfully used for detection, discrimination, identification, and classification of bacterial cells. (Burgula et al., 2007; Davis & Mauer, 2010; De Luca et al., 2011; Preisner et al., 2008; Preisner et al., 2012; Wenning & Scherer, 2013).

1.3.1 Electromagnetic radiation

The electromagnetic spectrum is consist of energy (E) that may act both as a particle and as a wave. The word **photon** is used when we identify this energy as a particle. The terms **frequency** (ν) and **wavelength** (λ) are used in the wave concept. The number of waves passing through a given point in a second is called frequency. Wavelength is described as the distance between the two adjacent wave crests. The inverse relation is present between frequency and wavelength, according to the equation where h is the Planck's constant and c is the speed of light.

$$(1) E = h\nu = hc / \lambda; \quad (2) c = \lambda \nu$$

Thus, when frequency increases, wavelength decreases. Based on these two equations, a new unit of measurement was introduced called the **wavenumber** ($\bar{\nu}$). The wavenumber is defined as a number of waves in one centimeter and has the units of reciprocal centimeters (cm^{-1}).

$$\bar{\nu} = \text{wavenumber} = (1/\lambda) \longrightarrow E = h \cdot \nu = h c / \lambda = h c \bar{\nu}$$

Because inverse proportionality is present between the wavenumber and wavelength, wavenumber is directly proportional to frequency and energy that renders it more convenient to use (Campbell & Dwek, 1984; Stuart, 2004).

1.3.2 IR spectroscopy

Spectroscopy is based upon the interaction of electromagnetic radiation with matter. The region extends from $10,000 \text{ cm}^{-1}$ to 10 cm^{-1} of the electromagnetic spectrum known as IR region is composed of near-infrared (NIR), mid-infrared (MIR) and far-infrared (FIR) regions (Burgula et al., 2007). IR spectroscopy is based on the absorption of IR radiation at specific wavelengths (or frequencies or wavenumbers) by IR active molecules that absorb energies within the mid-IR region ($400\text{-}4000 \text{ cm}^{-1}$) of the electromagnetic spectrum. In this region of spectrum, all molecules represent characteristic absorbance frequencies and primary molecular vibrations correlated with the presence of specific functional groups (for example, amide, carbonyl) (Marcelli et al., 2012). Molecules found in matters contain bonds that are continually vibrating and moving around. (Alvarez et al., 2011; Davis & Mauer, 2010). Infrared radiation (IR) changes the vibrational behavior of molecules by delivering energy quanta and changing their vibrational and rotational modes. It leads to excitation of specific molecular groups, and the vibration caused by the excited state only takes place at fixed wavelengths. That is when IR radiation is passed

through a sample; specific wavelengths are absorbed bringing about the chemical bond vibration in the material. Absorption of radiation takes place when the energy of vibrational mode is equal or close to the energy of a wavelength of radiation. In the mid-IR range, vibrations are mainly in stretching or bending fashion (Haris & Severcan, 1999; Davis & Mauer, 2010). Stretching and bending vibrations are determined by interferences (positive or negative) happening when specific frequencies (or wavelengths) of mid-IR radiation and the natural frequencies at which intra-molecular bond vibrations resonate. Stretching or bending alter the molecular dipole moment of the molecule. In polyatomic molecules, a number of potential vibrational modes reflecting the complexity of molecule can be simultaneously created by different parts of the molecule, while one normal mode of vibration is seen in bi-atomic molecules. Movement along the bond axis such that the interatomic distance increases or decreases creates stretching vibration (ν) while the change in the bond angle between bonds causes bending vibration (δ), e.g., scissoring, rocking, wagging, and twisting (Figure 3).

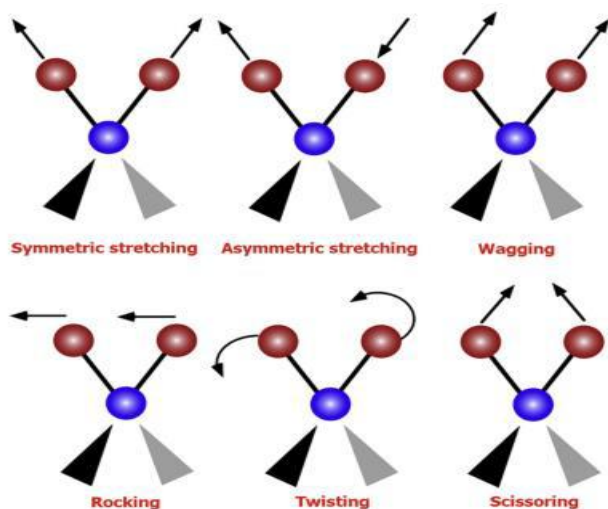


Figure 3. Simple presentations of some vibrational modes of chemical bonds (Marcelli et al., 2012).

Vibrations leading to a change of the dipole moment of the system create a certain number of peaks representing different vibrational modes and the number of vibrating components which contribute to the intensity value and shape (Figure 4). Spectral peaks can be situated to specific bonds or groups at specific wavenumber range (frequency). So a correlation is present between IR band positions and chemical structures in the molecule (Alvarez et al., 2011; Davis & Mauer, 2010; Marcelli et al., 2012).

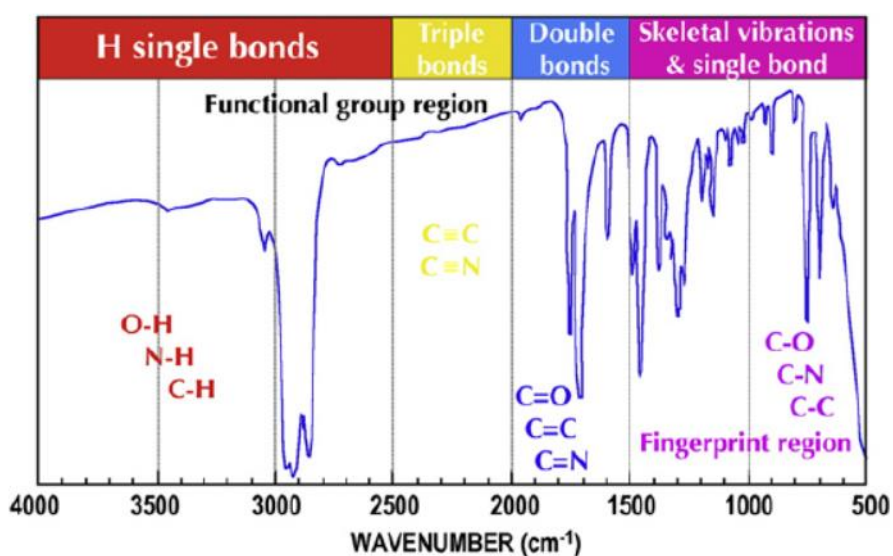


Figure 4. A typical mid-IR transmission spectrum showing peaks associated with vibrational modes of molecules (Marcelli et al., 2012).

An IR spectrum is evaluated by calculating the intensity of the IR radiation before and after passing through a specimen, and the spectrum is plotted. When plotting a spectrum, Y-axis and X-axis are used as absorbance and wavenumber units, respectively.

When IR spectrum is calculated according to transmittance (T), it is expressed as

$$\%T = I_S / I_R \quad (1)$$

I_S = intensity of IR beam after passing through the sample;

I_R = intensity of IR beam before passing through the sample;

T = transmittance.

Qualitative measurement is maintained by absorbance (A), where

$$A = -\log T \text{ or } A = \log_{10} (1/T) = \log (I_R/I_S) \quad (2)$$

Beer's law is valid for quantitative spectral analysis which defines the concentration of the sample regarding the path length (l), absorptivity (ϵ) and concentration (c):

$$A_\lambda = I\epsilon_\lambda C \quad (3)$$

Excitation caused by the absorption of IR radiation forms the absorption bands because of the energy exchange between discrete light quanta and the mechanical motion (vibrational modes) of the molecules. Concentration affects the intensity of absorbance peaks but, intensity variation may not always be linear due to intramolecular interactions, atmospheric changes, and instrumental limitations. An air background spectrum is needed

for analyzing spectra of biological samples to eliminate spectral variations resulting from instrumental error, variation in the surrounding atmosphere and absorbance of water vapor and CO₂ in the air. The absorbance or transmittance is measured without a sample in the chamber, and this measurement is compared to the sample spectrum to obtain a background spectrum employed to remove the effects of atmospheric conditions (Burgula et al., 2007).

1.3.3 Fourier Transform Infrared spectroscopy (FTIR)

In FTIR spectroscopy, radiation emitted from IR source is passed through a Michelson interferometer with a beam splitter (a semi-reflecting film usually made of KBr), a fixed mirror, and a moving mirror. The interferometer uses interference of radiation between two beams to measure the wavelength of light and produces interferogram, which is a signal formed as a result of the change of path length at a beam splitter (Stuart & Ando, 1997). Interferogram producing force is the recombination of two beams with different path length in the beam splitter producing an interference. When IR radiation is applied, some radiation is absorbed, and the rest is transmitted to the detector which measures the total interferogram from all the different IR wavelengths. Interferogram (an intensity versus time spectrum) is converted to an IR spectrum (an intensity versus frequency spectrum) by a mathematical function called Fourier transformation (Figure 5).

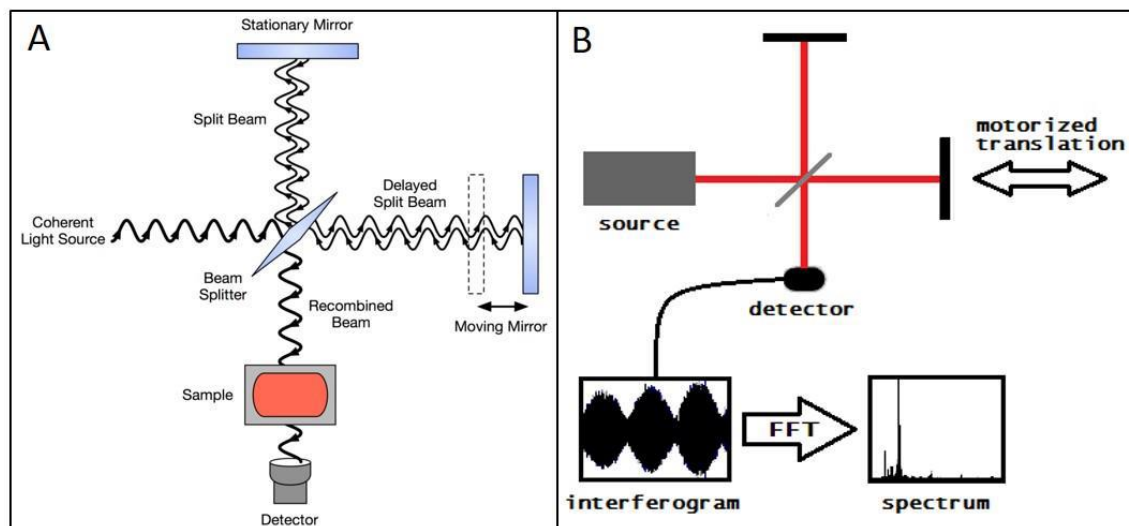


Figure 5. A) Schematic diagram of a Michelson interferometer configured for FTIR B) The general system flowchart of FTIR.

1.3.3.1 Advantages of FTIR spectroscopy

- 1- FT-IR is relatively fast and easy technique because, little or no sample preparation needed before application of the sample, and mostly 5 min is enough for spectral analysis (Mendelsohn, 1986; Movasaghi et al., 2008; Oust et al., 2004).
- 2- It is a nondestructive technique that cells remain intact during analysis. Furthermore, a small amount of sample (ng- μ g) is enough for spectral data acquisition (Aksoy et al., 2012; Burgula et al., 2007; Davis & Mauer, 2010)
- 4- It is a universal method. In other words, the instrument and software can be reached easily to use for routine analyses (Davis & Mauer, 2010; Garip et al., 2007).
- 5- In addition to providing qualitative information about cell composition and functional groups, FTIR analysis can be used for quantitative purposes by quantifying the number of cells or amount of functional groups present in a sample (Davis & Mauer, 2010; Kim et al., 2005; Movasaghi et al., 2008).

- 6- It is used for evaluation of multiple types of samples including liquid, gas, powder, solid, or film (Haris & Severcan, 1999; Davis & Mauer, 2010).
- 7- It is used for discrimination of bacteria according to their physiological state such as live, dead, injured, and treated (Davis & Mauer, 2010; Alvarez et al., 2011; Lin et al., 2004; Mecozzi, 2007; Oust et al., 2004).
- 8- Compared to several widely used methods, FTIR analysis is a relatively less expensive technique for bacterial identification (Naumann et al., 1996; Naumann, 2000; Mariey et al., 2001).

1.3.4 Attenuated Total Reflection- Fourier Transform Infrared (ATR-FTIR) Spectroscopy

Transmission, transfection and attenuated total reflection (ATR) are the three major IR-spectroscopic sampling modes. Each mode has advantages and disadvantages depending on sample type (Baker et al., 2014).

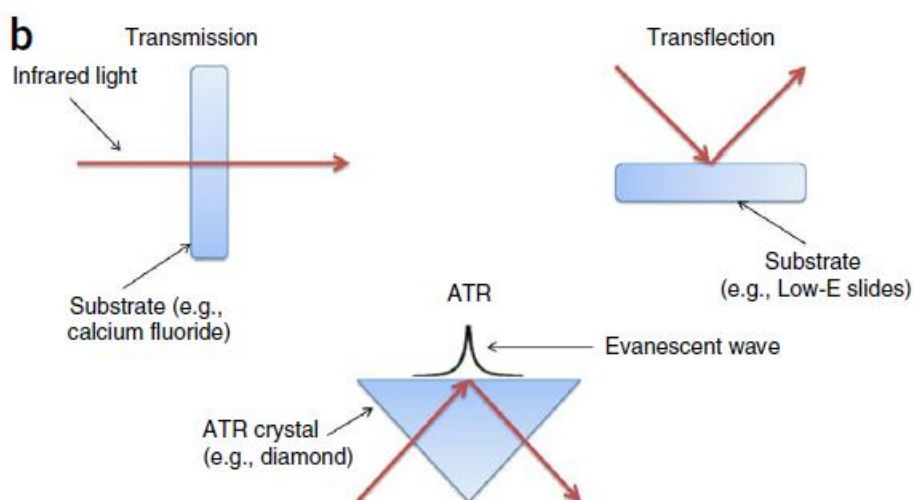


Figure 6. The three main sampling modes for FTIR spectroscopy (Baker et al., 2014).

Based on the phenomenon of total internal reflection, Attenuated Total Reflectance (ATR) spectroscopy is a powerful tool for studying biological materials. (Davis & Mauer, 2010; Marcelli et al., 2012). The ATR crystal, such as diamond, zinc, selenide, or germanium, with a high refractive index is used as an internal reflection element (IRE). The IR beam is directed through an internal reflection element (IRE) where evanescent wave penetrates the sample (Baker et al., 2014; Davis & Mauer, 2010). In particular, the IR beam reaches the interface between the ATR support and the sample at an angle which maintains total reflection of the beam by the interface and then beam penetrates into the sample as an evanescent wave, where it can be absorbed. The beam penetration depth is specified by the wavelength, the incident angle, as well as the refractive indices of the sample and the ATR element. This approach allows the measurement of samples without deposition onto an IR transparent support, and only need is a specimen to be in close contact with the ATR element (Ami et al., 2012). By placing the sample directly onto the IRE aperture of the ATR accessory, biofluids can be easily analyzed by bypassing any potential contributions from any substrate such as a microscope slide that the sample could be placed on. This approach provides a reduction in time needed for sample preparation (Baker et al., 2014). Furthermore, even though transmission and transflection modes have been commonly used in biological analysis, (Kazarian & Chan, 2006; Marcelli et al., 2012). Because of these properties, ATR mode of FTIR is a fast and inexpensive technique which can analyze different functional groups of molecules in the biological systems (Gaigneaux et al., 2006). Additionally, to reach sufficiently large absorbance intensity, the sample should be of adequate thickness. In transmission and transflection modes, the material thickness should be adjusted appropriately. If the excessively thick specimen is used, Beer-Lambert's law cannot be valid because of nonlinearity in detector response function which disrupts the subsequent quantitative and classification analyses. In contrast, samples must also not be excessively thin to prevent interactions of the evanescent wave with the underlying substrate. In ATR-FTIR spectroscopy, samples can be three- or fourfold thicker than the penetration depth. In other words, there is no restriction for thickness and specimens which are even a millimeter thick can be analyzed (Baker et al., 2014; Davis & Mauer, 2010).

1.4 Chemometric approaches

Chemometrics allow interpretation of complex spectral data which gives information about the structure and composition of cells by using multivariate statistical tools (Lavine, 2000). Multivariate statistical tools are divided into two categories supervised methods and unsupervised methods (Brereton, 2003 Wang & Mizaikoff, 2008). Unsupervised methods extrapolate the spectral data without prior knowledge about the sample studied. They are elegant tools for classifying spectra and obtaining an impression of the complexity, similarity and heterogeneity of data sets of unknown composition (Wenning & Scherer, 2013). By using these methods, spectral data is directly compared, and a subset of data is created based on spectral similarities (Burgula et al., 2007). In this study two of the unsupervised methods, Principal Component Analysis (PCA) and Hierarchical Cluster Analysis (HCA), were applied.

1.4.1 Principal Component Analysis (PCA)

Principal component analysis (PCA) based on statistical data reduction is a mathematical algorithm which reduces the multidimensionality of the data set into its most dominant components or scores while retaining most of the variation in the data set (Davis & Mauer, 2010; Ringnér, 2008). Multidimensionality is reduced neglecting the unimportant directions where samples variances are insignificant and defining directions called principal components (PCs) (Rusak et al., 2003). PCs are a new set of uncorrelated variables transformed from the original set of variables and contains maximal variation in the dataset. Mostly, >95% of the variance is maintained by the first few PCs. It investigates the variance-covariance or correlation structure of a sample set in vector form. Vectors composing variation are called eigenvectors (Tzeng & Berns, 2005). Principal components are independent (orthogonal) linear combinations of original variables. Sample variance of principal components is called eigenvalues and aligned with their magnitude. First principle component (PC) shows the largest amount of variation (in

eigenvalue) while the second largest variation is displayed by second principal component, along direction uncorrelated to the first component (Abdi et al., 2010; Al-Qadiri et al., 2008; Ami et al., 2012). The values used for detection of principal components are called factor scores, and these scores can be interpreted geometrically as the projections of the principal components. When factors are extracted, they account for less and less variability; data is reduced to a point in which there is only a minimal significant variability or to a merely random noise. As a result of the reduction of data, the new coordinate system is created. In this coordinate system, axes (eigenvectors) show the characteristic structure information of the data. Therefore PCA can be used to reduce a complex spectral data set into its most dominant components. It differentiates spectra consisting of hundreds of absorbance values without prior knowledge. The outcome of PCA presenting similarities and differences between the spectra is visualized as either two-dimensional (2D) (two PCs) or three-dimensional (3D) (three PCs) score plots. The pattern of similarity of the observations and the variables is also exhibited in PCA by displaying them as points in maps. Samples become closer with increasing similarity. Furthermore, PCA determines whether samples can be grouped or not (Davis & Mauer, 2010; Yu, 2005). The correlation between a component and a variable is known as loading. Loadings plots are used to determine which spectral regions provide the most significant contributions to data variation highlight the contribution of each variable (wavenumber) to each principal component. Large positive or negative loadings are related to spectral regions that are involved in sample differentiation (Abdi et al., 2010; Al-Qadiri et al., 2008).

1.4.2 Hierarchical Cluster Analysis (HCA)

Hierarchical cluster analysis (HCA) is one of the most used tools for the quick examination of complex spectral data of biological and medical samples. It is a ready, computerized instrument used for evaluating large sets of data for common characteristics. Therefore, cluster analysis can be used for discrimination of similarities between the spectra of cells by the help of the distances between spectra and aggregation algorithms.

Pearson product moment correlation coefficient and the Euclidian distance are mostly employed distances. Several algorithms such as Single-Linkage, Complete-Linkage, Average-Linkage, Weighted-Average-Linkage, Centroid, Median, have been developed for this purpose over the years. However, most popular algorithms used for clustering biological data are the Ward algorithm and average linkage algorithm (also called UPGMA, the unweighted pair group method with arithmetic mean) (Mariey et al., 2001). By using HCA, a complex set of observations are segregated into unique, mutually exclusive groups (clusters) of subjects similar to each other according to particular characteristics. Algorithms create a representative for each established cluster from the data set. Designated distance (or similarity) measures such as Euclidian distance or factorization are used for subsequent calculation of the distance between the clusters (Kniggendorf et al., 2011). Spectral data is separated into the most common spectral variations (factors, loadings, principal components) and the corresponding scores by using factorization which compresses the data and suppresses the noise. The arrangement of the clusters showing the relationships among different groups is visually represented by a dendrogram, tree diagram. Increasing variance or heterogeneity is displayed by the left vertical axis of a dendrogram. The number of spectra in a cluster and the similarities between them detect the magnitude of this heterogeneity (Chen et al., 2010; Davis & Mauer, 2010).

In our study, briefly, the ATR-FTIR spectroscopy monitored the overall chemical composition of the bacteria and generated highly specific whole-organism fingerprints. We analyzed our spectral data using unsupervised methods PCA and HCA. Therefore, we were able to evaluate molecular changes in bacterial strains acclimated to toxic concentrations of Cd and Pb.

1.5 Bacteriological Studies

Before subjected to ATR-FTIR spectroscopy, we acclimated environmental bacterial strains (*Brevundimonas* sp, *Gordonia* sp., and *M. oxydans*) to heavy metal (Cd and Pb) concentrations higher than their minimum inhibitory concentrations (MIC).

1.5.1 Minimum inhibitory concentration (MIC) Determinations

Minimum inhibitory concentration (MICs) is described as the lowest concentration of an antimicrobial agent including antibiotics, heavy metals, and other substances that kill (bactericidal) or inhibit the growth (bacteriostatic) of bacteria within a defined period of time (Andrews, 2001; Wiegand et al., 2008). In diagnostic laboratories, the MIC is mainly used to detect the resistance profile or to specify the in vitro activity of new antimicrobial agents (Andrews, 2001). The tested microorganism is classified as either clinically susceptible, intermediate or resistant to the antimicrobial agent. Different national organizations such as the Clinical and Laboratory Standards Institute (CLSI) in the USA and the European Committee on Antimicrobial Susceptibility Testing (EUCAST) publish the interpretative standards for these classifications. In the determination of the minimal inhibitory concentration (MIC), agar (solid growth media) dilution and broth (liquid growth media) dilution are the most commonly used techniques. In this study, we used broth dilution method to detect the minimum inhibitory concentration of Cd and Pb for *Brevundimonas* sp, *Gordonia* sp., and *Microbacterium oxydans*.

1.5.2 Broth dilution method

To detect MIC for an antimicrobial agent for any microorganism by broth dilution method, identical volumes of liquid growth media containing geometrically increasing concentrations (typically a twofold dilution series) of the antimicrobial agent are prepared. These media are inoculated with a defined number of bacterial cells. After incubation, the

presence of turbidity indicates growth of the bacteria (Figure 7). Then the MIC is defined as the lowest concentration ($\mu\text{g/ml}$ or mg/l) of the antimicrobial agent that completely prevents the visible growth of the microorganism under the defined conditions (Madigan et al., 2015; Wiegand et al., 2008).

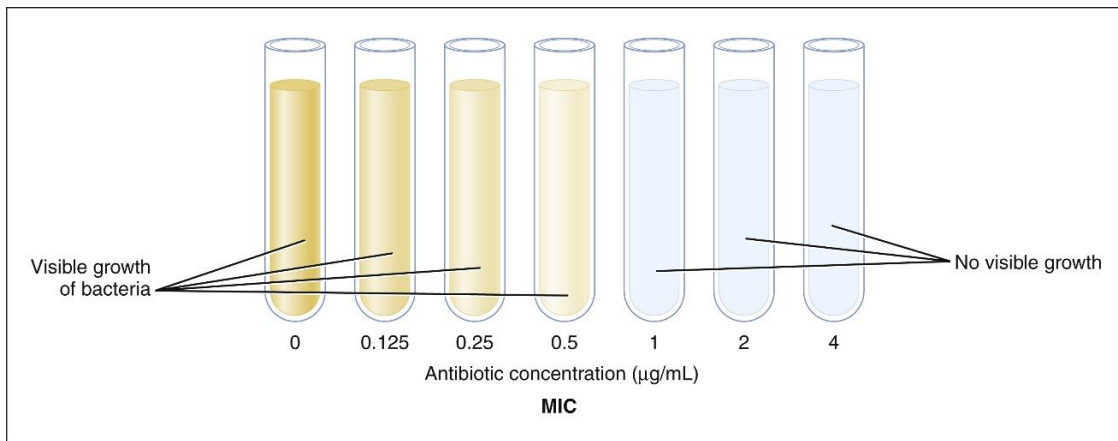


Figure 7. Detection of MIC by using broth dilution method

1. 5.3 Bacterial culture passaging

A particular strain or kind of organism growing in a laboratory medium is a culture. A subculture is called a passage. Any form of subculturing is considered to be a transfer/passage. The transfer of organisms from a viable culture (population of microorganisms) to fresh medium for the growth of the microorganisms is described as one passage. A small amount of initial culture is taken and added to another growth medium. When subculturing, microbes are transferred from one growth medium vessel, such as broth or agar medium, to another allowing the microbes to grow. Culture can be transferred from liquid to liquid, liquid to solid, or solid to solid media. By subculturing, microbes can be moved from one set of test parameters, such as temperature and media type, to another (U.S. Pharmacopeia, 2013).

1.5.4 Acclimation of bacterial strains to heavy metals

In our study, environmental strains were acclimated to heavy metal (Cd, Pb) concentrations higher than their corresponding MICs by sequential passaging. Increasing concentration of heavy metals was applied to acclimate bacterial strains predetermined metal concentration. During acclimation process, the amount of bacterial inoculum and volume of growth medium were kept constant. At every increasing concentration, bacteria were grown and subcultured (passaged) until the bacteria grow at a stable growth rate. Under the heavy metal exposure, growth slows down because of disruption of metabolic activities. During this period, bacteria may adjust its cell physiology to limit the distribution of heavy metal within the cell or to repair damages. That is why we passaged to bacterial strains to achieve a growth rate of fresh bacterial culture. For example, in a study done by Pagès et al. (2007) it was observed that when exposed to cadmium, *Pseudomonas brassicacearum* resumed the growth after long stasis period (lag phase of growth) (50 h). When Cd-exposed bacteria were inoculated directly into the Cd-containing medium, the lag phase was shortened to 26 h but remained much longer than the lag phase of the control in Cd-free medium (about 5 h). This situation was also seen in *E. coli* cells (Mitra et al., 1975).

1.6 Aim of the Study

Bacteria are capable of surviving, growing, getting acclimated and furthermore adapting to toxic Cd and Pb concentrations by using resistance mechanisms (section 1.2) (Nies, 1999). In their habitats, bacteria may be found very close to the source of the metal pollutant. In these cases, they are supposed to be experiencing acute exposures to the toxic concentrations of the metal. Alternatively, the bacteria may be situated at a distance from the pollution source. In this case, they may experience gradually increasing concentrations of the metal while metal is diffusing from the source. To become acclimated through either acute or gradual exposure, bacteria put one or more of its resistance mechanisms.

The process of acclimation occurs through several changes in structure, composition, and amounts of molecules (Harrison et al., 2007; Kamnev, 2008). These changes in the molecular profile of bacteria are affected by nature of acclimation (acute or gradual exposure to the heavy metal) which may lead to the formation of bacterial strains with different physiologies (Rouch et al., 1995; Liebert et al., 1991). From the application point of view, in bioremediation processes, acclimated bacteria are preferred, because acclimation leads to, for example, increase in production of metal complexing biopolymers (Kumar et al., 2011; Chang et al., 1995). Furthermore, bacteria can be genetically engineered to increase their biosorption capacity (Kermani et al., 2010; Kuroda et al., 2001; Singh et al., 2011; Valls et al., 2000; Valls & Lorenzo, 2002; Yoon & Pyo, 2003). To use bacteria in bioremediation applications and increase their biosorption capacity, it is important to select resistant microorganisms and to know which mechanisms are operational in the resistance (Hassan et al., 1999; Roosa et al., 2014; Xiong et al., 2015; Maynuad et al., 2014).

In this study, we aimed to determine differences in molecular profile changes between the acclimated bacterial cells which were acutely or gradually exposed to the heavy metals. We detected the extent of changes which may help the formation of resistant strains by using ATR-FTIR spectroscopy and evaluated the spectral data by taking chemometric approaches (PCA, HCA).

For this purpose, three environmental strains isolated from a freshwater source, *Brevundimonas* sp., *Gordonia* sp. and *Microbacterium oxydans*, were studied in the presence of Cd or Pb. By using two different acclimation procedures (acute, gradual), we tried to mimic the situation of being close to or distant from the source of heavy metals (Cd or Pb) for bacteria. The bacterial strains were acclimated to heavy metal (Cd or Pb) concentrations which were 2 to 4 times higher than their corresponding minimum inhibitory concentrations. Our results showed that the amount of lipid, protein, carbohydrate, nucleic acids changed.

In our study, we have shown for the first time that there were notable differences in molecular profiles of bacteria caused by nature of acclimation (acute, gradual). Moreover, the molecular profiles differed between the lead and cadmium acclimated bacteria. This

indicates that although the result is the acclimation to a certain condition, the way this acclimation achieved changes the current molecular status of the bacteria.

By using the knowledge that we have generated in this study different acclimation approaches may be taken to generate resistant bacterial strains with different physiological adaptations. We have seen that ATR-FTIR spectroscopy proves to be a useful tool in determining the molecular changes necessary for bacteria to acclimate themselves.

CHAPTER 2

MATERIALS AND METHODS

2.1 Bacterial strains

Three environmental strains, *Brevundimonas* sp., *Gordonia* sp. and *Microbacterium oxydans* were isolated from Lake Mogan, located in Ankara (Ozaktas et al., 2012). Their 16S rRNA sequences can be reached in NCBI GenBank database under accession numbers JF421706, JF421702, and JF421724 respectively.

2.2 Growth conditions

Bacterial strains were cultured in nutrient broth (5g/l of meat peptone and 3g/l meat extract, Merck) or nutrient agar (5 g of pancreatic digest of gelatin, 3 g of beef extract and 15 g/l agar, Becton Dickinson). Cadmium chloride (CdCl_2) stock solution was prepared by dissolving in distilled water (dH_2O). Lead nitrate ($\text{Pb}(\text{NO}_3)_2$) stock solution was prepared by first solubilizing in 1:10 diluted nitric acid (HNO_3) then dissolving in distilled water (metals from Sigma-Aldrich). Stock solutions were filter sterilized using 0.22 μm filters (Pall, USA). Before adding the metal solutions, growth media were autoclaved and cooled to 45-50 °C. Media dispersions and inoculations were performed in a laminar flow chamber (Esco, USA). The liquid cultures of bacterial strains were grown in an orbital shaker at 200 rpm under aerobic conditions at 28 °C (ZHWHY 200B, Zhicheng, CHINA). To determine the concentration of cells, the culture was serially diluted, then subsequently plated on nutrient agar (NA) and colony forming units (CFU) were counted. For each

culture, optical density (OD) were also measured at 600 nm. The working concentrations of bacteria were set at OD 0.5 which corresponded to 10^9 CFU/ml.

2.3. Determination of minimum inhibitory concentrations (MIC)

Broth dilution method was used to determine growth inhibition of bacterial strains (Table 5) as a result of metal exposure. Increasing concentrations of Cd (ranging between 0.5 and 100 $\mu\text{g/ml}$) and Pb (ranging between 5 and 500 $\mu\text{g/ml}$) were applied for all bacterial strains. Metal concentration (Cd, Pb) ranges for MIC studies were determined according to information obtained from literature (Bröker et al., 2004; Bröker et al., 2008; Jayanthi et al., 2016; Masoudzadeh et al., 2011; Masoudzadeh et al., 2014; Matyar et al., 2008). All experiments were conducted according to the rules specified by EUCAST (2003). All MIC studies were done in triplicates.

2.4 Acclimation of bacterial strains to cadmium and lead

The bacterial strains were acclimated to the Cd or Pb concentrations higher than their corresponding MIC values. Two different approaches were taken for acclimation studies; gradual versus acute. In the first approach (gradual), we subjected bacterial strains to gradually increasing Cd or Pb concentrations starting from the concentrations below the MIC values. At each metal concentration, several passages were made for bacterial cultures. Once the growth rate was stabilized, next concentration was then tried. Therefore, the cultures were supposed to be acclimated for desired metal concentration, when they show their maximal growth at the time that control reaches its maximal. In gradual acclimation for Cd, the concentrations were started from 5 $\mu\text{g/ml}$ and increased as multiples of 5 up to 30 $\mu\text{g/ml}$. The bacteria was acclimated to Pb upon gradual exposure similarly, but the concentrations were started from 20 $\mu\text{g/ml}$ and increased as 30, 40, 50, 60, 70, 80, and 90 $\mu\text{g/ml}$. In the second approach (acute), we subjected the bacteria to

higher concentrations as large pulses. Concentrations were begun from values higher than their MIC. At every concentration, bacterial strains were passaged several times until they reach their maximal growth rate. For Cd, the concentrations were applied as 20 and 30 $\mu\text{g/ml}$ at once, and for Pb as 45, 75, and 90 $\mu\text{g/ml}$. Number of passages could be seen in Tables 7, 8 as provided in section 3.2.

2.5 Bacteria Sample preparation for ATR-FTIR spectroscopy

Bacterial concentrations were standardized as OD 0.5 at 600 nm by using a spectrophotometer (UV-2600/2700, Shimadzu, Japan). After concentration adjustments, samples were centrifuged at 10,000 g for 10 min (Sigma 1-4 Microfuge, SciQuip, UK). Pellets were suspended in 15 μl of distilled water after removal of the supernatants. For each treatment in acute or gradual acclimation procedures, 10 samples were prepared (N=10). In tables and figures, “A” refers to the acute application of metals and “G” refers to the gradual application of metals (Table 1).

Table 1. Representations and numbers of samples for acute or gradual exposure procedures

Acute exposure		Gradual exposure	
Cadmium (Cd) / Lead (Pb)	Sample number	Cadmium (Cd) / Lead (Pb)	Sample number
<i>Brevundimonas</i> sp.-Cd(A)	10	<i>Brevundimonas</i> sp.-(G)	10
<i>Gordonia</i> sp.-Cd(A)	10	<i>Gordonia</i> sp.-Cd(G)	10
<i>M. oxydans</i> -Cd(A)	10	<i>M. oxydans</i> -Cd(G)	10
<i>Brevundimonas</i> sp.-Pb(A)	10	<i>Brevundimonas</i> sp.-Pb(G)	10
<i>Gordonia</i> sp.-Pb(A)	10	<i>Gordonia</i> sp.-Pb(G)	10
<i>M. oxydans</i> -Pb(A)	10	<i>M. oxydans</i> -Pb(G)	10

10 samples were also analyzed for each control (N=10). Controls were *Brevundimonas* sp., *Gordonia* sp. and *M. oxydans* cultures without metal exposure.

2.6 ATR-FTIR spectroscopy

IR spectroscopy measurements of bacterial samples were performed with Spectrum 100 FTIR spectrometer (PerkinElmer Inc., Norwalk, CT, USA) accompanied by an ATR equipment. To remove the atmospheric CO₂ and H₂O absorption bands of environmental air, air spectrum was used as background and automatically subtracted. Spectroscopic measurements of samples (5 μl) were conducted at 4 cm⁻¹ at room temperature. Before taking spectroscopic measurements, samples applied on a diamond/ZnSe crystal and were dried with a mild N₂ flux for 5 min. Then the samples were scanned between the ranges of 4000-650 cm⁻¹. From the same sample suspension (15 μl), three aliquots (5 μl each) were scanned as 100 times per aliquot and then averaged. Spectral data collection and manipulation were done with Spectrum 100 software (PerkinElmer).

2.7 IR Data Analysis

The second derivative of the spectrum was taken to increase the resolution of complex and overlapping bands as well as to determine the exact band positions by using Savitzky Golay algorithm. After taking the second derivatives, vector normalization of the spectral data was done. Absolute band intensities were calculated from the second derivative spectra with OPUS 5.5 software (Bruker Optics, GmbH).

2.8 Chemometric approaches

Complex spectral data can be analyzed by using multivariate statistical approaches. In this study, multivariate statistical analysis of ATR-FTIR spectra (chemometrics) was conducted by using unsupervised methods such as PCA and HCA. Those unsupervised methods let us extrapolate the spectral data without prior knowledge about the bacteria studied (Davis & Mauer, 2010; Wenning & Scherer, 2013).

2.8.1 Principle component analysis (PCA)

PCA reduces the multidimensionality of the data set into its most dominant components or scores while preserving most of the variation already exist in the data set (Davis & Mauer, 2010; Ringnér, 2008). Therefore, PCA can be used to evaluate and differentiate complex spectra consisting of hundreds of absorbance values by reducing it to one point in a multidimensional space (Wenning & Scherer, 2013). In our study, Unscrambler X software package (v. 10.0.1, Camo Software, Oslo, Norway) was used for PCA analysis of the spectral data obtained from bacterial strains. Followed by baseline correction, second derivatization, and vector normalization, the spectral data were subjected to PCA. PCA was employed to see the similarities and differences in the whole spectral region (4000-650 cm^{-1}), lipid region (3200-2800 cm^{-1}), protein region (1800-1500), and carbohydrate region (1200-900 cm^{-1}).

2.8.2 Hierarchical cluster analysis (HCA)

Hierarchical cluster analysis is used to define similarities among the spectra of samples with the help of the distances between spectra and aggregation algorithms. (Mariey et al., 2001). A dendrogram showing similarities between the spectra is generated. The dendrogram represents the arrangement of the clusters as an outcome of a clustering algorithm. The left vertical axis of a dendrogram exhibit the increasing variance or heterogeneity.

In our study, HCA was conducted by using by OPUS 5.5 software (Bruker Optics, GmbH). To find out spectral differences between 1) the heavy metal exposed and control, 2) acutely and gradually acclimated bacteria, vector normalized, second derivatized spectral data were used as input for HCA. The HCA analysis was applied to lipid, protein, carbohydrate and whole spectral regions. Results were visualized as dendrograms which represent the arrangement of clusters in two dimensions by graphical means. Ward's algorithm along with Euclidian distances was used to create the dendrograms. Sample

similarities were calculated by the help of Euclidean distance. The Ward's algorithm allowed clustering homogeneous samples as much as possible by collecting the spectra as the smallest distance in variance (Lasch et al., 2004; Severcan et al., 2010). Sensitivity and specificity values were acquired from the results of HCA (Tables 2, 3, 4). The sensitivity evaluates the ratio of real positives which are correctly defined. For instance, the percentage of the acutely acclimated bacteria (Cd or Pb) as being in the defined acutely acclimated group. On the other hand, the specificity evaluates the ratio of correctly defined negatives. For instance, the percentage of control bacteria defined as being not in the acclimated clusters (Table 2) (Severcan et al., 2010).

Table 2. Definitions for sensitivity and specificity for hierarchical cluster analysis based on FTIR data for acute acclimation

Cluster analysis results based on FT-IR data

	Positive (Cd or Pb)	Negative (Cd or Pb)	
Acute	A	B	Sensitivity= A/A+B
Control	C	D	Specificity= D/C+D

A: The number of acutely acclimated (for Cd or Pb) bacteria clustered in acutely acclimated group (true positive)

B: The number of acutely acclimated (for Cd or Pb) bacteria clustered in control group (false negative)

C: The number of control bacteria clustered in acutely or gradually acclimated (for Cd or Pb) group (false positive)

D: The number of control bacteria clustered in control group (true negative)

Table 3. Definitions for sensitivity and specificity for hierarchical cluster analysis based on FTIR data for gradual acclimation

Cluster analysis results based on FT-IR data

	Positive (Cd or Pb)	Negative (Cd or Pb)	
Gradual	E	F	Sensitivity= $E/E+F$
Control	C	D	Specificity= $D/C+D$

E: The number of gradually acclimated (for Cd or Pb) bacteria clustered in gradually acclimated group (true positive)

F: The number of gradually acclimated (for Cd or Pb) bacteria clustered in control group (false negative)

C: The number of control bacteria clustered in acutely or gradually acclimated (for Cd or Pb) group (false positive)

D: The number of control bacteria clustered in control group (true negative)

Table 4. Definitions for sensitivity and specificity for hierarchical cluster analysis based on FTIR data for acute and gradual acclimation

Cluster analysis results based on FT-IR data

	Positive (Cd or Pb)	Negative (Cd or Pb)	
Acute	G	H	Sensitivity= $G/G+H$
Gradual	J	K	Specificity= $K/J+K$

G: The number of acutely acclimated (for Cd or Pb) bacteria clustered in acutely acclimated group (true positive)

H: The number of acutely acclimated (for Cd or Pb) bacteria clustered in gradually acclimated group (false negative)

J: The number of gradually acclimated (for Cd or Pb) bacteria clustered in acutely acclimated group (false positive)

K: The number of gradually acclimated (for Cd or Pb) bacteria clustered in gradually acclimated group (true negative)

2.9 Statistics

The results were displayed as means (\pm SEM). One way ANOVA test (GraphPad Software, Inc.) was used for comparison of acclimated bacterial strains (group A and group G) with control groups under the exposure of cadmium or lead. Also, acclimated groups were compared with each other. Absolute intensities of the spectral bands in the control groups were taken as 100 and intensities of acclimated groups were corrected proportional to that. A *p-value* of less than 0.05 was considered statistically significant. Degrees of significance were denoted as $p < 0.05^*$, $p < 0.01^{**}$, $p < 0.001^{***}$, $p < 0.0001^{****}$.

CHAPTER 3

RESULTS AND DISCUSSION

3.1. Minimum Inhibitory Concentrations (MIC) for bacterial strains

Minimum inhibitory Cd concentrations were 15 µg/ml (82 µM) for *Brevundimonas* sp. and *M. oxydans*, 10 µg/ml (54.5 µM) for *Gordonia* sp. (Table 5). Results indicated that *Brevundimonas* sp. and *M. oxydans* strains were more resistant than *Gordonia* sp. to Cd. For Pb the MIC values were 35 µg/ml (106 µM), 22.5 µg/ml (68 µM) and 37.5 µg/ml (113 µM) for *Brevundimonas* sp., *Gordonia* sp. and *M. oxydans*, respectively (Table 5). As it was shown that *M. oxydans* was the most resistant strain to Pb.

Table 5. Minimum inhibitory Cd and Pb concentrations for environmental strains

Bacteria Strains	MIC	
	Cadmium (Cd) µg/ml	Lead (Pb) µg/ml
<i>Brevundimonas</i> sp.	15	35
<i>Gordonia</i> sp.	10	22.5
<i>M. oxydans</i>	15	37.5

In the literature, different MIC values have been reported. The MIC ranges for Cd or Pb exposed *Brevundimonas* sp., *Gordonia* sp., and *M. oxydans* are given in Table 6. All studies mentioned in Table 6 were conducted on bacteria isolated from different

polluted environments. Therefore, MIC difference between previous studies and ours may be caused by differences in environments where the samples had been derived, in media composition or growth conditions as well as strain (Kardas et al., 2014).

Table 6. Minimum inhibitory Cd and Pb concentrations in the related literature

Bacteria Strains	MIC		References
	Cd ($\mu\text{g/ml}$)	Pb ($\mu\text{g/ml}$)	
<i>Brevundimonas</i> sp.	5-50	5- > 20	Masoudzadeh et al., 2011 Masoudzadeh et al., 2014 Jayanthi et al., 2016
<i>Gordonia</i> sp.	25-3200	12.5-3200	Bröker et al., 2004, 2008 Matyar et al., 2008
<i>M. oxydans</i>	91-910	365-2745	Nedelkova et al., 2007 Sanchez et al., 2016 Abou-Shanab et al., 2007

3.2 Acclimation of bacterial strains for cadmium or lead

In this step of our study, *Brevundimonas* sp., *Gordonia* sp. and *M. oxydans* strains were acclimated to grow in Cd or Pb-containing media upon gradual or acute exposure. Because resistance levels differed among bacteria when exposed to Cd or Pb, the concentrations evaluated and the number of passage were adjusted for each bacterial strains. Applied concentrations of heavy metals and number of passages are given in Tables 7 and 8. The gradual acclimation procedures for Cd and Pb are presented in Tables 7A and 7B, respectively. Table 8A and 8B show acute acclimation procedures for Cd and Pb, respectively.

Table 7. Gradual acclimation of bacterial strains to Cd or Pb

A

Gradual acclimation of bacterial strains to Cd through subculturing

Concentrations ($\mu\text{g/ml}$)	Number of passages for the Bacteria		
	<i>Brevundimonas</i> sp.	<i>Gordonia</i> sp.	<i>M. Oxydans</i>
5	1	2	1
10	3	4	3
15	4	4	4
20	4	4	4
25	4	4	4
30	7	7	7

B

Gradual acclimation of bacterial strains to Pb through subculturing

Concentrations ($\mu\text{g/ml}$)	Number of passages for the Bacteria		
	<i>Brevundimonas</i> sp.	<i>Gordonia</i> sp.	<i>M. Oxydans</i>
20	-	2	-
30	2	3	2
40	4	4	4
50	4	4	4
60	4	4	4
70	4	4	4
80	4	4	4
90	7	7	7

Table 8. Acute acclimation of bacterial strains for heavy metals

A

Acute acclimation of bacterial strains to Cd through subculturing

Concentrations ($\mu\text{g/ml}$)	Number of passages for the Bacteria		
	<i>Brevundimonas</i> sp.	<i>Gordonia</i> sp.	<i>M. Oxydans</i>
20	7	8	7
30	10	10	10

B

Acute acclimation of bacterial strains to Pb through subculturing

Concentrations ($\mu\text{g/ml}$)	Number of passages for the bacteria		
	<i>Brevundimonas</i> sp.	<i>Gordonia</i> sp.	<i>M. oxydans</i>
45	7	8	7
75	7	7	7
90	10	10	10

3.3. ATR-FTIR spectroscopy

FTIR spectroscopy has been used for characterization and identification of microbial cells for about four decades (Davis et al., 2010; Garip et al., 2009; Helm & Naumann, 1995; Naumann et al., 1988; Wenning & Scherer, 2013). IR spectroscopy has been proved to be a useful tool for detection of molecular changes including alterations in structure, composition, and quantities of proteins, carbohydrates, lipids and nucleic acids caused by metal exposure (Choudhary & Sar, 2009; Kamnev, 2008; Kardas et al., 2014). ATR-FTIR spectra give information on qualities as well as quantities of the molecules subjected to change under a given set of condition. One such spectrum is shown in Figure 8 to demonstrate a general ATR-FTIR recording in the case of *Gordonia* sp. Band assignments were done according to the related literature (Table 9).

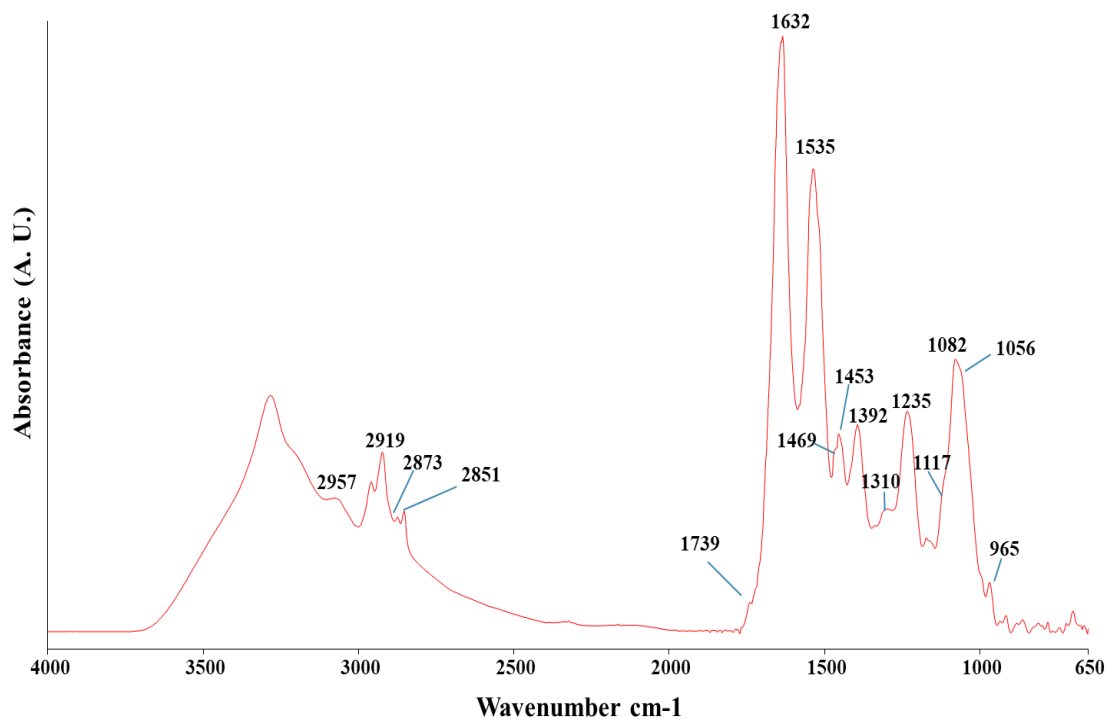


Figure 8. A representative ATR-FTIR spectrum of *Gordonia* sp. showing band assignments in the 4000-650 cm⁻¹ region

Table 9. General band assignments in the spectrum obtained from bacteria

Wave number (cm^{-1})	Types of molecular vibrations
2957	CH ₃ antisymmetric stretching of fatty acids
2919	CH ₂ antisymmetric stretching of mainly lipids
2873	CH ₃ symmetric stretching of mainly proteins
2851	CH ₂ symmetric stretching of mainly lipids
1739	Ester CO stretching of triglycerides and cholesterol esters
1632	Amide I: mainly CO stretching of proteins
1535	Amide II: N–H bending, C–N stretching of proteins
1469	CH ₂ scissoring: lipids
1453	CH ₂ bending of lipids
1392	COO [–] symmetric stretching of fatty acids
1310	CO stretching of carboxylic acids: exopolymer formation
1235	PO ₂ [–] antisymmetric stretching of mainly nucleic acids
1117	CC symmetric stretching of RNA ribose
1082	PO ₂ symmetric stretching of nucleic acids and phospholipids
1056	C–O–C, P–O–C symmetric stretching of polysaccharides
965	RNA and DNA backbone CC stretching of nucleic acids

In the present study, we performed ATR-FTIR spectroscopy to detect molecular alterations in two acclimation groups of the bacteria. One group was acclimated through acute high concentrations of heavy metals. The other group was acclimated through a gradual increase in heavy metal concentrations. Both groups were compared to their corresponding controls. Representative IR spectra of Cd or Pb acclimated *Brevundimonas* sp. (acute or gradual) and control groups in the 4000-650 cm^{-1} spectral region is given in Figure 9. Similar representative IR spectra for other working groups are given in Appendix

A1-A5. To evaluate heavy metal concentration-related changes, the second derivative of spectra were used to increase the resolution of broad spectral bands. The second derivatization lets the overlapping peaks be resolved, and spectral bands be discriminated. Then spectra were vector normalized. Figures 10A, B, and C show representative second derivative, vector normalized, average spectra of the control *Brevundimonas* sp., *Gordonia* sp. and *M. oxydans* in the 3000-2800, 1800-1350 and 1350-900 cm^{-1} regions, respectively.

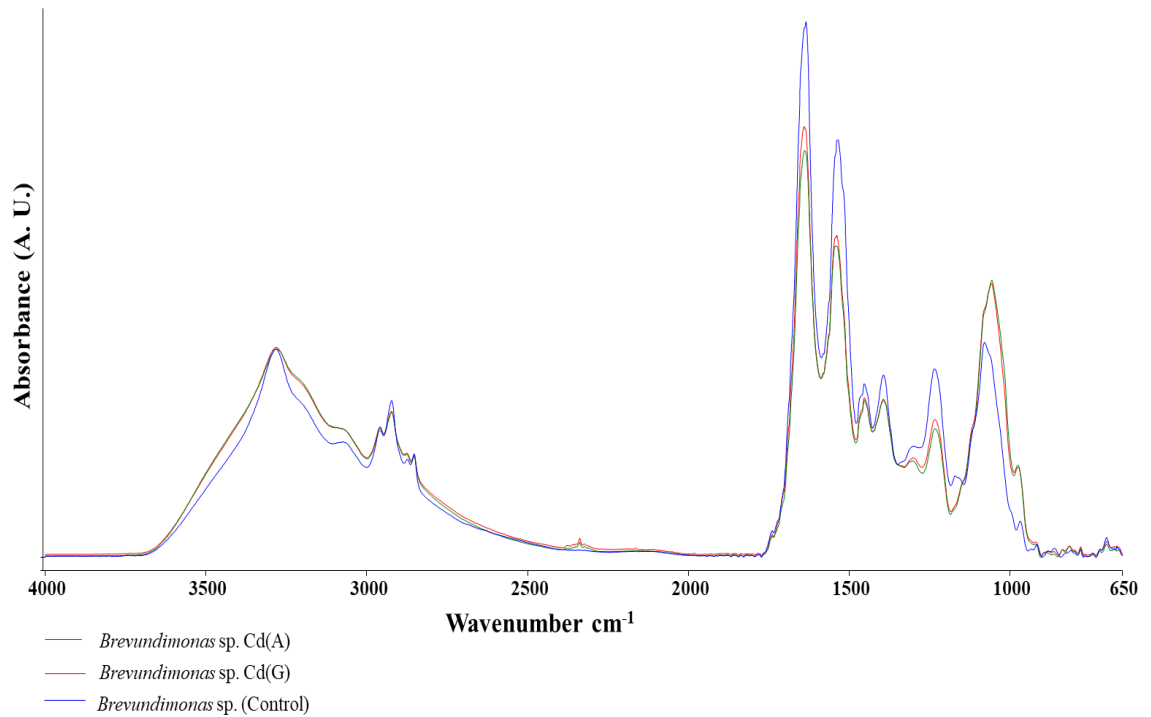
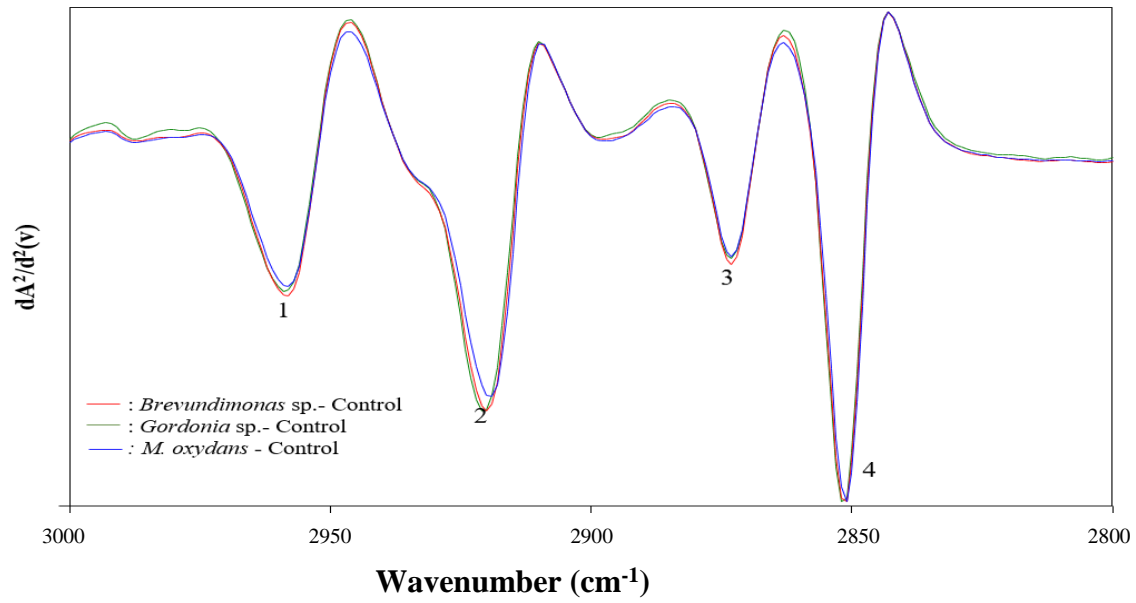
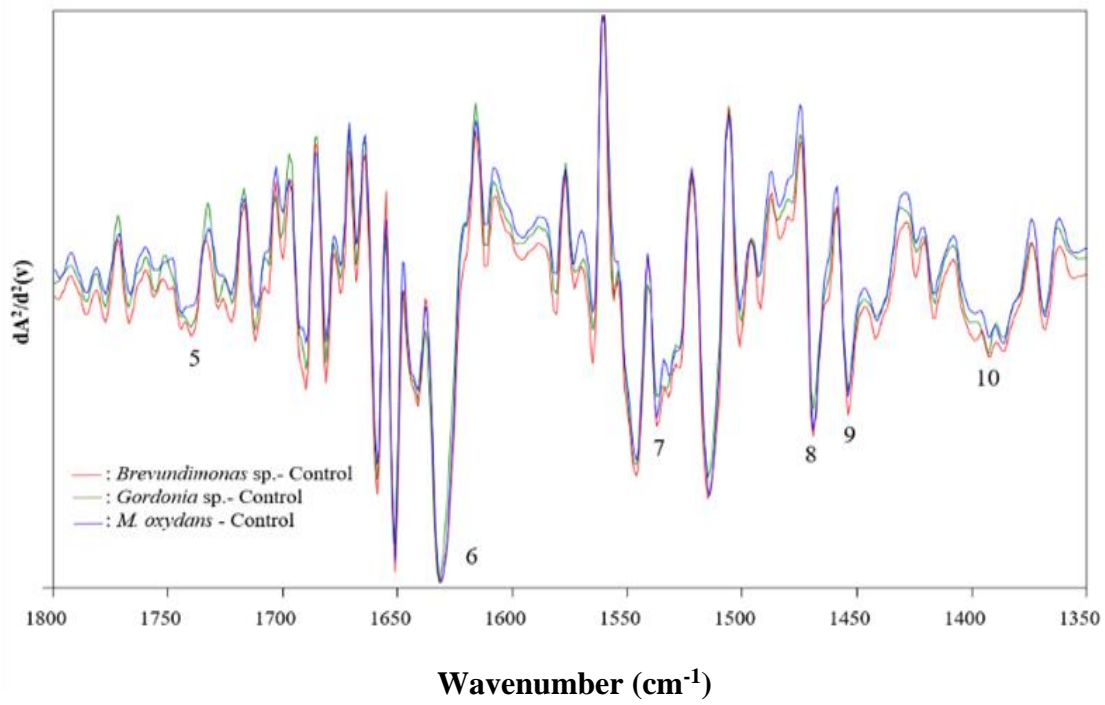


Figure 9. ATR-FTIR spectra of Cd-acclimated (acute: A, gradual: G) and control groups of *Brevundimonas* sp. in the 4000-650 cm^{-1} spectral region

A



B



C

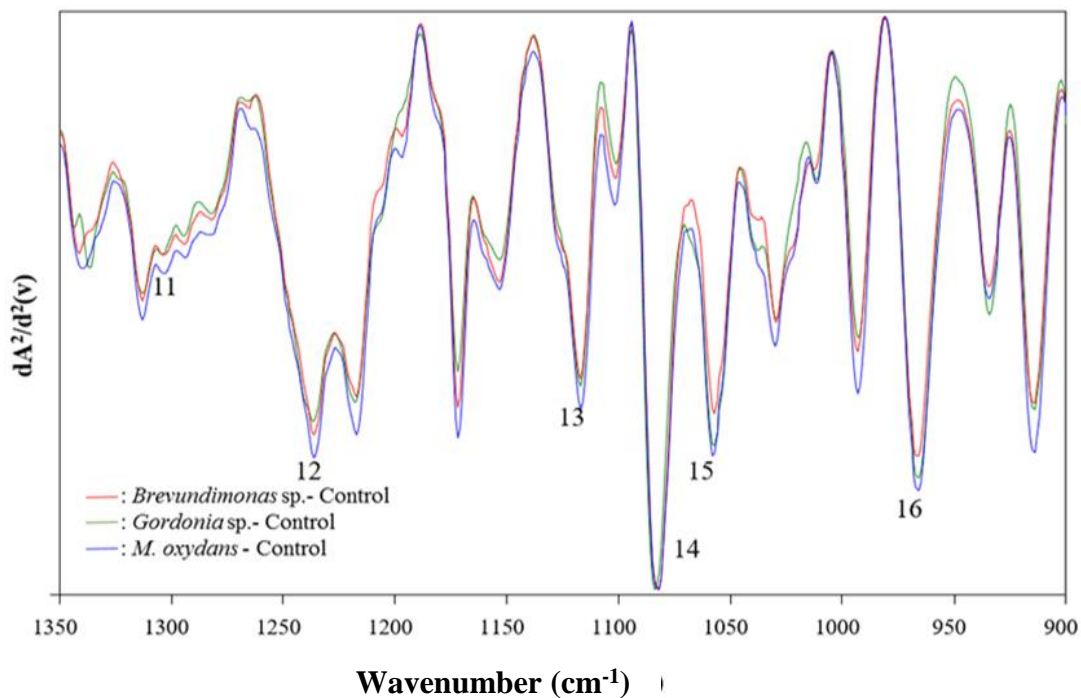


Figure 10. Representative second derivative, vector normalized, average spectra of controls without metal exposure; **A-** 3000-2800 cm^{-1} , **B-** 1800-1350 cm^{-1} , and **C-** 1350-900 cm^{-1} regions

Figures 11, 12 and 13 (A, B, C for Cd and D, E, F for Pb) show representative second derivative, vector-normalized, average spectra of the acclimated (acute or gradual) and control groups of *Brevundimonas sp.*, *M. oxydans* and *Gordonia sp.* in the 3000-2800, 1800-1350 and 1350-900 cm^{-1} regions, respectively. As a result of Cd or Pb exposure, changes in the intensities, band shapes and wave number values of spectral bands can be deduced from these figures.

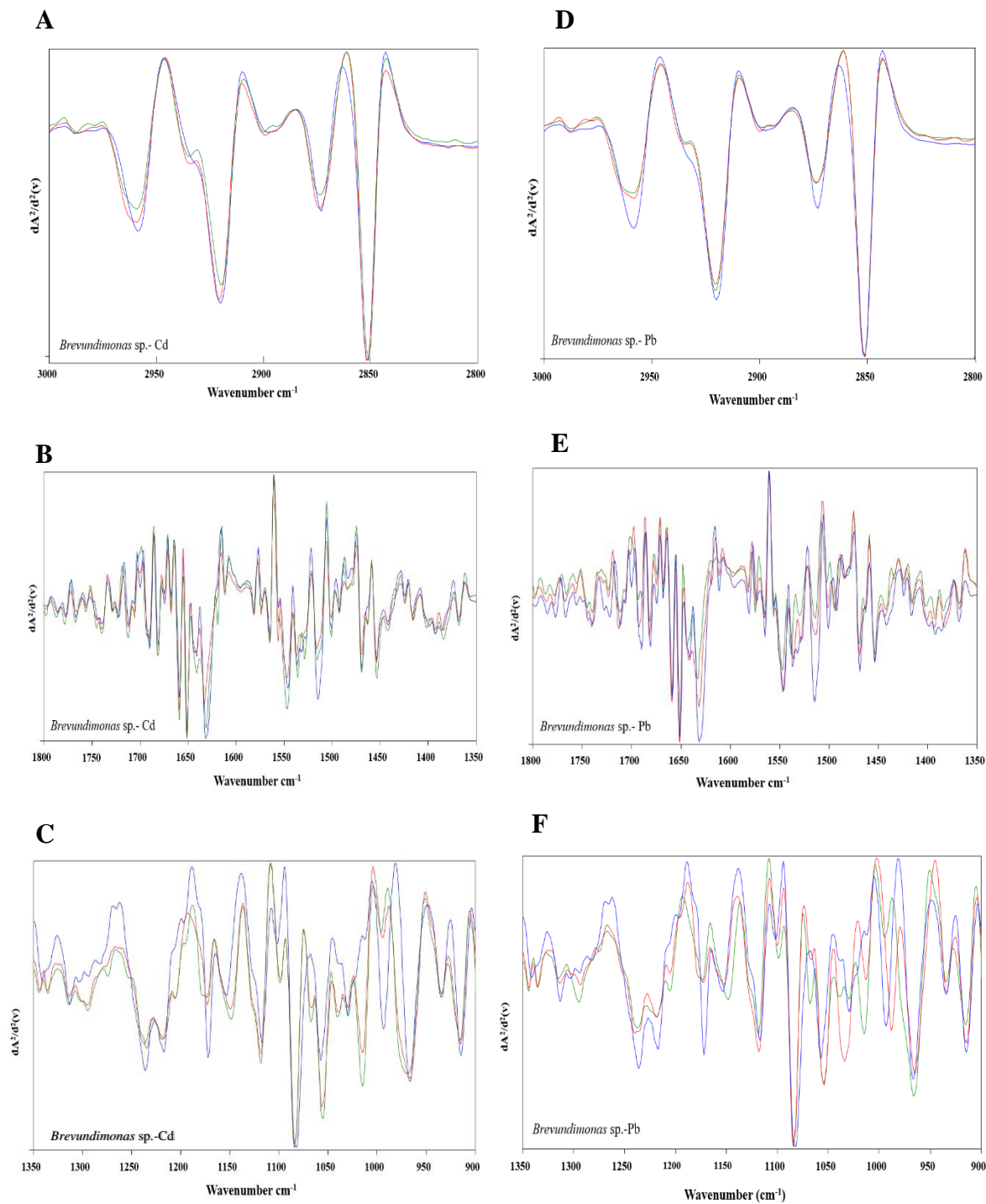


Figure 11. Representative second derivative, vector-normalized, average spectra of the acclimated (acute: A, gradual: G) and control groups of *Brevundimonas* sp. (A-F) in the presence of Cd or Pb; — ; Acute, — ; Gradual, — ; Control

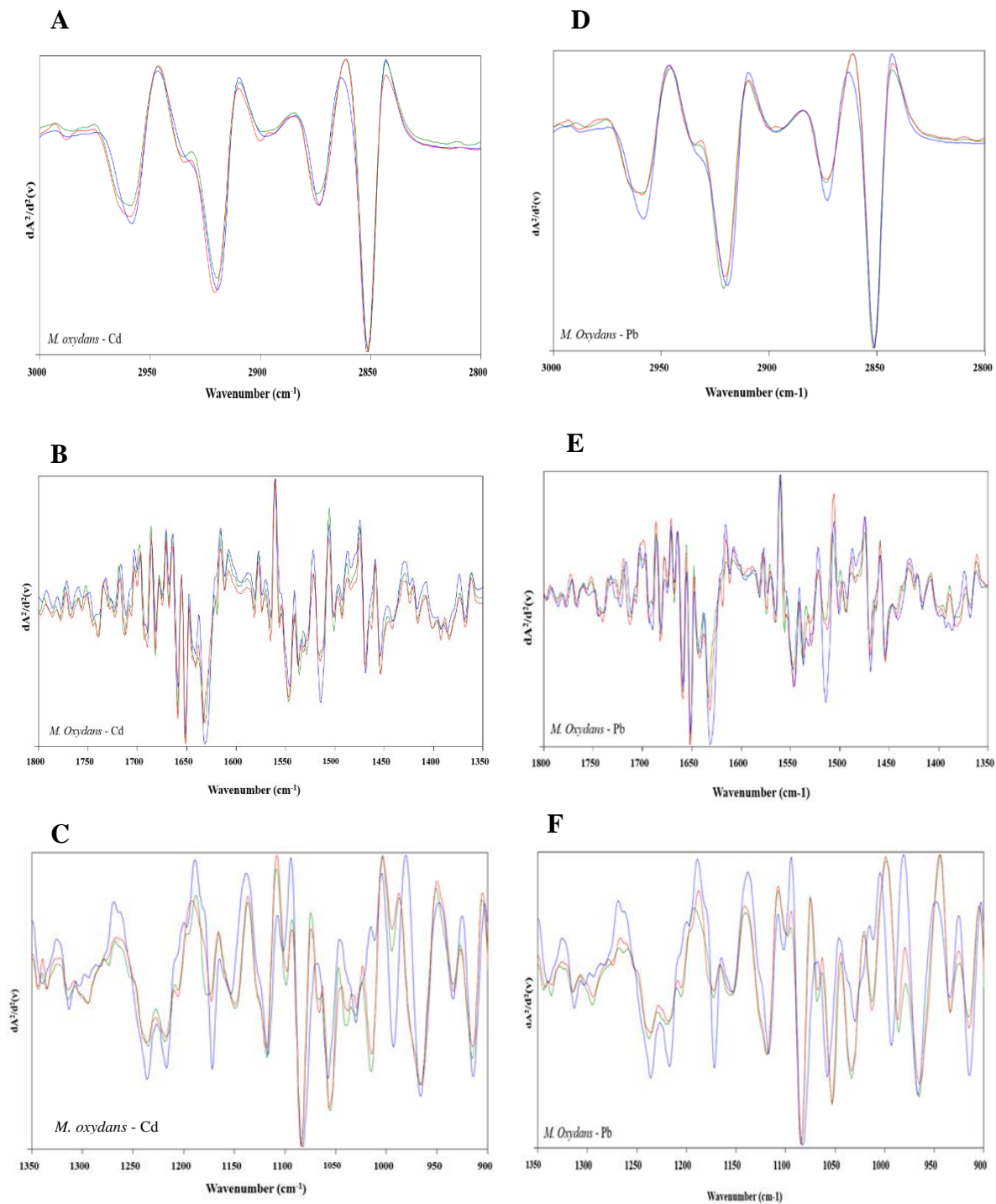


Figure 12. Representative second derivative, vector-normalized, average spectra of the acclimated (acute: A, gradual: G) and control groups of *M. oxydans* (A-F) in the presence of Cd or Pb — green ; Acute, — red ; Gradual, — blue ; Control

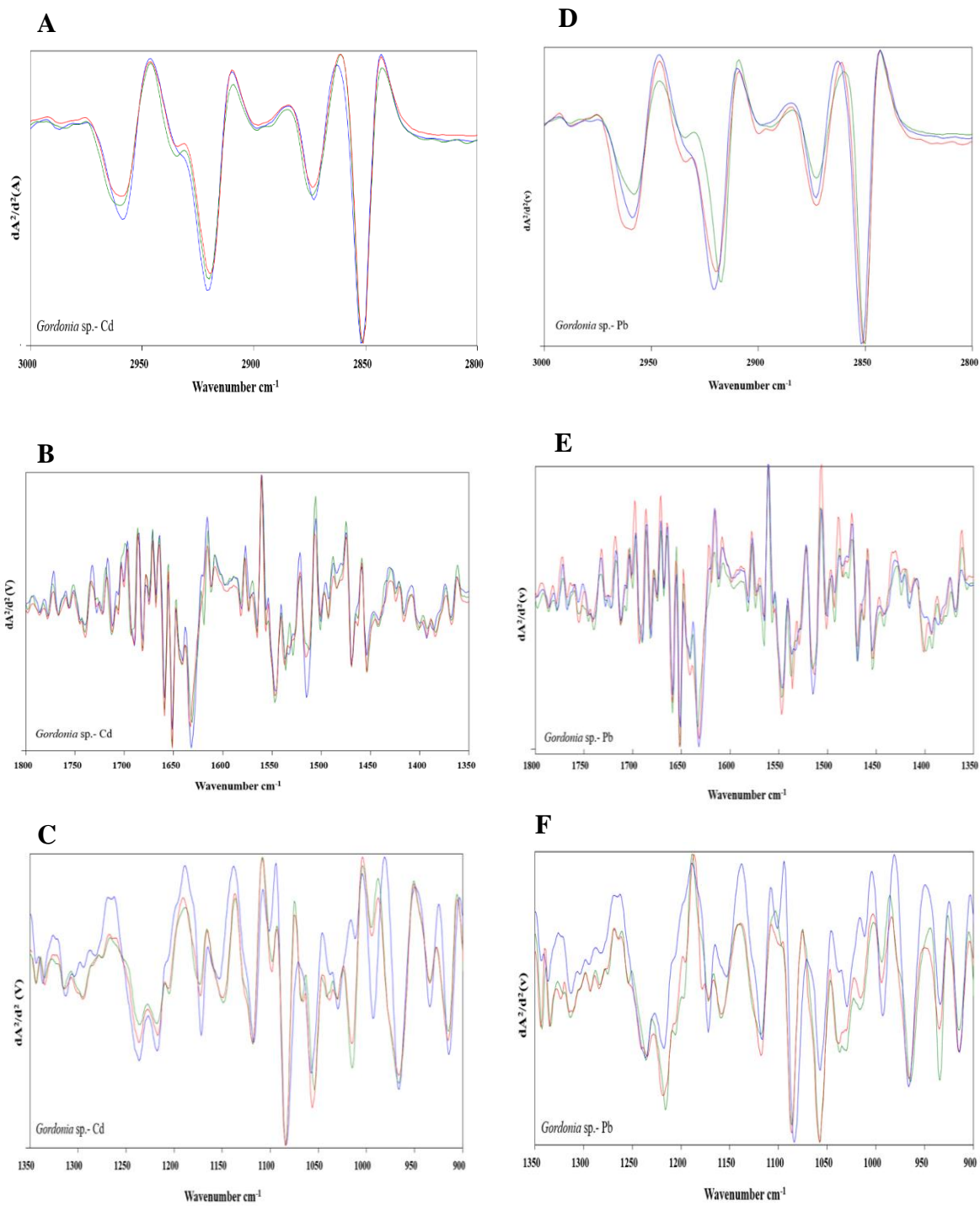


Figure 13. Representative second derivative, vector-normalized, average spectra of the acclimated (acute: A, gradual: G) and control groups of *Gordonia sp.* (A-F) in the presence of Cd or Pb — green ; Acute, — red ; Gradual, — blue ; Control

Absorption intensity of spectral bands gives information about the concentration of the functional groups belonging to proteins, carbohydrates, lipids and nucleic acids (Cakmak et al., 2003; Cakmak et al., 2006; Ozek et al., 2010). As a consequence of Cd or Pb acclimation, significant differences in the spectral band intensities occurred. These differences in the 3000-900 cm^{-1} spectral region are given in Tables 10, 11 and 12 for *Brevundimonas* sp., *Gordonia* sp., and *Microbacterium oxydans*, respectively.

Table10. The changes in spectral band intensities in Cd or Pb acclimated *Brevundimonas* sp. with respect to control group; A; acute, G; gradual

Wave Number (cm^{-1})	Spectral band intensities of <i>Brevundimonas</i> sp.				
	Cadmium (A)	Cadmium (G)	Control	Lead (A)	Lead (G)
2956	79.783 ± 2.237****	81.837 ± 0.756****	100 ± 2.132	61.729 ± 0.874****	70.918 ± 1.034****
2919	96.401 ± 1.394*	97.636 ± 0.365	100 ± 0.783	103.651 ± 0.438**	98.865 ± 0.94
2873	84.534 ± 2.418****	96.461 ± 0.856	100 ± 1.833	74.345 ± 0.697****	56.675 ± 1.852****
2851	106.651 ± 1.735**	101.508 ± 0.5	100 ± 1.589	108.662 ± 0.377****	108.623 ± 0.436****
1739	121.5 ± 7.785	146.5 ± 4.285****	100 ± 8.658	149 ± 8.225***	159 ± 4.876****
1632	81.009 ± 1.366****	84.416 ± 1.547****	100 ± 2.452	70.41 ± 4.214****	73.817 ± 0.664****
1535	100.964 ± 1.007	98.071 ± 3.453	100 ± 2.449	118.595 ± 4.214***	93.801 ± 1.035
1469	89.322 ± 1.415****	88.411 ± 0.627****	100 ± 0.795	93.88 ± 1.122**	80.468 ± 1.632****
1453	115.572 ± 2.17****	119.847 ± 2.453****	100 ± 1.496	127.328 ± 2.674****	107.175 ± 0.814*
1392	79.651 ± 3.552****	92.732 ± 1.011	100 ± 1.162	115.988 ± 5.209	100.29 ± 6.284
1310	155.555 ± 7.408****	169.4444 ± 4.986****	100 ± 4.536	280.555 ± 48.027***	188.888 ± 5.555
1235	96.837 ± 2.584	86.561 ± 0.922***	100 ± 2.045	99.604 ± 2.485	111.067 ± 2.315**
1117	158.1 ± 3.729****	136.871 ± 2.082****	100 ± 1.002	144.134 ± 4.982****	195.53 ± 5.77****
1082	149.767 ± 3.781****	139.069 ± 1.028****	100 ± 1.801	182.093 ± 3.023****	188.372 ± 3.553****
1056	238.565 ± 3.828****	200.896 ± 1.609****	100 ± 2.593	225.112 ± 4.109****	240.807 ± 4.632****
965	99.644 ± 8.252	114.234 ± 2.085	100 ± 2.513	192.882 ± 10.882****	170.462 ± 5.871****

Table 11. The changes in spectral band intensities in Cd or Pb acclimated *Gordonia* sp. with respect to the control group; A; acute G; gradual

Wave Number cm ⁻¹	Spectral band intensities of <i>Gordonia</i> Sp.				
	Cadmium (A)	Cadmium (G)	Control	Lead (A)	Lead (G)
2956	80.471 ± 1.11****	74.298 ± 1.226****	100 ± 3.156	92.783 ± 3.408	102.502 ± 2.215
2919	96.96 ± 0.318	96.919 ± 0.872	100 ± 1.564	101,169 ± 4.315	86.018 ± 0.909***
2873	98.209 ± 0.741	94.903 ± 3.21	100 ± 2.874	92.286 ± 4.132	102.341 ± 2.932
2851	105.088 ± 0.514*	107.054 ± 1.946**	100 ± 0.732	114.070 ± 3.022****	99.036 ± 2.67
1739	138 ± 6.55**	162.5 ± 4.487****	100 ± 11.785	142.5 ± 5.23**	109 ± 8.425
1632	77.736 ± 0.702****	86.889 ± 1.74****	100 ± 1.931	85.961 ± 0.962****	84.662 ± 0.795****
1535	102.647 ± 1.365	101.176 ± 3.388	100 ± 3.835	122.941 ± 4.28***	131.617 ± 3.148****
1469	95.294 ± 0.814	101.47 ± 2.02	100 ± 6.58	98.97 ± 2.622	73.382 ± 2.241***
1453	123.559 ± 1.055****	128 ± 1.715****	100 ± 3.145	128.474 ± 2.242****	106.61 ± 3.13
1392	65.721 ± 2.437****	84.536 ± 1.374****	100 ± 2.025	127.577 ± 3.587****	97.422 ± 5.079
1310	165.789 ± 4.021****	160.526 ± 6.366****	100 ± 5.263	300 ± 26.081****	215.789 ± 9.447****
1235	85.401 ± 1.354***	94.525 ± 3.46	100 ± 1.114	96.715 ± 5.967	91.605 ± 2.69
1117	147.169 ± 2.201****	112.735 ± 4.066**	100 ± 1.17	66.981 ± 2.31****	111.32 ± 2.741**
1082	167.237 ± 2.079****	139.186 ± 2.513****	100 ± 3.111	108.993 ± 1.254*	115.417 ± 1.702****
1056	177.926 ± 1.518****	169.899 ± 3.065****	100 ± 7.484	190.301 ± 2.362****	188.963 ± 4.026****
965	142.939 ± 3.988****	108.357 ± 4.994	100 ± 2.469	100.576 ± 2.484	97.118 ± 3.412

Table 12. The changes in spectral band intensities in Cd or Pb acclimated *M. oxydans* with respect to the control group; A; acute G; gradual

Wave Number (cm ⁻¹)	Spectral band intensities of <i>M. oxydans</i>				
	Cadmium (A)	Cadmium (G)	(Control)	Lead (A)	Lead (G)
2956	79.249 ± 1.859****	81.145 ± 0.768****	100 ± 3.897	63.686 ± 0.772****	72.847 ± 0.916****
2919	94.619 ± 1.602*	97.389 ± 0.777	100 ± 1.825	104.315 ± 0.235*	97.815 ± 0.963
2873	85.771 ± 2.259*	95.973 ± 1.911	100 ± 4.889	74.228 ± 1.401****	64.832 ± 2.669****
2851	104.828 ± 1.593	100.678 ± 0.513	100 ± 2.771	105.733 ± 0.463	107.061 ± 2.058*
1739	209.285 ± 12.685***	220.714 ± 4.185****	100 ± 8.826	158.671 ± 10.364****	192.657 ± 8.25****
1632	77.538 ± 1.085****	83.753 ± 1.106****	100 ± 2.211	81.6 ± 1.342****	76.43 ± 1.024****
1535	96.124 ± 1.236	86.95 ± 3.369**	100 ± 3.153	108.656 ± 3.259	89.534 ± 1.388*
1469	75.451 ± 1.412****	81.347 ± 1.123***	100 ± 4.392	77.256 ± 1.421****	75.451 ± 1.281****
1453	115.764 ± 1.234***	122.292 ± 2.079****	100 ± 3.848	131.21 ± 2.375****	112.42 ± 1.346**
1392	71.81 ± 2.202****	108.308 ± 2.392*	100 ± 1.535	73.9 ± 3.614****	74.48 ± 3.842****
1310	136.842 ± 3.507****	173.684 ± 4.297****	100 ± 5.263	310.526 ± 25.963****	271.052 ± 11.13****
1235	94.346 ± 1.828	84.452 ± 1.702***	100 ± 3.206	92.932 ± 3.028	96.113 ± 1.956
1117	141.148 ± 4.294****	117.703 ± 1.626***	100 ± 2.516	149.282 ± 1.717****	161.722 ± 3.173****
1082	161.848 ± 3.604****	149.289 ± 1.413****	100 ± 2.753	177.251 ± 1.759****	190.521 ± 1.875****
1056	194.16 ± 2.359****	178.632 ± 2.929****	100 ± 3.273	201.824 ± 4.868****	215.328 ± 1.884****
965	128.086 ± 4.629***	118.209 ± 4.438*	100 ± 3.228	163.58 ± 3.904****	159.259 ± 4.808****

The 3000-2800 cm^{-1} spectral region contains the C-H stretching dominated by lipid-associated bands including CH_3 antisymmetric stretching of fatty acids, CH_2 antisymmetric and CH_2 symmetric stretching of lipids (Helm et al., 1991; Naumann et al., 1995). As a result of Cd acclimation, the intensity of the CH_3 antisymmetric stretching band at 2956 cm^{-1} significantly ($P < 0.0001$) decreased in all heavy metal acclimated *Brevundimonas* sp., *Gordonia* sp. and *Microbacterium oxydans* with respect to their corresponding control groups. These results were supported by another fatty acid associated spectral band at 1392 cm^{-1} except for gradual Cd-acclimated *M. oxydans* (Tables 10, 11, 12). In the Pb-acclimated bacterial groups, except in *Gordonia* sp. (acute, gradual), the intensity of the CH_3 antisymmetric stretching band remarkably reduced ($P < 0.0001$) (Tables 10, 11, 12). Similarly, the intensity of the COO^- symmetric stretching at 1392 cm^{-1} was low for only Pb-acclimated (acute, gradual) *M. oxydans* groups (Table 12). In Pb-acclimated *Gordonia* sp. (acute, gradual) the CH_3 antisymmetric stretching band was not different. However, the intensity of the COO^- symmetric stretching band (1392 cm^{-1}) remarkably increased in acutely Pb-acclimated *Gordonia* sp. ($P < 0.0001$) (Table 11) while no change was recorded for gradually acclimated counterparts. The significant decreases in intensities of spectral bands in 2956 cm^{-1} and 1392 cm^{-1} suggested a reduction in the amount of lipids and change in the composition of the acyl chains. Figure 14 represents significant changes in the intensity of the CH_3 antisymmetric stretching band that occurred as a result of Cd (A, C, E) or Pb (B, D) exposures.

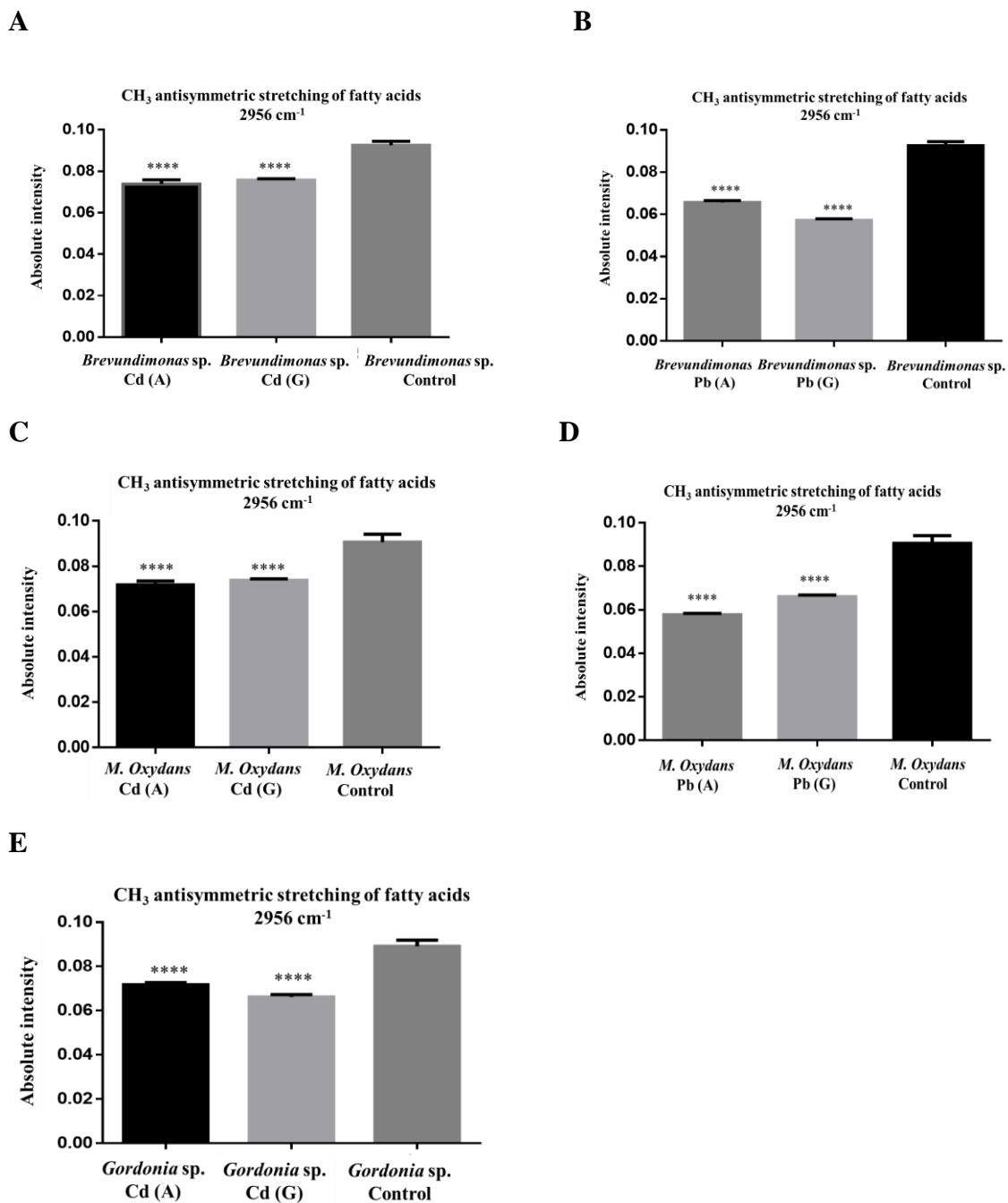


Figure 14. The CH₃ antisymmetric stretching band intensities of Cd (A, C, E) or Pb (B, D) acclimated and control groups of *Brevundimonas sp.*, *Gordonia sp.* and *M. oxydans*

The CH₂ antisymmetric stretching at 2919 cm⁻¹ and the CH₂ symmetric stretching at 2851 cm⁻¹ are associated with saturated lipid concentration of membranes. Therefore, it affects membrane fluidity (Kardas et al., 2014; Markovicz et al., 2010). Decreases at 2919 cm⁻¹ were significant ($P<0.05$) in acutely acclimated *Brevundimonas* sp. and *M. oxydans* while increases at 2851 cm⁻¹ were significant ($P<0.05$) in acutely acclimated *Brevundimonas* sp. and both acclimation groups of *Gordonia* sp. (Tables 10, 11, 12). In acutely Pb-acclimated *Brevundimonas* sp. and *M. oxydans* groups, the intensity of the CH₂ antisymmetric stretching band located at 2919 cm⁻¹ was higher with respect to controls ($P<0.05$) (Tables 10, 12). In *Gordonia* sp., change in the intensity of this spectral band was not significant in acute exposure cases. In gradually acclimated groups a significant change was measured only in *Gordonia* sp. ($P<0.05$). The CH₂ symmetric band intensity located at 2851 cm⁻¹ was significantly higher compared to controls in of Pb-acclimated groups (acute, gradual) in *Brevundimonas* sp. ($P<0.0001$). The pattern also repeated in acutely acclimated *Gordonia* sp. ($P<0.05$) and gradually acclimated *M. oxydans* ($P<0.05$) (Tables 10, 11, 12). Under the light of this information about the CH₂ antisymmetric and symmetric stretching bands, we can say that there was not a prominent change in the concentration of saturated membrane lipids in both of Cd-acclimated groups of *Brevundimonas* sp. On the contrary, in the Pb-acclimated groups (acute, gradual) of *Brevundimonas* sp., saturated membrane lipids increased. In *Gordonia* sp., amount of saturated membrane lipids increased in both of Cd-acclimated groups (acute, gradual) and acutely Pb-acclimated group. In contrast, the saturated lipids decreased in the gradually Pb-acclimated group. In *M. oxydans*, the concentration of the saturated membrane lipids increased in Pb-acclimated groups (acute, gradual) while decreased in the acutely Cd-acclimated group. Upon gradual Cd-acclimation of *M. oxydans*, saturated lipid concentration did not change. The reduction in saturated lipid concentration may be caused by decreased lipid biosynthesis or degradation via lipid peroxidation (Ozek et al., 2010; Ozek et al., 2014). As Markowicz et al. (2010) pointed out by increasing saturated lipid concentration bacteria increase the rigidity of their membranes (Kardas et al., 2014; Ozek et al., 2010). Another factor affecting membrane structure and dynamics is protein-to-lipid ratio. Protein-to-lipid ratio is calculated as the ratio of the intensity of the Amide I (1632 cm⁻¹)+Amide II (1535 cm⁻¹) to the intensity of C=O ester stretching (1739 cm⁻¹)

(Garip et al., 2009). The protein-to-lipid ratio significantly decreased in all Cd and Pb acclimated bacterial groups except gradually Pb-acclimated *Gordonia* sp. (Table 13). Figure 15 displays significant alterations in the protein to lipid ratio caused by the exposure to the Cd (A, C, E) or Pb (B, D, F) in terms of bar graphs.

Table 13. The protein-to-lipid ratio (Amide I + Amide II / C=O stretching) of Pb and Pb acclimated bacteria

	P/L ratio		Control	P/L ratio	
	Cd (A)	Cd (G)		Pb (A)	Pb (G)
<i>Brevundimonas</i> sp.	9**	7.086***	12.509	6.04****	5.878****
<i>Gordonia</i> sp.	7.201**	6.478***	13.437	7.945*	11.115
<i>M. oxydans</i>	7.0756***	6.621****	17.725	10.159**	7.322***

Another spectral band found in the C-H region is protein associated CH₃ symmetric stretching band positioned at 2873 cm⁻¹. The intensity of this band decreased in all acutely Cd-acclimated *Brevundimonas* sp. and *M. oxydans* species. Intensities of all Pb-acclimated *Brevundimonas* sp. and *M. oxydans* species were significantly ($P < 0.0001$) lower than the controls (Tables 10 and 12). In *Gordonia* sp., noteworthy changes did not occur regarding CH₃ symmetric stretching band located at 2873 cm⁻¹ (Table 11). The decreases in the intensity of the CH₃ symmetric stretching band implied a reduction in protein concentration in the membrane (Garip et al., 2009; Kardas et al., 2014). This agrees with Markowicz et al. (2010) as they correlate increased the rigidity of the membranes with the decreased proton translocation. Furthermore, It was also known that bacteria could use permeability barrier as a resistance mechanism to protect metal-sensitive, essential cellular components. For example, bacteria can reduce production of membrane channel protein porin and decrease penetration of heavy metals. Therefore the decrease in intensity of the CH₃ symmetric band could be caused by decreased production of porins (Bruins et al., 2000; Rouch et al., 1995).

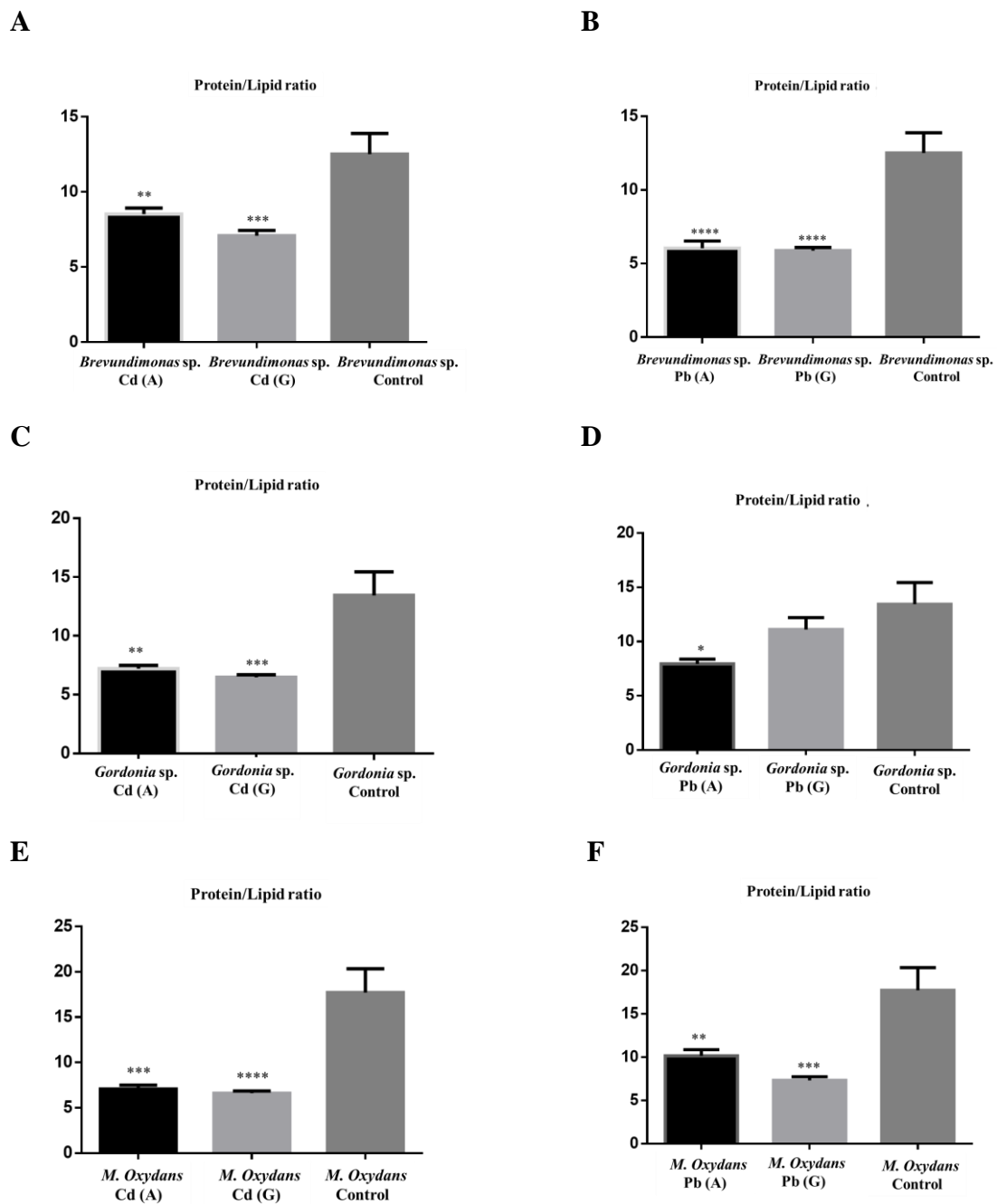


Figure 15. The protein-to-lipid ratio of Cd (A, C, E) or Pb (B, D, F) acclimated and control groups of *Brevundimonas* sp., *Gordonia* sp. and *Microbacterium oxydans*

The 1800-1500 cm^{-1} region of the bacterial spectrum is known as amide region dominated by amide I and amide II bands (Helm et al., 1991; Naumann, 2000). Highly significant ($P < 0.0001$) decrease in the intensity of the amide I band at 1632 cm^{-1} was recorded in all bacterial groups corresponds to a reduction in protein concentration as a result of Cd or Pb acclimation (Tables 10, 11, 12). Bar graphs displaying changes in the absorption intensities of amide I band in the Cd (A, C, E) or Pb (B, D, F) acclimated *Brevundimonas* sp., *Gordonia* sp. and *M. oxydans* are given in Figure 16. The 1535 cm^{-1} region harbor amide II band. The intensity of this band remarkably was lower only in gradually-acclimated *M. oxydans* in the Cd presence. As a consequence of Pb acclimation, there was significant amide II band intensity (at 1535 cm^{-1}) decrease in gradually-acclimated *M. oxydans* and, an increase in acutely-acclimated *Brevundimonas* sp., and both acclimation groups of *Gordonia* sp.. Increases in the intensity of Amide II band may result from the production of metal binding proteins (metallothioneins) involved in resistance. Metallothioneins sequester heavy metals including Pb intracellularly and immobilize them (Jarosławiecka & Piotrowska-Seget, 2014; Naik et al., 2013). Because sequestering agents become easily saturated, sequestration mechanisms acting alone are not sufficient to maintain high-level of resistance. However, they contribute the overall resistance of bacteria. Rouch et al. (1995) hypothesized that when metals gradually accumulate in the environment creating metal concentration gradients, stepwise selection of multiple mutations occurs. It increases general tolerance by the cumulative effect of these mutations. Stepwise selection of multiple mutations in *smt* locus is characterized in the studies conducted by Gupta et al. (1992) and Gupta et al. (1993). The *smt* locus of *Synechococcus* PCC 6301 contains the *smtA* gene encoding a metallothionein that sequesters Cd and Zn, and *smtB* gene which encodes a repressor of *smtA* expression. Stepwise selection with Cd leads to amplification in the *smtA* and deletion in the *smtB* gene (Rouch et al., 1995). MT induction in Cd and Pb exposed cells were also represented in several studies (Chaturvedi et al. 2012; Khan et al., 2016; Klaassen et al. 2009).

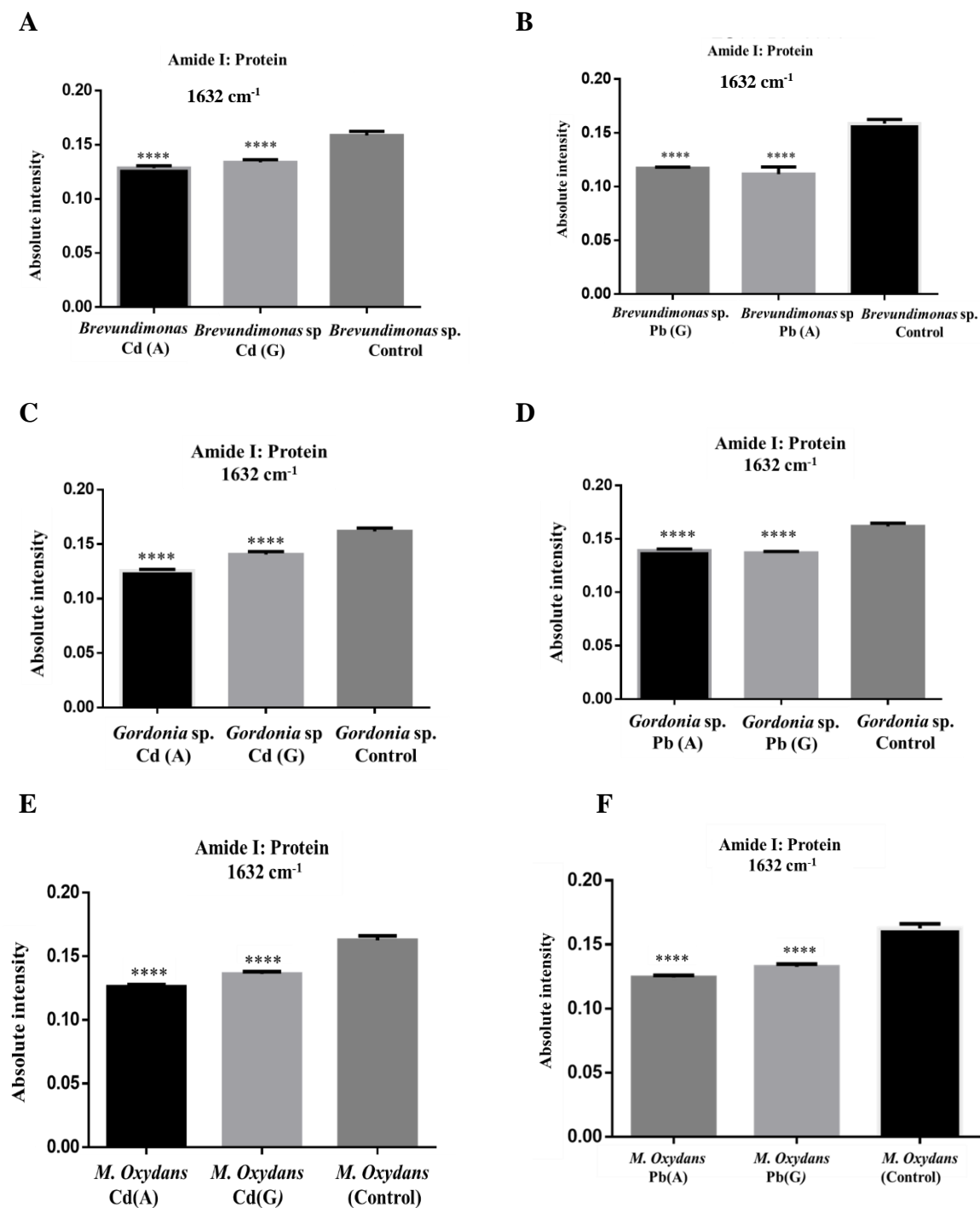


Figure 16. Changes in spectral band intensities in Cd acclimated (A, C, E), Pb acclimated (B, D, F), and control groups of *Brevundimonas* sp., *Gordonia* sp. and *M. oxydans*

The amide I to amide I + amide II ratio is related to the total protein concentration (Kardas et al., 2014). Although, there was an increase in the intensity of Amide II band in the Pb acclimated bacteria (Tables 10 and 11) total protein concentration decreased in all acclimated bacteria except gradually Cd-acclimated *M. oxydans* (Table 14). A probable cause of this decrease would be as a result of the inhibition of synthesis of several enzymes and proteins.

Table 14. The relative protein concentration (amide I/amide I+ amide II) of acute and gradual and acclimated environmental strains

<i>Brevundimonas sp.</i>				
<u>Cadmium (A)</u>	<u>Cadmium (G)</u>	<u>Control</u>	<u>Lead (A)</u>	<u>Lead (G)</u>
0.636 ± 0.0028****	0.653 ± 0.0056****	0.685 ± 0.0036	0.632 ± 0.0024****	0.632 ± 0.0025****
<i>Gordonia sp.</i>				
0.643 ± 0.0021****	0.6717 ± 0.0053**	0.7041 ± 0.01	0.625 ± 0.0071****	0.605 ± 0.0042****
<i>M. oxydans</i>				
0.628 ± 0.005****	0.670 ± 0.0069	0.677 ± 0.0043	0.612 ± 0.0094****	0.6419 ± 0,003**

For example, inhibition of the synthesis of proteins and enzymes involved in quorum sensing, biofilm formation, and iron chelation was shown in several studies under Cd or Pb exposure (Vega et al., 2014; Nithya et al., 2011; Gaonkar & Bhosle, 2013). Quorum sensing mechanism provides cell-cell communication among microorganisms by production and reception of signal molecules. Quorum sensing coordinates and regulates a number of mechanisms in a cell population such as occurring in biofilm formation (Vega et al., 2014). Similar inhibition of protein synthesis was shown to occur under Nickel exposure as well (Vega et al., 2014). In another study, inhibition of quorum sensing and biofilm formation was presented in Cd and Pb resistant *Bacillus arsenicus* and *Bacillus*

indicus isolates (Nithya et al., 2011). Furthermore, in many bacteria, siderophore (an iron chelating molecule) production is regulated via quorum sensing (Guan, 2000; Popat et al., 2017; Stintzi et al., 1998). It has been reported that when quorum sensing is inhibited, siderophore production declines. For instance, in a study performed by Gaonkar & Bhosle (2013), siderophore production was inhibited up to 90 and 70% as a consequence of Cd and Pb exposure, respectively. Reduction in protein amount could also be caused by inhibition respiratory protein synthesis by Cd and Pb in bacterial cells (Gibbons et al., 2011; Khan et al., 2016; Zeng et al., 2012). The 1800-1500 cm^{-1} region also includes lipid-associated the C=O ester stretching band positioned at 1739 cm^{-1} . The C=O ester stretching band is related to the production of polyester storage compounds, such as poly-3-hydroxybutyrate (PHB). Polyesters are known to be produced by bacteria under stress conditions (Helm, 1995; Naumann, 2000; Schuster et al., 1999) including heavy metal stress (Kamnev, 2008; Kardas et al., 2014). Polyesters are stored as energy and carbon source. Except, acutely Cd-acclimated *Brevundimonas* sp. and gradually Pb-acclimated *Gordonia* sp. in all other bacterial groups, the intensity of the C=O ester stretching band increased (Tables 10, 11, 12). Another spectral band correlated to PHB production appeared at 1453 cm^{-1} spectral region (Kamnev, 2008). In all Cd and Pb acclimated bacterial groups, the intensity of the CH₂ bending located at 1453 cm^{-1} significantly increased except gradually Pb-acclimated *Gordonia* sp. (Tables 10, 11, 12).

Another lipid associated band was located at 1469 cm^{-1} . The intensity of this band decreased in gradually Pb-acclimated *Gordonia* sp and all acclimated groups of *Brevundimonas* sp., *M. oxydans*.

C-O stretching of carboxylic acid at 1310 cm^{-1} demonstrates the presence of exopolymer (EPS) (Garip et al., 2009; Nichols et al., 1985). Exopolysaccharides (EPS) are biopolymers secreted by bacterial cells and composed of macromolecules such as polysaccharides, proteins, nucleic acids, humic substances, lipids, and other nonpolymeric constituents of low molecular weight (Bramhachari & Dubey, 2006; Bramhachari et al., 2007; Morillo 2006; Naik et al., 2012). Due to their cation exchange capacity, exopolymers efficiently bind toxic metal ions and prevent their internalization by the cell.

In this way, metal-sensitive cellular components are protected (Bruins et al., 2000; Jarosławiecka & Piotrowska-Seget, 2014). In all Cd and Pb acclimated groups, extraordinary ($P < 0.0001$) increases occurred in the intensity of this band (Tables 10, 11, 12). Figure 17 displays changes in the intensity of C-O stretching of carboxylic acid at 1310 cm^{-1} in Cd (A, C, E) or Pb (B, D, F) acclimated *Brevundimonas* sp., *Gordonia* sp. and *M. oxydans*. In biosorption studies dealing with Cd and Pb removal, the increase in exopolymers production by bacterial cells was documented by using FTIR spectroscopy (Amoozegar et al., 2012; Freire-Nordi et al., 2005; Naik & Dubey, 2013; Jaroslaviecka & Piotrowska-Seget, 2014; Pagès et al., 2007; Salehizadeh & Shojaosadati, 2003; Watcharamusik et al., 2008). For example, Ha et al. (2010) showed that cell wall-associated EPS of *Shewanella oneidensis* adsorbed more Zn(II), and Pb(II) compared to an EPS production inhibited strain. In another study dealing with immobilization capacity of EPS, when capsular EPS was removed from *Azotobacter* cells, no significant metal ion binding took place. However, when EPS was present, Cd^{2+} ions bound to bacterial cells with high affinity (Joshi & Juwarkar, 2009). Wei et al. (2011) studied the role of EPS in Cd(II) absorption using FTIR spectroscopy. They found that EPS containing bacterial cells absorbed a higher amount of Cd(II) than EPS free bacteria. Also, as we mentioned before, in the study conducted by Nithya et al. (2011), along with the inhibition of biofilm formation and quorum sensing related protein production an enormous amount of exopolymer production was reported. Their finding implied the key role of EPS in heavy metal resistance.

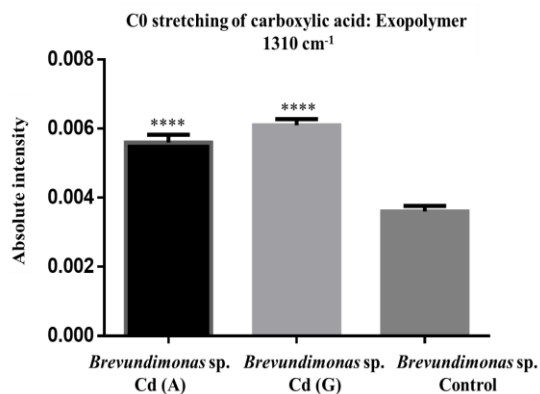
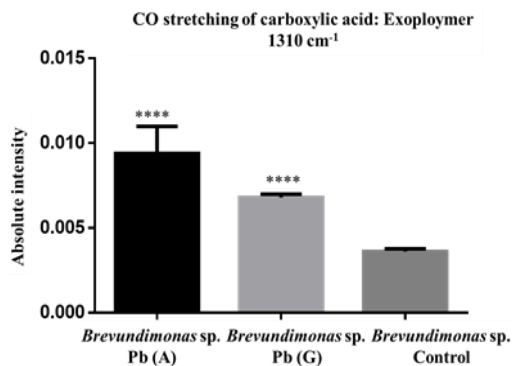
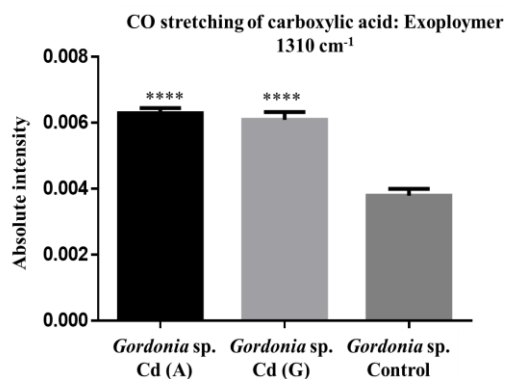
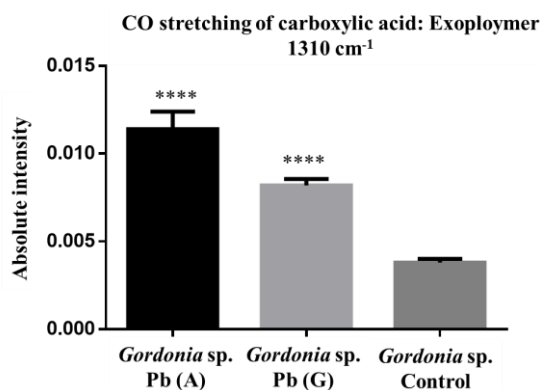
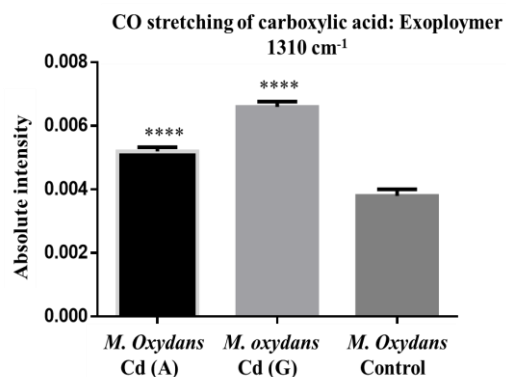
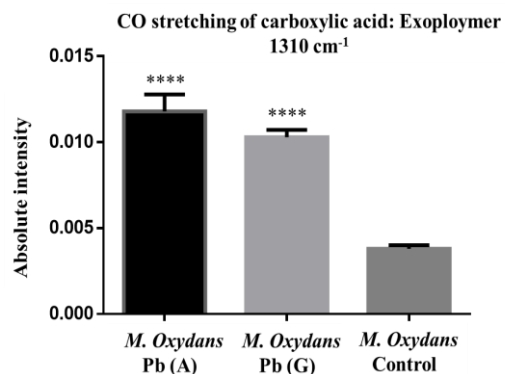
A**B****C****D****E****F**

Figure 17. Changes in intensity of C-O stretching of carboxylic acid at 1310 cm^{-1} in the Cd or Pb-acclimated *Brevundimonas* sp., *Gordonia* sp., and *M. oxydans*; A: acute, G: gradual

Spectral bands in carbohydrate region ($1200\text{-}900\text{ cm}^{-1}$) include exopolysaccharide, and EPS associated phospholipids, RNA-ribose and nucleic acids bands. In our study, the intensity of CC symmetric stretching of RNA-ribose at 1117 cm^{-1} increased in all Cd or Pb acclimated groups except acutely Pb-acclimated *Gordonia* sp. (Tables 10, 11, 12). The intensity of PO_2 symmetric stretching band (at 1082 cm^{-1}) belonging to nucleic acids and phospholipids significantly ($P < 0.0001$) increased in all Cd and Pb acclimated bacterial groups (Tables 10, 11, 12). The intensity of the C-O stretching band at 1056 cm^{-1} is associated with polysaccharide concentration. This band was significantly ($P < 0.0001$) high in all Cd and Pb acclimated groups (Tables 10, 11, 12). As an indicator of nucleic acid concentration, the intensity of CC stretching at 965 cm^{-1} increased in acutely Cd-acclimated *Gordonia* sp., both Pb-acclimated groups (acute, gradual) of *Brevundimonas* sp. and all acclimation groups of *M. oxydans* (Tables 10, 11, 12). Because exopolymers contain polysaccharides, proteins, nucleic acids, and lipids, the band intensity increases, referring increases in yield, at 1117 , 1082 , 1055 and 965 cm^{-1} indicated extensive exopolymer production (Tables 10, 11, 12). In the literature, similar results were obtained in studies conducted by using FTIR, concerning Cd and Pb resistant bacterial strains (Naik et al., 2012; Nithya et al., 2011). Figures 18, 19, and 20 exhibit significant changes in intensities of spectral bands in the carbohydrate region (1117 , 1082 , 1055 , and 965 cm^{-1}) for Cd (A, C, E, and G) or Pb (B, D, F, and H).

Furthermore, EPS production is known to be inducible, and when heavy metal concentrations were high, more EPS was produced (Iyer et al., 2005; Watcharamusik et al., 2008; Yue et al., 2015). Accordingly, in our study, huge amount of EPS was measured in acclimated bacterial strains at high concentrations of Cd or Pb. Also, bacteria can modify their EPS as a result of metal exposure and increase their metal binding capacity. For example, carboxyl and phosphoric content increase binding capacity of exopolysaccharides to Cd and Pb (Comte et al., 2006, Guibaud et al., 2003; Guibaud et al., 2005). Our results agree with the previous findings in a way that we also found elevated amounts of phosphoric ion content (based on the intensities and positions at 1082 and 1055 cm^{-1}). A report on EPS production by *Desulfovibrio desulfuricans* demonstrated that the composition of EPS was significantly changed after metal exposure. In their study,

while in the presence of Cu^{2+} and Zn^{2+} , protein content decreased, polysaccharide content increased, in the presence of Cd^{2+} protein amount increased and polysaccharide amount decreased in EPS (Yue et al., 2015). On the contrary to their, in our study, carbohydrate concentration increased while protein concentration decreased as a result of metal exposure. It could be due to the difference of bacteria and environmental factors. Since it is known that composition and amount of EPS vary among bacterial species based on the conditions in the environment such as pH, temperature, metal content, nutrient level and type (Guibaud et al., 2003; Guo et al., 2010).

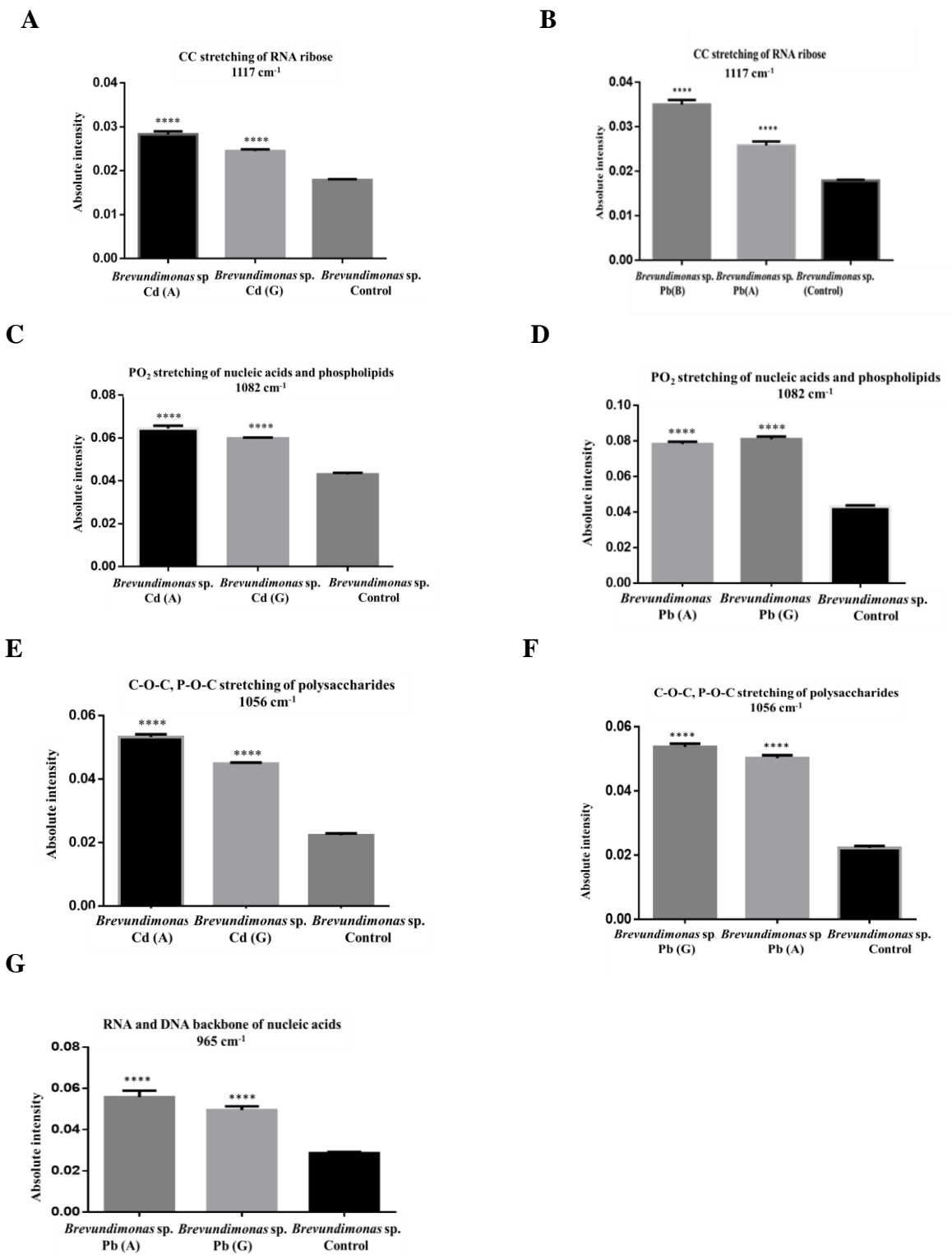


Figure 18. Spectral band intensity changes at 1117, 1082, 1056, and 965 cm⁻¹ (carbohydrate region) in Cd or Pb acclimated *Brevundimonas* sp.

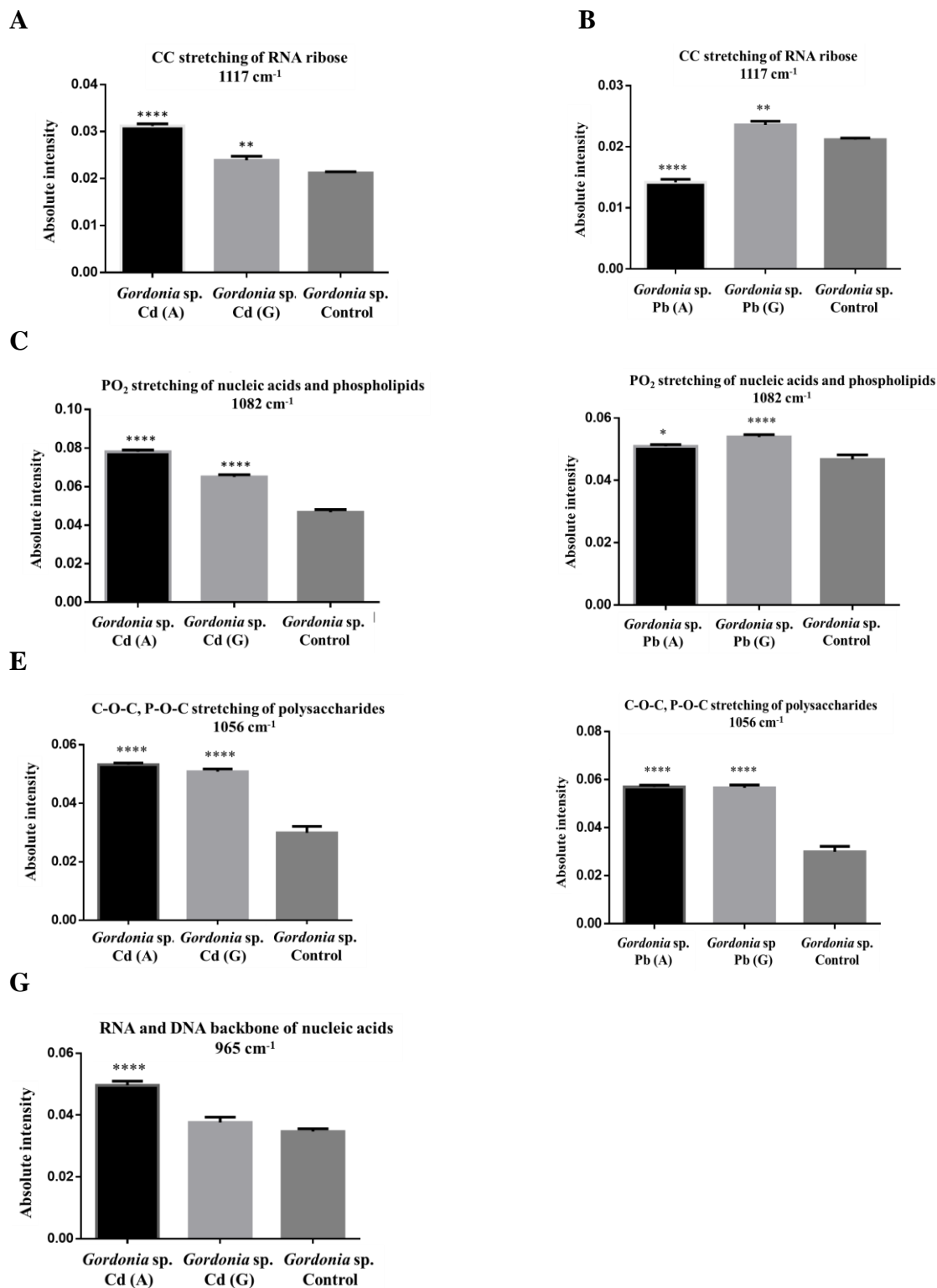


Figure 19. Spectral band intensity changes at 1117, 1082, 1056, and 965 cm⁻¹ (carbohydrate region) in Cd or Pb acclimated *Gordonia sp.*

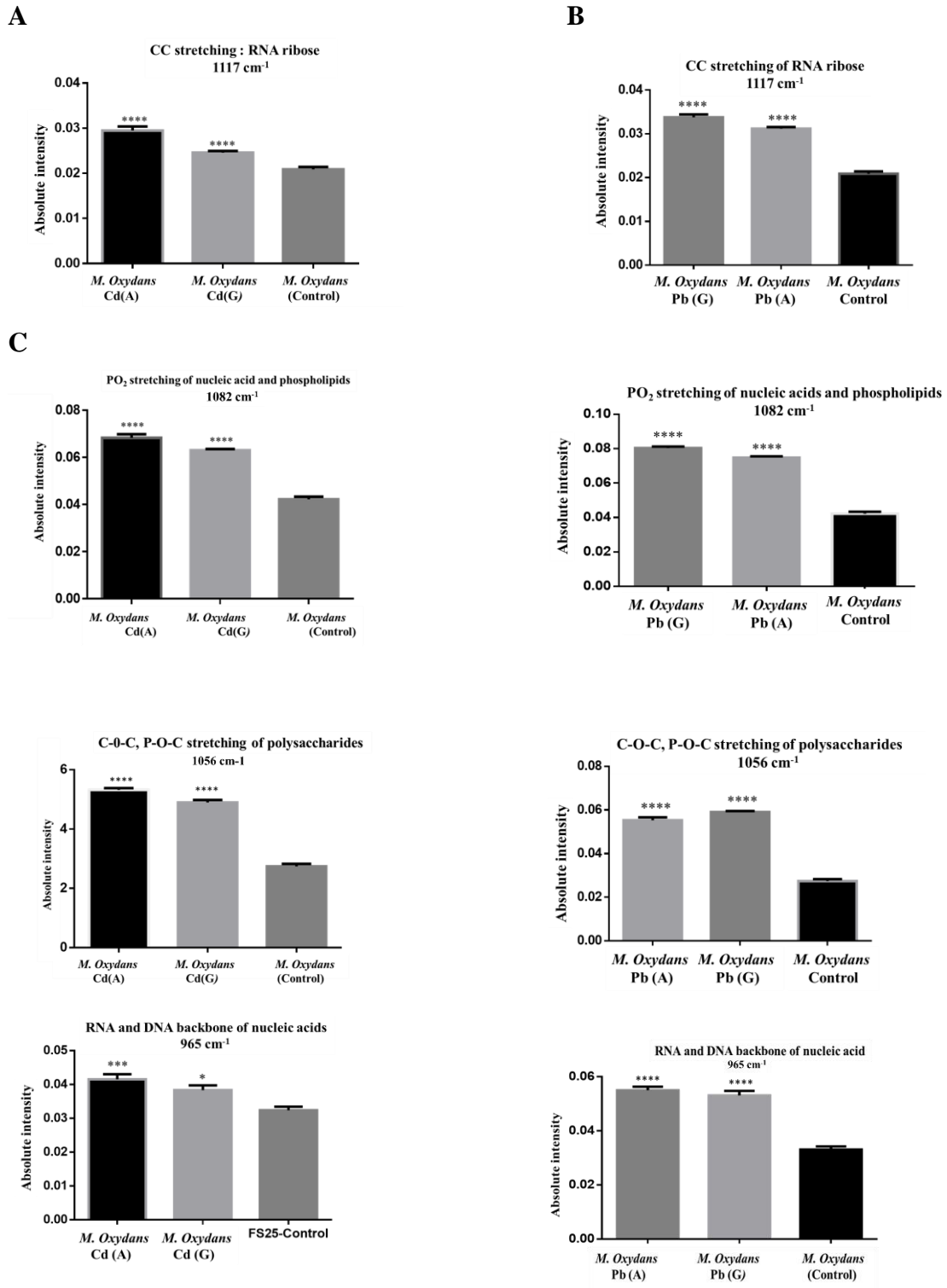


Figure 20. Spectral band intensity changes at 1117, 1082, 1056, and 965 cm⁻¹ (carbohydrate region) in Cd or Pb acclimated *M. oxydans*

So far we have presented the results of comparison between the treatment and control groups. In addition, we also compared the spectral profile differences between the acutely and gradually metal exposed groups of the same bacterial strains. For example, acutely Cd-exposed *Gordonia* sp. Profile vs. gradually Cd-exposed *Gordonia* sp. (Tables 15, 16, 17).

Table 15. Differences in spectral band intensity change between acutely and gradually Cd or Pb-acclimated *Brevundimonas* sp.

Wave number	Cd (A)	Cd (G)	<i>p</i>
2873	84.534 ± 2.418	96.461 ± 0.856	***
2851	106.651 ± 1.735	101.508 ± 0.5	*
1739	121.5 ± 7.785	146.5 ± 4.285	*
1392	79.651 ± 3.552	92.732 ± 1.011	***
1235	96.837 ± 2.584	86.561 ± 0.922	**
1117	158.1 ± 3.729	136.871 ± 2.082	****
1082	149.767 ± 3.781	139.069 ± 1.028	**
1056	238.565 ± 3.828	200.896 ± 1.609	****
	Pb (A)	Pb (G)	<i>p</i>
2956	61.729 ± 0.874	70.918 ± 1.034	***
2919	103.651 ± 0.438	98.865 ± 0.94	***
2873	74.345 ± 0.697	56.675 ± 1.852	****
1535	118.595 ± 4.214	93.801 ± 1.035	****
1469	93.68 ± 1.122	60.468 ± 1.632	****
1453	127.528 ± 2.674	107.175 ± 0.814	****
1235	99.604 ± 2.485	111.067 ± 2.315	**
1117	146.368 ± 4.696	195.53 ± 5.77	****
1056	225.112 ± 4.109	240.807 ± 4.6	*

In carbohydrate region, intensities of acutely Cd-acclimated groups were significantly higher than the intensities of gradually acclimated counterparts in all three bacteria (Tables 15, 16, 17).

Table 16. Differences in spectral band intensity change between acutely and gradually Cd or Pb-acclimated *Gordonia* sp.

Wave number	Cd (A)	Cd (G)	<i>p</i>
1632	77.736 ± 0.702	86.889 ± 1.4	***
1392	65.721 ± 2.437	84.536 ± 1.374	****
1235	85,401 ± 1,354	95.52 ± 3.46	*
1117	147.169 ± 2,201	112.735 ± 4.066	****
1082	167.237 ± 2,079	139.186 ± 2.513	****
965	142.939 ± 3,988	108.357 ± 4.994	****
	Pb (A)	Pb (G)	<i>p</i>
2956	89.674 ± 4.351	105.162 ± 3.313	*
2919	107.442 ± 5.481	86.018 ± 0.909	***
2873	88.705 ± 5.146	102.341 ± 2.932	*
2851	114.070 ± 3.022	99.036 ± 2.67	***
1739	142.5 ± 5.23	109 ± 8.425	*
1469	98.97 ± 2.622	73.382 ± 2.241	***
1453	128.474 ± 2.242	106.61 ± 3.13	****
1392	127.577 ± 3.587	97.422 ± 5.079	****
1300	300 ± 26,081	215.789 ± 9.447	**
1117	66.981 ± 2.31	111.32 ± 2.741	****

On the other hand, in the lead exposed bacteria, spectral band intensities of gradually acclimated strains were significantly higher than those of the acutely acclimated ones (Tables 15, 16, 17). This situation was not so for spectral bands found in lipid and protein regions. In lipid and protein regions, differences in spectral band intensities were variable.

Table 17. Differences in spectral band intensity change between acutely and gradually Cd or Pb-acclimated *M. oxydans*

Wave number	Cd (A)	Cd (G)	<i>p</i>
1632	77.538 ± 1.085*	83.753 ± 1.106	*
1392	71.81 ± 2.202	108.308 ± 2.392	****
1300	136.842 ± 3.507	173.684 ± 4.297	****
1235	94,346 ± 1.828	84.452 ± 1.702	*
1117	141.148 ± 4,294	117.703 ± 1.626	****
1082	161.848 ± 3.604	149.289 ± 1.413	**
1056	194.16 ± 2.359	178.632 ± 2.929	**
	Pb (A)	Pb (G)	<i>p</i>
2956	63.686 ± 0.772	72.847 ± 0.916	*
2919	104.315 ± 0.235	97.815 ± 0.963	**
1535	108.656 ± 3.259	89.534 ± 1.388	***
1453	131.21 ± 2.375	112.42 ± 1.346	***
1117	149.282 ± 1.717	161.722 ± 3.173	**
1082	177.251 ± 1759	190.521 ± 1.875	***
1056	201.824 ± 4.868	215.328 ± 1.884	*

Briefly, heavy metal toxicity leads to DNA damage, inhibition of enzyme activity, and change in structure and composition of lipids (Gibbons et al. 2011; Lemire et al., 2013; Sabdono 2011; Schirawski et al., 2002; Stohs et al., 1995). It also creates reactive oxygen species (ROS) causing lipid peroxidation (Howlett et al., 1997; Rouch et al., 1995; Ozek et al., 2010).

In our study, significant changes (increase or decrease) in the saturated lipid concentration, prominent decreases in the fatty acid and protein concentrations, as well as the protein-to-lipid ratio, pointed out membrane modification in response to heavy metal exposure. The nature modifications differed between gradually and acutely metal-acclimated bacteria. Furthermore, the modifications vary depending on the metal (whether Cd or Pb).

Total protein concentration decreased in all acclimated groups except gradually-Cd acclimated *M. oxydans*. However, the increase in the amid II band intensity in some treatments indicated the elevated protein synthesis (acutely Pb-acclimated *Brevundimonas* sp. and both groups of Pb-acclimated *Gordonia* sp.). It could be caused by selective activation of some protection mechanisms in response to heavy metal stress such as metallothionein production, efflux pump proteins. The total protein concentration is calculated from the ratio of amid I over amid I plus amid II. Therefore, it does not discriminate the amount variations among the individual proteins. The decreases measured in the total protein may imply the inhibition of several anabolic pathways.

Changes occurred in amount, structure, and composition of molecules in lipid and protein regions to cope with Cd or Pb toxicity in the three bacteria. However, the most striking changes occurred in exopolysaccharide concentrations. It seemed that main exopolysaccharide deposition on the outer surface of the bacteria was the main protection mechanism, against heavy metal toxicity. There were two interesting outcomes of the exopolymer measurements. Firstly, acutely Cd-acclimated bacteria had significantly higher exopolymer content than that of gradually acclimated ones. Secondly, gradually Pb-acclimated bacteria had significantly higher exopolymer content than that of acutely acclimated ones.

3.4. Chemometric Approaches

Followed by the characterization using the spectral changes, we applied PCA and HCA, for further characterization and discrimination of the IR data.

3.4.1. Principle Component Analysis (PCA)

One of the most frequently used multivariate methods, PCA decomposes the data matrix and concentrate the source of variability in the data into the first few PCs (Hori & Sugiyama, 2003). Score plot of PCA exhibit discriminations between the sample groups. Loading plots were used to determine the contribution of each variable (wavenumber) to each principal component. It detects which spectral regions maintain the most significant contributions to data variation. Large positive or negative loadings are associated with spectral regions that are involved in differentiation (Al-Qadiri et al., 2008).

In this study, PCA was performed to find out discrimination between the heavy metal (Cd or Pb) acclimated strains (A or G) and control groups. It was applied to *Brevundimonas* sp., *Gordonia* sp. and *M. oxydans* in the whole IR region (4000-650 cm^{-1}), lipid region (3200-2800 cm^{-1}), protein region (1800-1500 cm^{-1}), and carbohydrate region (1200-900). Figures 21-26 demonstrate score plots showing the variation among the sample groups. As a result of Cd or Pb exposure, there were sufficient variations among the bacteria (acute, gradual and control groups) in all of the IR spectral regions that we analyzed (Figures 21-26). We used lodings of PCA to detect which spectral regions provide the most significant contributions to the data variation in the applied area. When evaluating discriminations in the all spectral region, we observed clear differentiations in the experimental groups of bacteria (acclimated and control groups). Loading plots of PCAs presenting both positive and/or negative lodings in lipid (3200-2800 cm^{-1}), protein (1800-1500 cm^{-1}), and carbohydrate (1200-900 cm^{-1}) regions provided the differentiation (Appendix B, Figures 1-6). Score plot of *Brevundimonas* sp., *Gordonia* sp., and *M. oxydans* sp. exhibited clear discriminations between the acclimated (A, G) and control

groups in the whole spectral region (4000-650 cm^{-1}) in the presence of Cd or Pb. Percentage of variation and discrimination of sample groups in the whole region are presented in Figures 21-26 (A panels). We then evaluated the loading plots of PCA in the whole spectral region (4000-650 cm^{-1}) for the Cd or Pb-acclimated bacteria and corresponding control groups. We determined the contribution of lipid, protein, and carbohydrate to the variation in profiles from the loading plots (Appendix B; Figures 1-6 A panels). Evaluation of the loading plots for each bacteria was done for lipid, protein and carbohydrate regions separately based on Cd or Pb exposures (Appendix B; Figures 1-6). In the lipid region (3200-2800 cm^{-1}), most of the variation was due to the spectral bands located at 2956, 2919, 2873, and 2851 cm^{-1} (Appendix B; Figures 1-6, B panels). In the protein region (1800-1500 cm^{-1}), the major contribution to variation was due to 1739, 1632 and 1535 cm^{-1} spectral bands (Appendix B; Figures 1-6, C panels). Furthermore, in carbohydrate region (1200-900 cm^{-1}), spectral bands at 117, 1082, 1055, and 965 cm^{-1} contributed the most loading in the variation (Appendix B; Figures 1-6, D panels).

The PCA was done for Cd-acclimated (A, G) and control groups for *Brevundimonas* sp., in lipid (3200-2800 cm^{-1}), protein (1800-1500 cm^{-1}), and carbohydrate (1200-900 cm^{-1}) regions. In lipid region, the PCA score plot showed that sample groups are discriminated, as being 83% ($\text{PC1}+\text{PC2}= 62+21= 83$) (Figure 21B). In protein region, acclimated groups (A, G) and control group clearly segregated from each other (Figure 21C). The localization of sample groups in the score plot indicated that more molecular changes occurred in acutely-acclimated bacteria compared to gradually-acclimated. It was supported by the ATR-IR results that total protein concentration in acutely- acclimated bacteria was significantly lower than the gradually-acclimated counterparts (Table 14). The total variation contributed by PC1 and PC2 was 70% ($\text{PC1}+\text{PC2}= 48+22= 70$).

In carbohydrate spectral region of *Brevundimonas* sp. were well separated depending on the acute vs. gradual-acclimation (Figure 21D). According to positions of sample groups in score plot, more molecular changes occurred in acutely-acclimated bacteria. This outcome was in agreement with the spectral analysis results (Table 10). PC1 and PC2 identifies 88% variation ($\text{PC1}+\text{PC2}= 62+26= 88$) in this region. According to positions of

sample groups in score plot, more molecular changes occurred in acutely acclimated samples. This outcome overlapped the spectral analysis results that spectral band intensities of acutely-acclimated bacteria were apparently higher than those of gradually acclimated ones in carbohydrate region.

Figure 22B shows the PCA for acutely or gradually Pb-acclimated and the control groups of *Brevundimonas* sp. in lipid region. There was not apparent discrimination between the acutely acclimated and the control. However acclimated groups separated from each other. It appears that similar modifications occurred in acclimation groups whether gradual or acute exposure causing the acclimation. This can be seen from the spectral analysis results presented in Table 10. For the lipid region, PC1 and PC2 explained 82% of the total variation. In the protein region, discrimination was apparent among the treatments (A, G) and control (Figure 22C; $PC1+PC2= 41+32= 73$). Figure 22D shows the discrimination in carbohydrate region. The score plot implied that there were more molecular changes in gradually-acclimated bacteria than acutely-acclimated one.

The PCA score plots for Cd-acclimated (A, G) and control groups of *Gordonia* sp. in lipid, protein, and carbohydrate regions are shown in Figures 23B, C, and D.

In the lipid region, the acclimation and control groups were clearly separated from each other (Figure 23B). The variation was bigger between the acutely Cd-acclimated *Gordonia* and the control. The gradually acclimated bacteria varied less from the control than the acutely acclimated counterparts. Figure 23C shows the variation in protein region for the treatment and control groups of *Gordonia* sp. As extrapolated from the location of samples in score plot, acutely-acclimated samples further differentiated from samples of control groups as can be attributed to the intensity of amide I band (1632 cm^{-1}) and total protein concentration of acutely acclimated samples (Tables 11, 14). In carbohydrate region, the clear separation between the treatment and control groups was obtained (Figure 23D). Score plot of PCA represented that PC1 and PC2 explain 90% of total variation ($PC1+PC2= 84+6= 90$) in this region.

The PCA score plots for Pb-acclimated (A, G) and control groups of *Gordonia* sp. in lipid, protein, and carbohydrate regions are shown in Figures 24B, C, and D.

In lipid region, as represented in the PCA score plot, although Pb-acclimated groups (A, G) were separated from the control group, the treatment groups overlapped (Figure 24B). The overlap implies that similar molecular changes took place during the acclimation processes whether the exposure was acute or gradual (Table 11). As revealed by the PCA score plot belonging to the protein region, in addition to the clear separation between the treatment groups and control, 77% of variation provided by PC1 and PC2 ($PC1+PC2=55+22=77$) (24C). In carbohydrate region, the variation between the treatments and the control groups was defined by the PC1 and PC2 as being 76% of the total variation ($PC1+PC2=60+16=76$) (Figure 24D).

The PCA score plots for Cd-acclimated (A, G) and control groups of *Microbacterium oxydans* in lipid, protein, and carbohydrate regions are shown in Figures 25B, C, and D. Figure 25 B shows the separation among treatment and control groups in lipid region. PC1 and PC2 explained 90% of total variation ($PC1+PC2=82+8=90$). In protein region, members of the acutely-acclimated group separated from the gradually-acclimated and control groups based on PC1 (25C). PC1 and PC2 described the 68% of total variation ($PC1+PC2=53+15=68$) in this region. The clear-cut separation of the acutely Cd-acclimated *M. oxydans* from the gradually-acclimated and the control groups appeared to be due to the total protein concentration decrease upon acute acclimation (Table 14). Also, there was no change in total protein concentration of gradually-acclimated counterparts (Tables 12, 14). In carbohydrate region, separation of the sample groups is shown in Figure 25 D. PC1, and PC2 of score plot explained 90% of total variation ($PC1+PC2=80+10=90$).

Finally, we applied PCA for Pb-acclimated (A, G) and control groups of *M. oxydans*. In lipid region (Figure 26B), PC1 and PC2 defined 89% of the total variation ($PC1+PC2=80+9=89$). In PC1 the most loading was due to four bands at 2956, 2919, 2878 and 2851 cm^{-1} (Appendix B, Figure 6B). In protein region (Figure 26C) 73% of total variation was due to PC1 and PC2 ($PC1+PC2=44+29=73$). Loading plot (Appendix B, Figure 6C) shows the contributing bands to variation the most. Likewise, in carbohydrate region, the discrimination was obvious between sample groups (Figure 26D). Gradually Pb-

acclimated *M. oxydans* varied from control group more than the acutely acclimated group. PC1 and PC2 defined 93% of the total variation ($PC1+PC2= 85+9= 93$) in this region.

To sum up, the information presented in the score plots, we can say that in lipid region of bacteria, there were fewer modifications to cope with the heavy metals. Furthermore, the modifications were similar between the two acclimated groups (A and G). In protein and carbohydrate region clear separation was present among all sample groups (A, G, and control). It implies that more modification occurred in these regions to cope with the heavy metal presence. Furthermore, in carbohydrate region, the modifications in the Cd-acclimated bacteria upon acute exposure appeared to be segregated more than the gradual as compared to control. In the case of Pb, the reverse relation was detected.

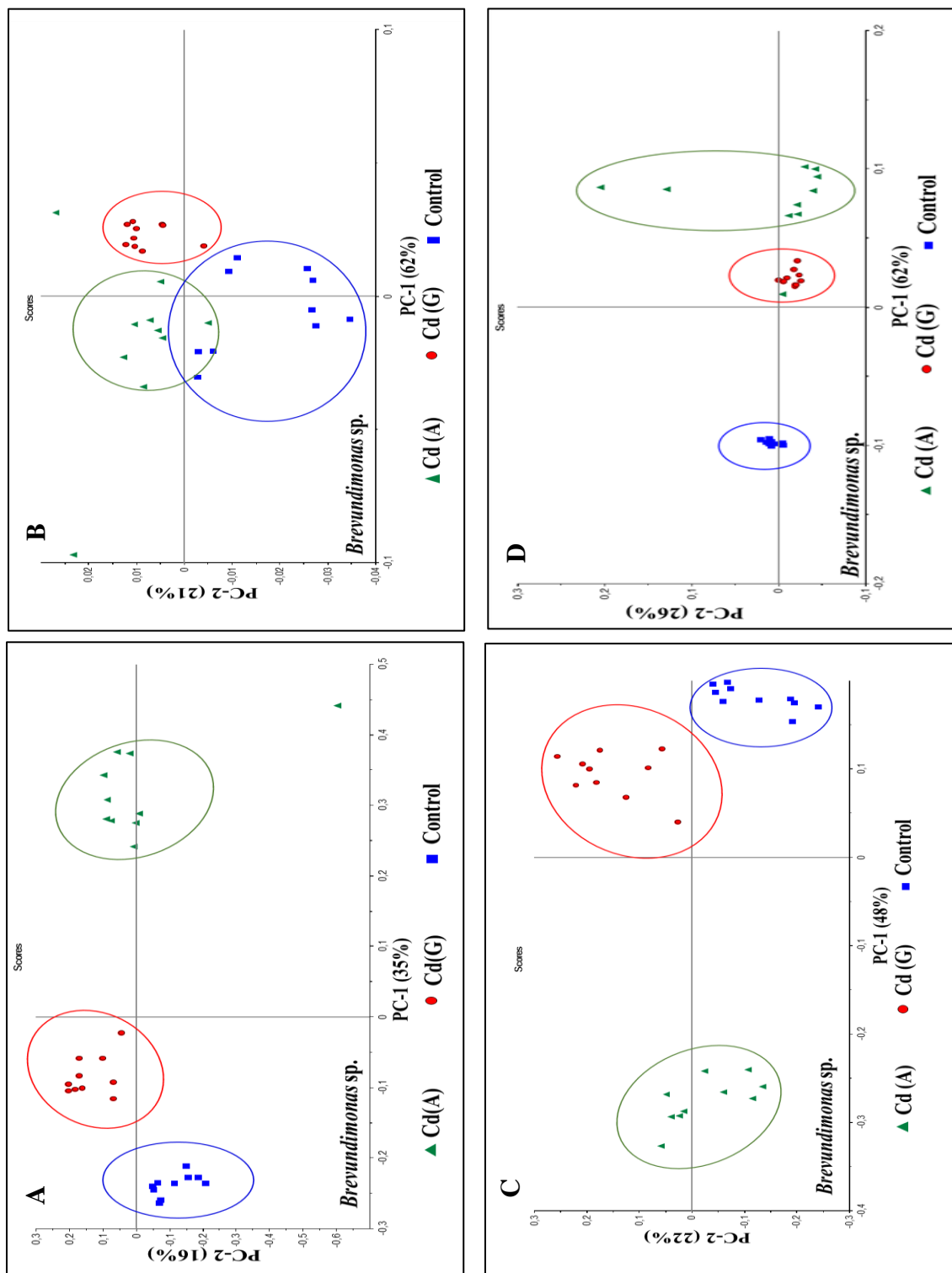


Figure 21. PCA score plots; (A) whole spectral region (4000-650 cm^{-1}) (B) lipid region (3200-2800 cm^{-1}) (C) protein region (1800-1500 cm^{-1}) (D) carbohydrate region (1200-900 cm^{-1}) for Cd-acclimated (A: acute, G: gradual) and control groups of *Brevundimonas* sp.

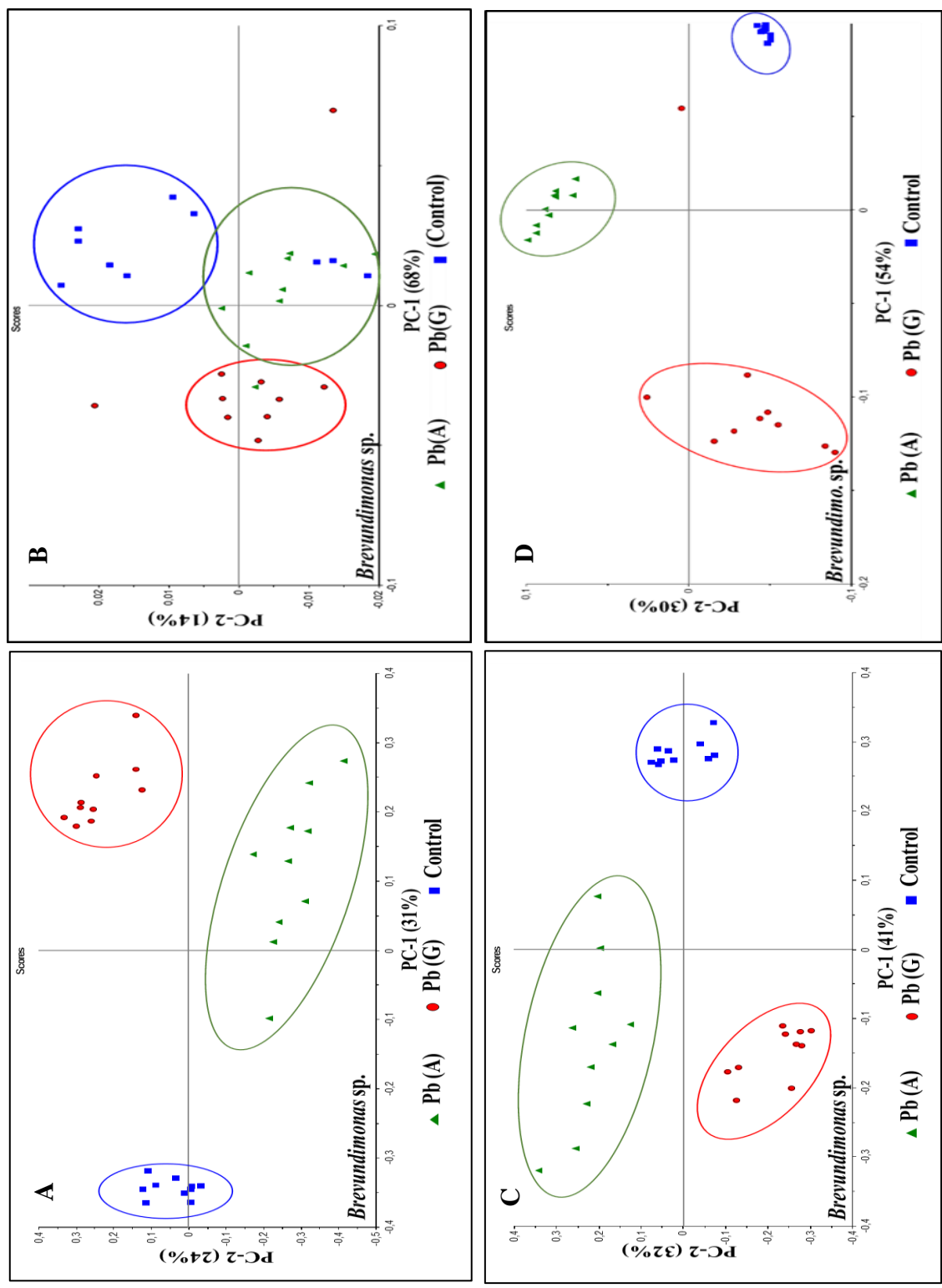


Figure 22. PCA score plots; (A) whole spectral region (4000-650 cm^{-1}) (B) lipid region (3200-2800 cm^{-1}) (C) protein region (1800-1500 cm^{-1}) (D) carbohydrate region (1200-900 cm^{-1}) for Pb-acclimated (A: acute, G: gradual) and control groups of *Brevundimonas sp.*

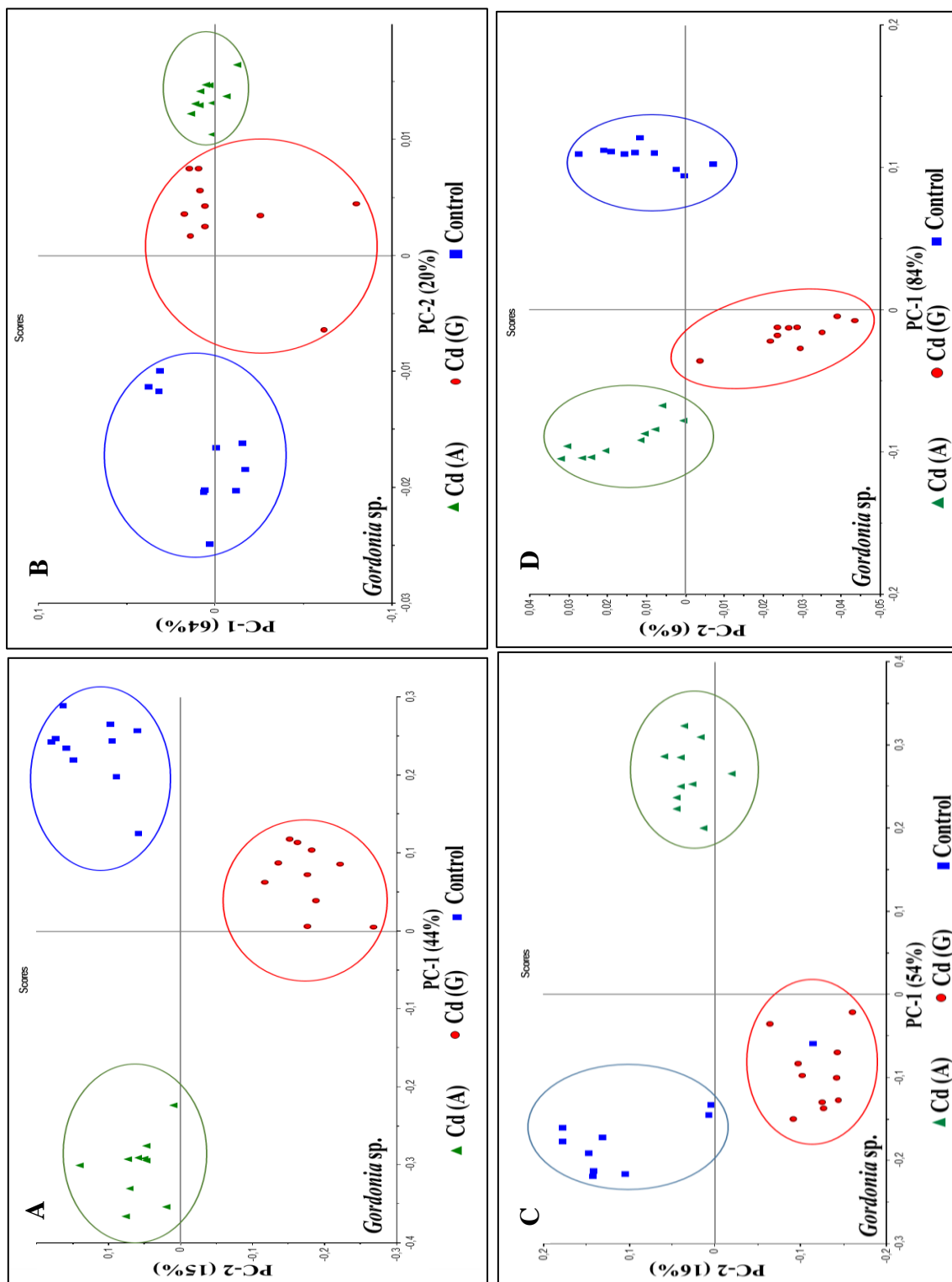


Figure 23. PCA score plots; (A) whole spectral region (4000-650 cm^{-1}) (B) lipid region (3200-2800 cm^{-1}) (C) protein region (1800-1500 cm^{-1}) (D) carbohydrate region (1200-900 cm^{-1}) for Cd-acclimated (A: acute, G: gradual) and control groups of *Gordonia* sp.

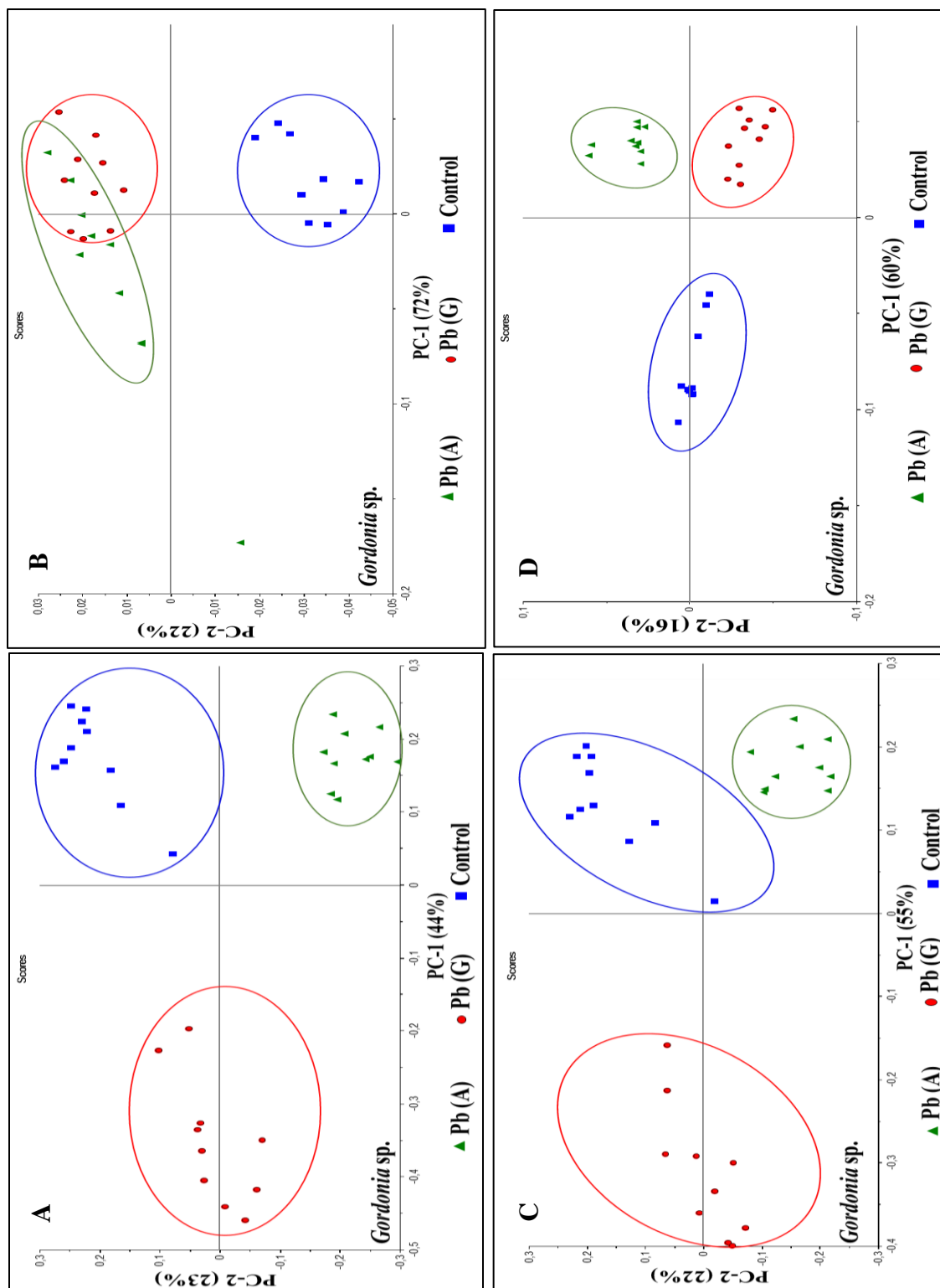


Figure 24. PCA score plots; (A) whole spectral region (4000-650 cm^{-1}) (B) lipid region (3200-2800 cm^{-1}) (C) protein region (1800-1500 cm^{-1}) (D) carbohydrate region (1200-900 cm^{-1}) for Pb-acclimated (A: acute, G: gradual) and control groups of *Gordonia sp.*

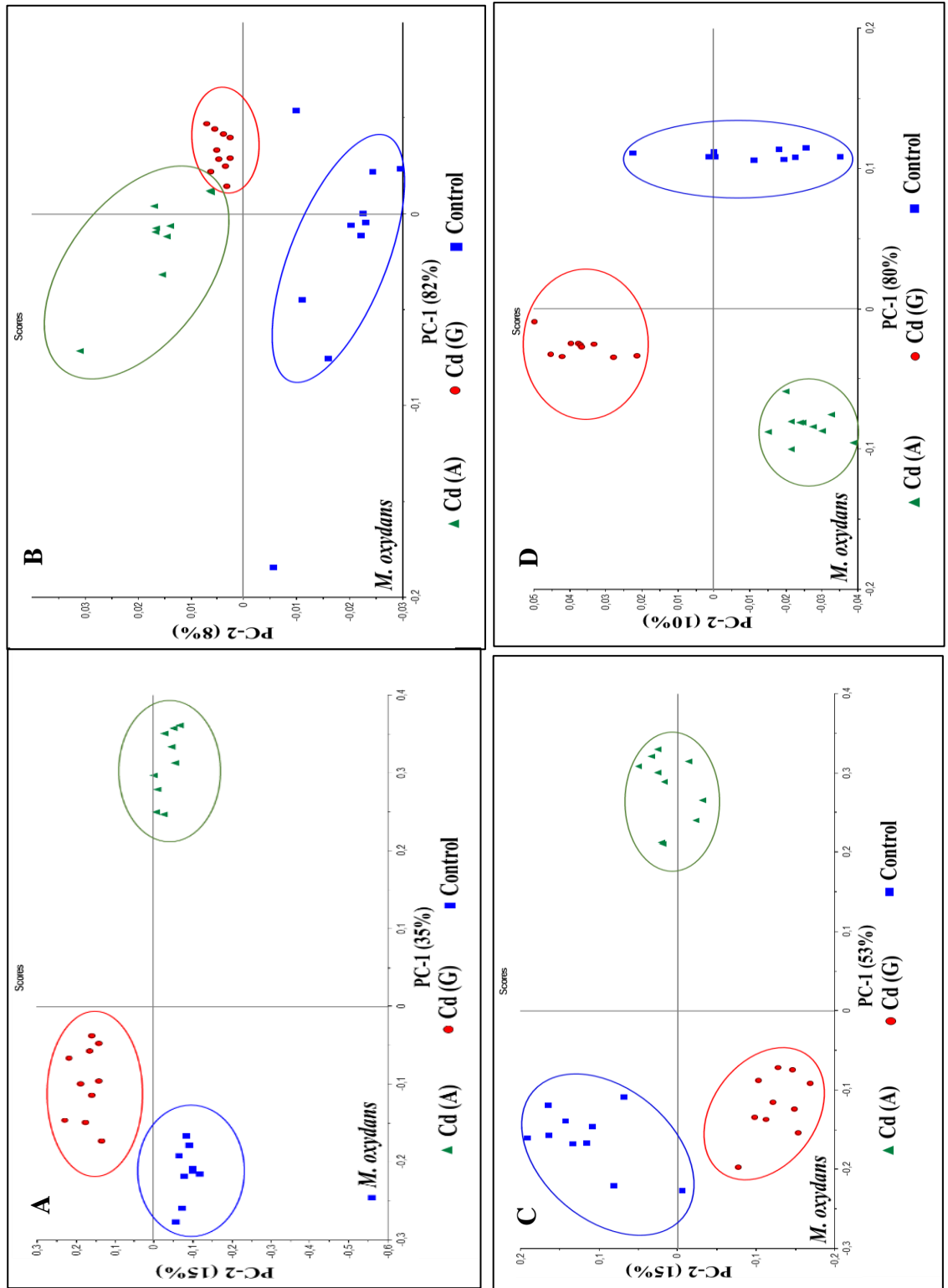


Figure 25. PCA score plots (A) whole spectral region (4000-650 cm^{-1}) (B) lipid region (3200-2800 cm^{-1}) (C) protein region (1800-1500 cm^{-1}) (D) carbohydrate region (1200-900 cm^{-1}) for Cd-acclimated (A: acute, G: gradual) and control groups of *M. oxydans*

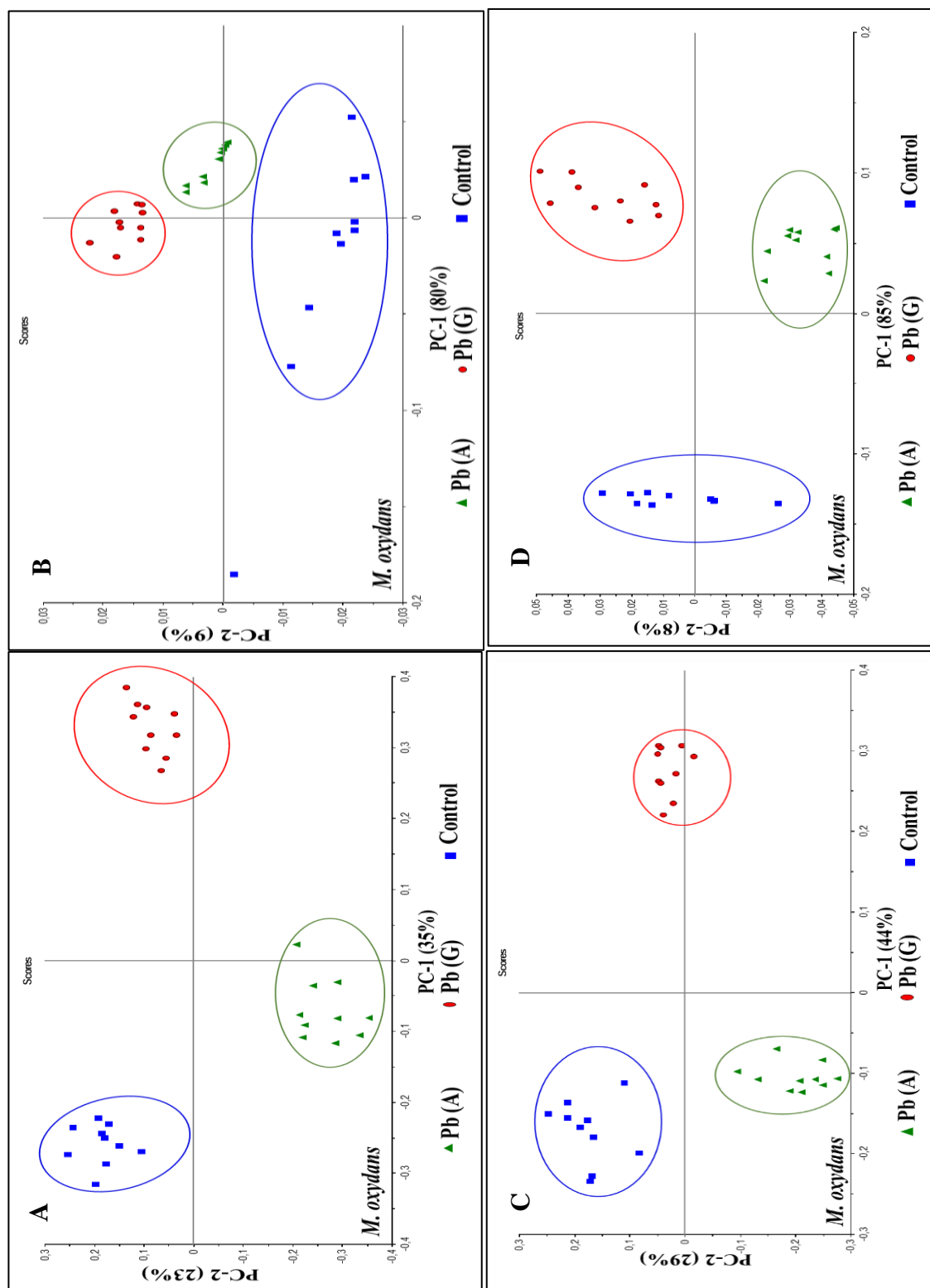


Figure 26. PCA score plots (A) whole spectral region (4000-650 cm^{-1}) (B) lipid region (3200-2800 cm^{-1}) (C) protein region (1800-1500 cm^{-1}) (D) carbohydrate region (1200-900 cm^{-1}) for Pb-acclimated (A: acute, G: gradual) and control groups of *M. oxydans*

3.4.2. Hierarchical Cluster Analysis (HCA)

In the second chemometric approach as an alternative to PCA analysis, we have done HCA. This analysis uses a different algorithm than the one used for PCA. Use of PCA and HCA together has been becoming a trend in IR data analysis. The hierarchical cluster analysis (HCA) is based on similarities between the spectra of samples (Dziuba et al., 2007). We applied HCA to discriminate acclimated (acutely or gradually) bacterial groups from control groups. In HCA derived dendrograms, the differences between clusters are represented as heterogeneity values. The dendrograms illustrate the arrangement of the clusters. In these clusters, samples with the highest correlations are clustered together, while samples with small correlations are widely separated (Xue et al., 2011). In our study, HCA was applied to the data covering whole spectral region (4000-650 cm^{-1}), lipid region (3200-2800 cm^{-1}), protein region (1800-1500 cm^{-1}) and carbohydrate region (1200-900) for the bacteria. The dendrograms that were constructed based on the HCA are represented in Figures 27-32 (A; whole region: 4000-650 cm^{-1} , B; lipid region: 3200-2800 cm^{-1} , C; protein region: 1800-1500 cm^{-1} , D; carbohydrate region: 1200-900 cm^{-1}). Cd-acclimated (Acute or Gradual) groups of *Brevundimonas* sp., *Microbacterium oxydans*, and *Gordonia* sp. were differentiated from control groups with 100% sensitivity and 100% specificity in all the analyzed regions (whole region, lipid region, protein region and carbohydrate region) (Figures 27, 29, 31) except for lipid regions of *Brevundimonas* sp. and *M. oxydans* (Figures 27B, 31B). In this region, acutely acclimated *Brevundimonas* sp. and *M. oxydans* groups differentiated from the control group with 90% sensitivity and 100% specificity. As a result of lead exposure, all acclimated (acute or gradual) strains were separated from control groups with 100% sensitivity and 100% specificity for all spectral regions (Figures 28, 30, 32). These results indicated that Cd and Pb acclimation caused definite molecular changes in these bacterial strains. As a consequence of these molecular changes, bacteria could live and grow at Cd and Pb concentrations well above lethal in un-acclimated cases. Furthermore, acutely Cd-acclimated *Brevundimonas* sp., *Microbacterium oxydans*, and *Gordonia* sp. differentiated from gradually acclimated ones in the whole, protein, and carbohydrate regions (Figures 27, 29, 31 panels; A, C and D).

The same differentiation was apparent for Pb as well (Figures 28, 30, 32 panels; A, C, D). There were 100% sensitivity and specificity in discrimination between acutely and gradually heavy metal exposed bacteria. These discrimination values demonstrated that the way in which they got acclimated (acute or gradual) changed the molecular profiles of the bacteria at the end. Even though, all the acclimated ones were living and growing at the same concentration by the end. In the case of lipid regions (3200-2800 cm^{-1}), the discrimination was not as sensitive or as specific compared to protein and carbohydrate regions. Acutely Cd-acclimated *Brevundimonas* sp. and *M. oxydans* were separated from gradually acclimated ones with 70% sensitivity and 100% specificity (Figures 27B and 31B). Likewise, acutely Pb-acclimated *Gordonia* sp. were differentiated from gradually acclimated ones with 80% sensitivity and 70% specificity (Figure 30B). The modifications that different bacteria apply to survive and grow metal exposure appears to have common features as long as the lipids are concerned.

The heterogeneity values (ranging between 1.2 to 3) were the lowest for lipid region data. These values pointed out fewer differences among Pb or Cd-acclimated samples of *Brevundimonas* sp., *Gordonia* sp. and *Microbacterium oxydans*. HCA yielded the highest heterogeneity values (ranging between 6 to 9) for the data points covering carbohydrate region in Cd or Pb exposed bacteria. Heterogeneity appeared to be a function of amount rather than composition as obtained from the intensities of the spectral bands. When we evaluated the distances of acclimated samples from the control samples, acutely acclimated samples of bacteria were clustered at a greater distance than those of gradually acclimated ones in the Cd-exposed cells in protein and carbohydrate regions. On the other hand, in the presence of Pb, gradually acclimated samples were located at a greater distance than those of acutely acclimated ones in all bacterial strains in the protein and carbohydrate regions. This situation was not valid for lipid region under Cd or Pb-exposures. It appears that the amounts of lipids were not changing dramatically. However, the compositions seemed to be altered to cope with the metals.

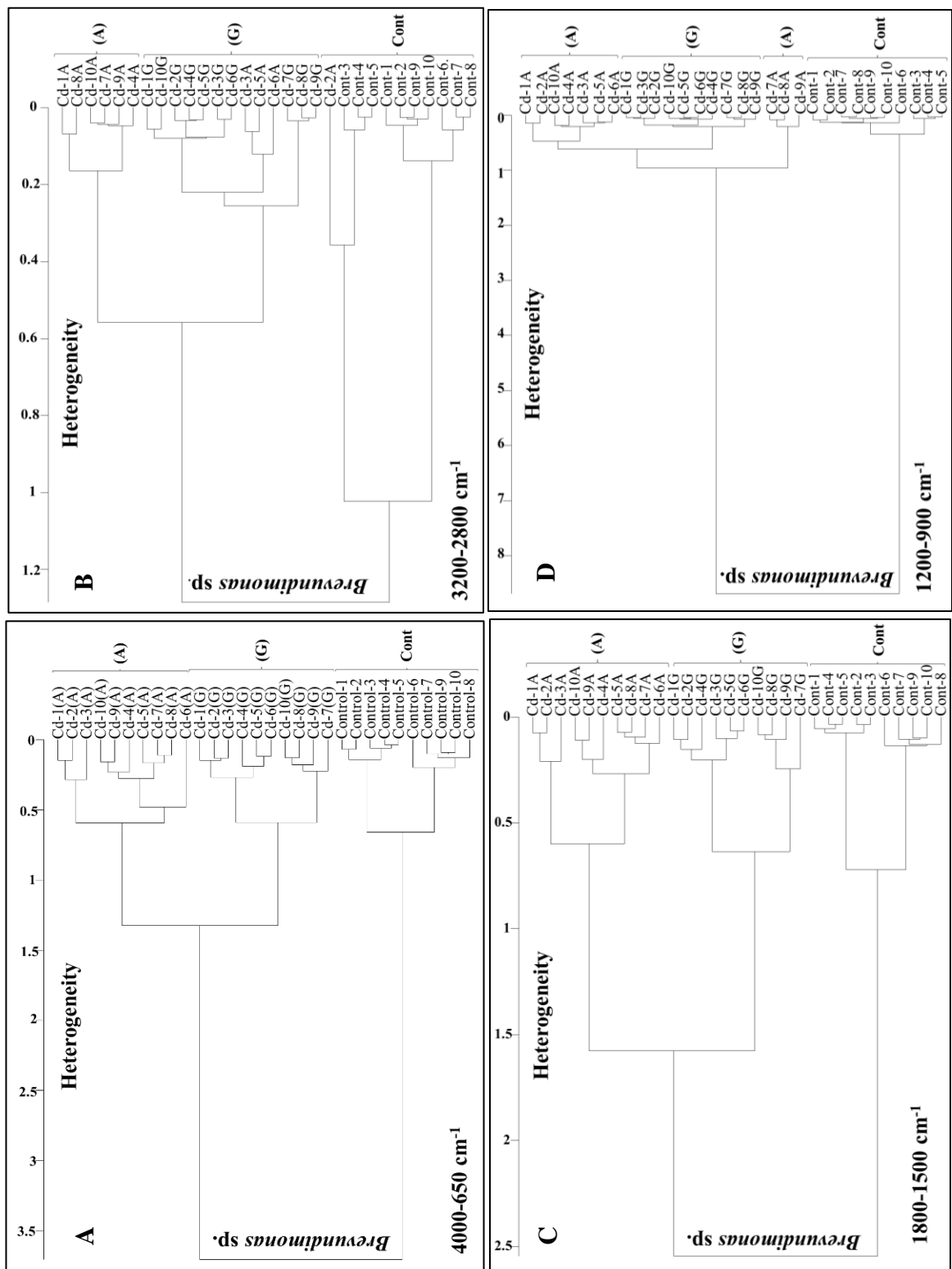


Figure 27. HCA of (A) whole, (B) lipid, (C) protein, and (D) carbohydrate region for Cd-acclimated (A: acute, G: gradual) and control *Brevundimonas sp.*

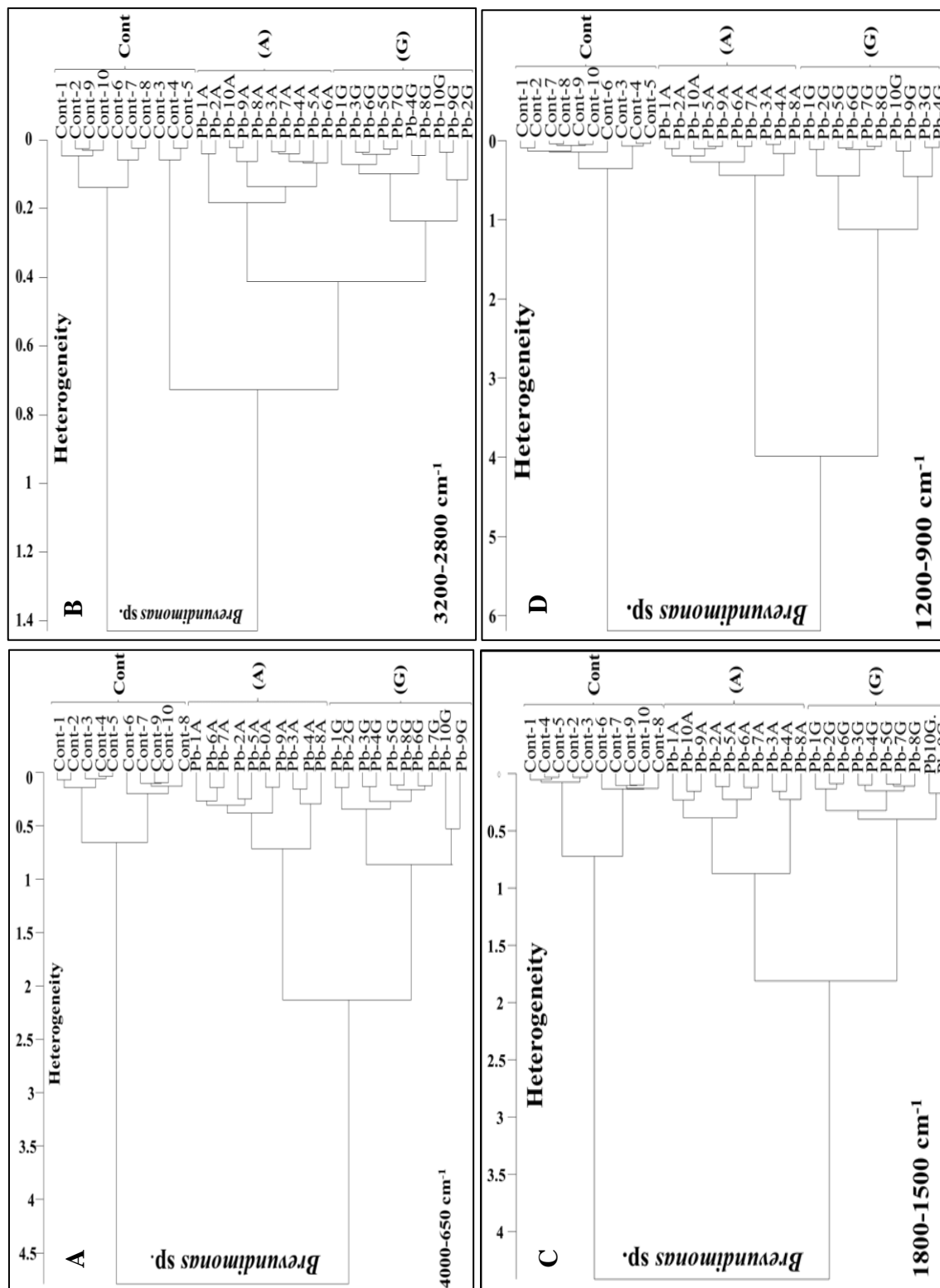


Figure 28. HCA of (A) whole, (B) lipid, (C) protein, and (D) carbohydrate region for Pb-acclimated (A: acute, G: gradual) and control *Brevundimonas* sp.

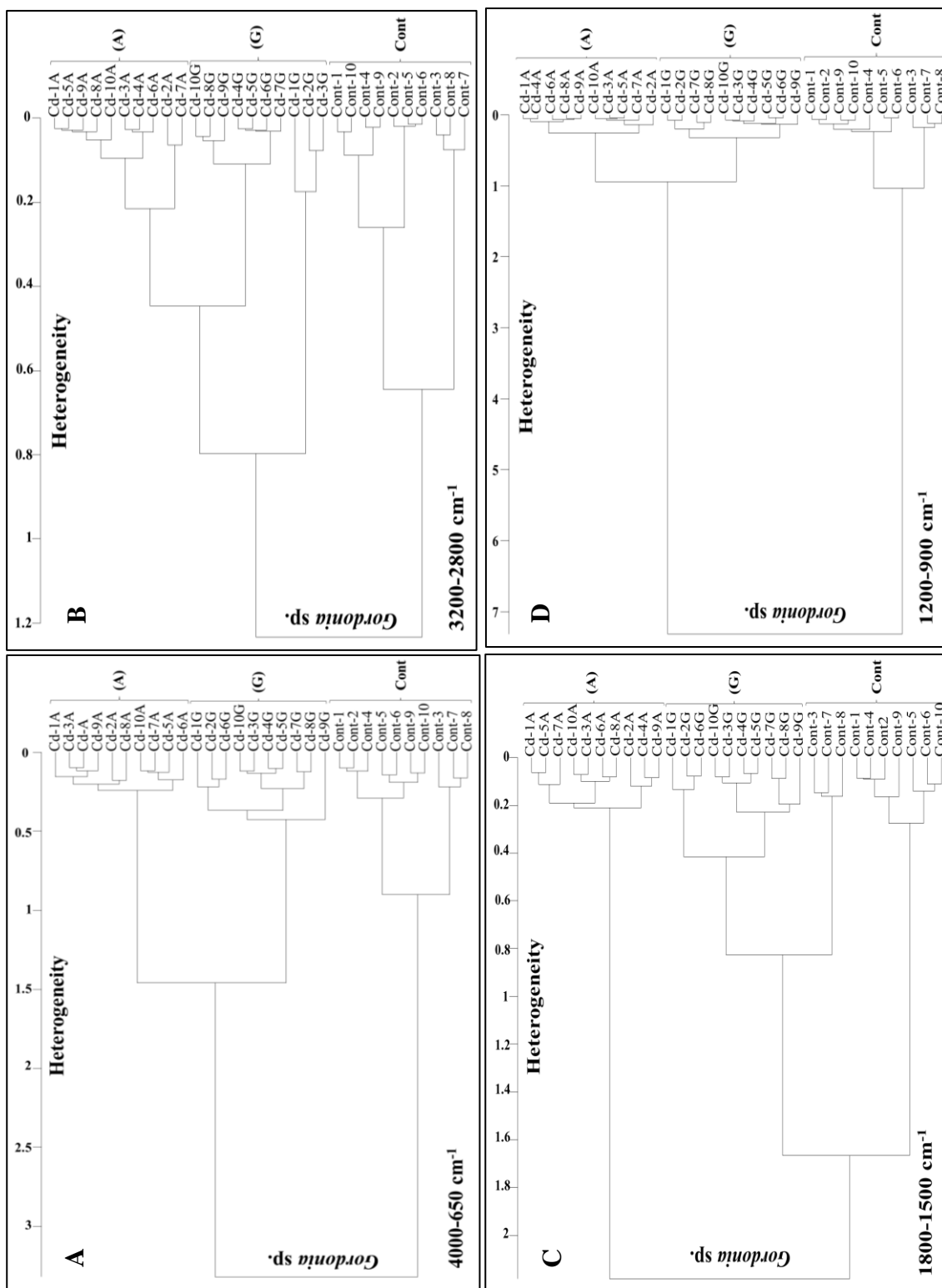


Figure 29. HCA of (A) whole, (B) lipid, (C) protein, and (D) carbohydrate region for Cd-acclimated (A: acute, G: gradual) and control *Gordonia* sp.

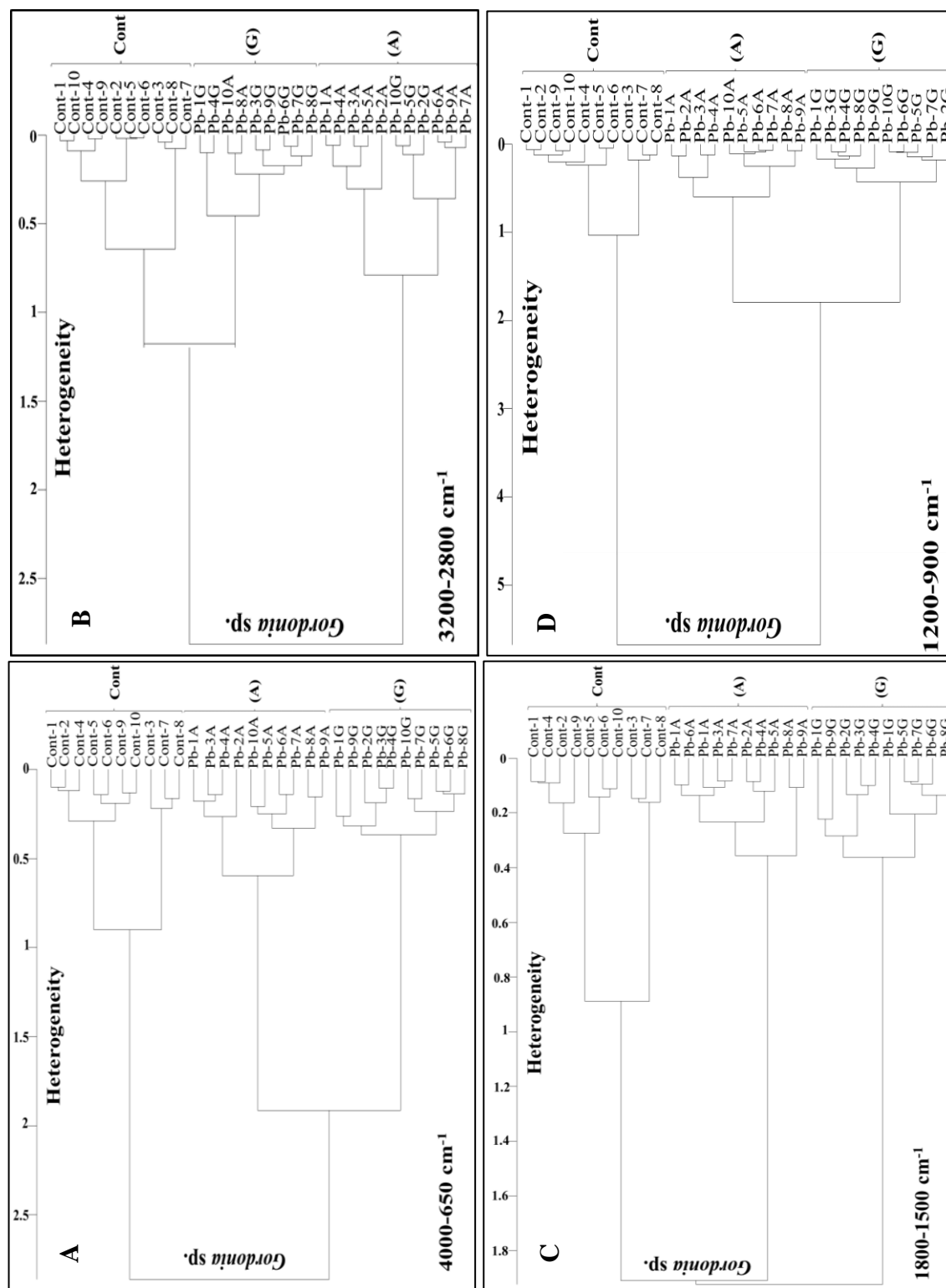


Figure 30. HCA of (A) whole, (B) lipid, (C) protein, and (D) carbohydrate region for Pb-acclimated (A: acute, G: gradual) and control *Gordonia* sp.

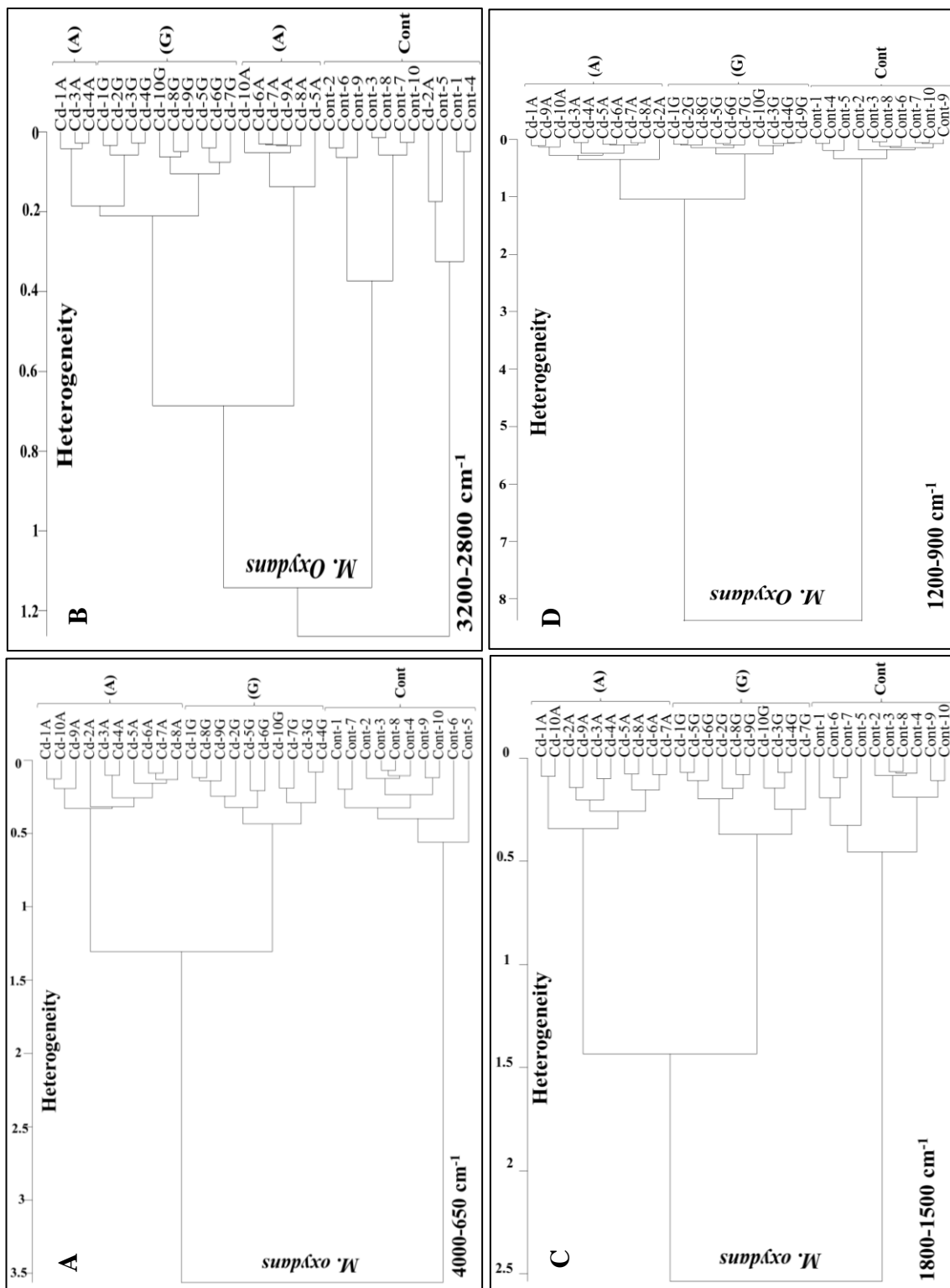


Figure 31. HCA of (A) whole, (B) lipid, (C) protein, and (D) carbohydrate region for Cd-acclimated (A: acute, G: gradual) and control *M. oxydans*

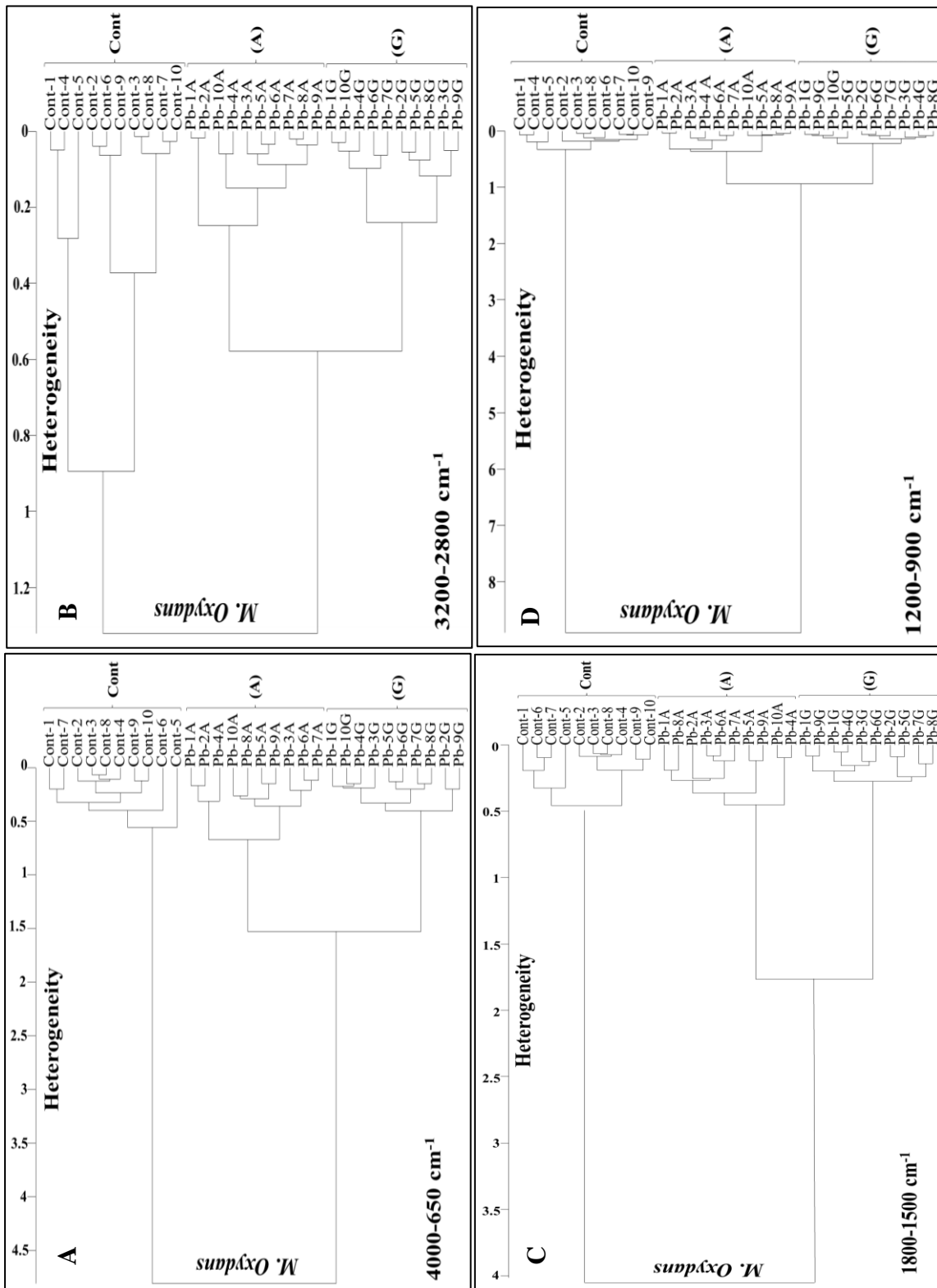


Figure 32. HCA of (A) whole, (B) lipid, (C) protein, and (D) carbohydrate region for Pb-acclimated (A: acute, G: gradual) and control *M. oxydans*

The information we have obtained through PCA and HCA on IR data revealed definite quantitative molecular changes upon acute or gradual exposure of bacteria to Cd or Pb. Bacterial strains exhibiting a high resistance to a particular heavy metal can be used to detoxify the polluted environments (Nithya et al., 2011; Ahluwalia & Goyal, 2007). When the concentration of applied heavy metal is gradually increasing in the environment, bacterial generations with higher metal resistance arise (Antonioli et al. 2007; Zaki & Farag, 2010). Since, acclimation leads to new and advanced features in microorganisms, in bioremediation processes, acclimated bacteria are preferred (Bestawy et al., 2013; Chang et al., 1995; Kumar et al., 2010; Kumar et al., 2011; Principia et al. 2006). One of the advanced features is the increase in the production of metal complexing biopolymers. These polymers serve in biosorption dependent bioremediation (Capdevila et al., 1994; Cols et al., 1997; Kermani et al., 2010; Klauser et al., 1990; Singh et al., 2011; Valls et al., 2000; Valls & Lorenzo, 2002). The information we generated in this study showed that the IR spectroscopy measurements along with PCA and HCA could be used to evaluate the bacteria regarding their features necessary for bioremediation.

CHAPTER 4

CONCLUSION

After extended exposure bacteria can be acclimated to live and grow in the existence of high heavy metal concentrations using several resistance mechanisms provided by the change in structure, composition, and the amount of molecules. In this study, we determined the differences in molecular changes took place in Cd or Pb-acclimated bacteria upon gradual or acute exposure via ATR-FTIR spectroscopy. We acclimated *Brevundimonas* sp., *Gordonia* sp. and *Microbacterium oxydans* for toxic Cd or Pb concentrations (higher than their minimum growth inhibitory concentrations). The significant changes were detected in concentrations of proteins, carbohydrates, and lipids. Structure and composition of bacterial membranes changed in acclimated groups. Changes in bacterial membranes included decreases in fatty acid and protein concentrations as well as the protein-to-lipid ratio. The saturated lipid concentrations were also affected. Total protein concentration decreased which could be caused by inhibition of synthesis. The increase in polysaccharide appeared to be due to the increase in exopolysaccharide production. In other words, *Brevundimonas* sp., *Gordonia* sp. and *M. oxydans* coped with toxic concentrations of Cd and Pb mainly through elevated exopolymer production. Moreover, acutely Cd-acclimated strains produced the significantly higher amount of polysaccharide and phospholipids than gradually acclimated ones. In lead exposure, production of polysaccharide and phospholipids were significantly higher in gradually acclimated strains. Further evaluation of spectroscopic data with PCA and HCA represented that acutely or gradually acclimated bacterial strains and control strains were discriminated from each other based on the bands in the whole, lipid, protein, and carbohydrate IR regions. The discrimination in lipid region was not as striking as to the discrimination in protein and carbohydrate regions indicating similarity in modifications. HCA gave the highest heterogeneity in carbohydrate regions. It proved

that most molecular changes happened in carbohydrate amounts arising from exopolymer production.

Metal resistance properties of bacteria have been used in bioremediation practices. Furthermore, acclimated bacteria are preferred, because acclimation leads to increase in production of metal complexing biopolymers suitable for biosorption purposes. In this study, we have shown that by using ATR-FTIR spectroscopy, we could determine the which bacteria would be suitable for bioremediation work. We have also shown how to physiologically modify bacteria through acclimation procedures for desired properties regarding their molecular profiles. In our study, for the first time, we proved that the molecular profiles of bacteria acclimated to the same metal concentration differ depending on whether the acclimation attained through gradual or acute exposure.

REFERENCES

Abdi, H., Williams, L. J. (2010). Principal component analysis. *Wiley & Sons, Inc.* (*wires.wiley.com/compstatsJohn*), 2: 433-459

Abou-Shanab, R. A. I., van Berkum, P., Angle, J. S. (2007). Heavy metal resistance and genotypic analysis of metal resistance genes in gram-positive and gram-negative bacteria present in Ni-rich serpentine soil and in the rhizosphere of *Alyssum murale*. *Chemosphere*, 68: 360-367.

Ahemad, M. (2014). Remediation of metalliferous soils through the heavy metal resistant plant growth promoting bacteria: Paradigms and prospects. *Arabian Journal of Chemistry*, xxx, xxx-xxx

Ahluwalia, S.S. & Goyal, D. (2007). Microbial and plant derived biomass for removal of heavy metals from wastewater. *Bioresource Technology*, 98: 2243-2257.

Aksoy, C., Guliyev. A., Kilic, E., Uckan, D., Severcan, F. (2012). Bone Marrow Mesenchymal Stem Cells in Patients with Beta-Thalassemia Major: Molecular Analysis with Attenuated Total Reflection-Fourier Transform Infrared Spectroscopy Study as a Novel Method. *Stem Cells and Development*, 21(11): 2000-2011.

Al-Qadiri, H. M., Al-Alami, N. I., Al-Holy, M. A., Rasco, B. A. (2008). Using Fourier Transform Infrared (FT-IR) Absorbance Spectroscopy and Multivariate Analysis to Study the Effect of Chlorine-Induced Bacterial Injury in Water. *J. Agric. Food Chem.*, 56: 8992-8997.

Alvarez-Ordóñez, A., Mouwen, D. J. M., López, M., Prieto, D. J. M. (2011). Fourier transform infrared spectroscopy as a tool to characterize molecular composition and stress response in foodborne pathogenic bacteria. *Journal of Microbiological Methods*, 84: 369-378.

Ami, D., Mereghetti, P., Doglia, S. M. (2012). Multivariate Analysis for Fourier Transform Infrared Spectra of Complex Biological Systems and Processes (Chapter 10). *Multivariate Analysis in Management, Engineering and the Sciences*, Intech.

Amoozegar, M. A., Ghazanfari, N. & Didari, M. (2012). Lead and cadmium bioremoval by *Halomonas* sp., an exopolysaccharideproducing halophilic bacterium. *Prog Biol Sci*, 2: 1–11.

Andrews J. M. (2001). Determination of minimum inhibitory concentrations. *J. Antimicrob. Chemother*, 48(1): 5-16.

Baker, M. J., Trevisan, J., Bassan, P., Bhargava, R., Butler, H. J., Dorling, K. M., Fielden, P. R., Fogarty, S. W., Fullwood, N. J., Heys, K. A., Hughes, C., Lasch, P., Martin-Hirsch, P. L., Obinaju, B., Sockalingum, G. D., Sulé-Suso, J., Strong, R. J., Walsh, M. J., Wood, B. R., Gardner, P., Martin, F. L. (2014). Using Fourier transform IR spectroscopy to analyze biological materials. *Nature Protocols*, 9: 1771-1791.

Bar, C., Patil, R., Doshi, J., Kulkarni, M. J., Gade, W. N. (2007). Characterization of the proteins of bacterial strain isolated from contaminated site involved in heavy metal resistance - A proteomic approach. *Journal of Biotechnology*, 128: 444-451.

Bhaskar PV, Bhosle NB (2006) Bacterial extracellular polymeric substances (EPS) a carrier of heavy metals in the marine food-chain. *Environ Int* 32:192–198.

Bramhachari, P., Dubey, S. K. (2006). Isolation and characterization of exopolysaccharide produced by *Vibrio harveyi* VB23. *Lett Appl Microbiol*, 43: 571-577.

Bramhachari, P. V., Kavi Kishor, P. B., Ramadevi, R., Kumar, R., Rao, B. R., Dubey, S.K. (2007). Isolation and characterization of mucous exopolysaccharide produced by *Vibrio furnissii* VB0S3. *J Microbiol Biotechnol*, 17: 44-51.

Brereton, R. G. (2003). *Chemometrics: data analysis for the laboratory and chemical plant*. Wiley.

Bröker, D., Arenskotter, M., Legatzki, A., Nies, D. H., Steinbüchel, A. (2004). Characterization of the 101-Kilobase-Pair Megaplasmid pKB1, Isolated from the Rubber-Degrading Bacterium *Gordonia westfalica* Kb1. *Journal of Bacteriology*, 186(1): 212-225.

Bröker, D., Arenskötter, M., Steinbüchel, A. (2008). Transfer of megaplasmid pKB1 from the rubber-degrading bacterium *Gordonia westfalica* strain Kb1 to related bacteria and its modification. *Appl Microbiol Biotechnol*, 77: 1317-1327.

Bruins M. R., Kapil S., Oehme M., K. (2000). Microbial resistance to metals in the environment. *Ecotoxicology and Environmental Safety*, 45: 198-207.

Burgula, Y., Khali, Y., Kim, S., Krishnan, S. S., Cousin, M. A., Gore, J P., Reuhs B. L., Mauer, L. J. (2007). Review of mid-infrared Fourier Transform-Infrared Spectroscopy applications for bacterial detection. *Journal of Rapid Methods & Automation in Microbiology*, 15: 146-175.

Cakmak, G., Togan, I., Severcan F. (2006). 17 β -Estradiol induced compositional, structural and functional changes in rainbow trout liver, revealed by FT-IR spectroscopy: A comparative study with nonylphenol. *Aquatic Toxicology*, 77: 53-63.

Cakmak, G., Togan, I., Uguz, C., Severcan F. (2003). FT-IR Spectroscopic Analysis of Rainbow Trout Liver Exposed to Nonylphenol. *Applied Spectroscopy*, 57(7): 835-841.

Campbell, I. D., & Dwek, R. A. (1984). *Biological spectroscopy*. Benjamin/Cummings Pub. Co.

Capdevila, M., Cols, N., Romero-Isart, N., González-Duarte, R., Atrian, S., González-Duarte, P. (1997). Recombinant synthesis of mouse Zn³-β and Zn⁴-α metallothionein 1 domains and characterization of their cadmium(II) binding capacity. *Cellular and Molecular Life Sciences*, 53(8): 681-688.

Chaturvedi A.K., Mishra A, Tiwari, V., Jha, B. (2012) Cloning and transcript analysis of type2 metallothionein gene (*SbMT 2*) from extreme halophyte *Salicornia brachiata* and its heterologous expression in *E. coli*. *Gene*; 499:280-287.

Chang, D., Fukushi, K., Ghosh, S. (1995). Stimulation of activated sludge cultures for enhanced heavy metal removal. *Water Environment Research*, 67 (5): 822-827.

Chen, H., Ferrari, C., Angiulib, M., Yaoa, J., Raspic, C., Bramantib, E. (2010). Qualitative and quantitative analysis of wood samples by Fourier transform infrared spectroscopy and multivariate analysis. *Carbohydrate Polymers*, 82: 772-778.

Chudobova, D., Dostalovaa, S., Ruttkay-Nedeckya, B., Gurana, R., Rodrigoa, M. A. M., Tmejovaa, K., Krizkovaa, S., Zitkaa, O., Adama, V., Kizek, R. (2015). The effect of metal ions on *Staphylococcus aureus* revealed by biochemical and mass spectrometric analyses. *Microbiological Research*, 170: 147–156.

Choudhary, S., & Sar, P. (2009). Characterization of a metal resistant *Pseudomonas* sp. isolated from uranium mine for its potential in heavy metal (Ni²⁺, Co²⁺, Cu²⁺, and Cd²⁺) sequestration. *Bioresource Technology*, 100: 2482-2492.

Comte, S., Gilles Guibaud, G., Baudu, M. (2006). Biosorption properties of extracellular polymeric substances (EPS) resulting from activated sludge according to their type: Soluble or bound. *Process Biochemistry*, 41: 815–823.

Cols, N., Romero-Isart, N., Capdevila, M., Oliva, B., González-Duarte, P., González-Duarte, R., Atrian, S. (1997). Binding of excess cadmium(II) to Cd7-metallothionein from recombinant mouse Zn7-metallothionein 1. UV-VIS absorption and circular dichroism studies and theoretical location approach by surface accessibility analysis. *J. Inorg. Biochem*, 68(3): 157-166.

Davis R. & Mauer L. J. (2010). Fourier transform infrared (FT-IR) spectroscopy: A rapid tool for detection and analysis of foodborne pathogenic bacteria. *Current research, technology and education topics in applied microbiology and microbial biotechnology*, 2: 1582-1594.

Dziubaa, B., Babuchowskia, A., Nalecz, D., Niklewicz, M. (2007). Identification of lactic acid bacteria using FTIR spectroscopy and cluster analysis. *International Dairy Journal*, 17:183–189.

European Committee for Antimicrobial Susceptibility Testing (EUCAST) of the European Society of Clinical Microbiology of the Infectious Diseases (ESCMID). (2003). Determination of Minimum Inhibitory Concentrations (MIC) of Antibacterial Agents by Broth Dilution. *Clinical microbiology and infection*, 9(8): 1-7.

Freire-Nordi, C. S., Vieira, A. A. H., Nakaie, C. R., Nascimento, O. R. (2005). Effect of polysaccharide capsule of the microalgae *Staurastrum iversenii* var. *americanum* on diffusion of charged and uncharged molecules, using EPR technique. *Braz J Phys*, 36: 75–82.

Gaigneaux, A., Ruyschaert, J. M., Goormaghtigh, E. (2006). Cell Discrimination by Attenuated Total Reflection–Fourier Transform Infrared Spectroscopy: The Impact of Preprocessing of Spectra. *Applied Spectroscopy*, 60: 1022-1028.

Gaonkar, T., & Bhosle, S. (2013). Effect of metals on a siderophore-producing bacterial isolate and its implications on microbial assisted bioremediation of metal contaminated soils. *Chemosphere*, 93: 1835–1843.

Garip, S., Bozoglu, F., Severcan, F. (2007). Differentiation of Mesophilic and Thermophilic Bacteria with Fourier Transform Infrared Spectroscopy. *Applied Spectroscopy*, 61: 186-192.

Garip, S., Gozen, A. C., Severcan, F. (2009). Use of Fourier transform infrared spectroscopy for rapid comparative analysis of Bacillus and Micrococcus isolates. *Food Chemistry*, 113: 1301–1307.

Gibbons, S. M., Feris, K., Mc Guirl, M. A., Morales, S. E., Hynninen, A., Ramsey, P. W., Gannon, J. E. (2011). Use of microcalorimetry to determine the costs and benefits to *Pseudomonas putida* strain kt2440 of harboring cadmium efflux genes. *Appl Environ Microbiol*, 77:108-113.

Guan L. L., & Kamino K. (2001). Bacterial response to siderophore and quorum-sensing chemical signals in the seawater microbial community. *BMC Microbiology*, 1:27

Guan, L. L., Onuki, H., Kamino, K. (2000). Bacterial Growth Stimulation with Exogenous Siderophore and Synthetic *N*-Acyl Homoserine Lactone Autoinducers under Iron-Limited and Low-Nutrient Conditions. *Applied and Environmental Microbiology*, 66(7): 2797-2803.

Guibaud, G., Comte, S., Bordas, F., Dupuy, S., Baudu, M. (2005). Comparison of the complexation potential of extracellular polymeric substances (EPS), extracted from activated sludges and produced by pure bacteria strains, for cadmium, lead, and nickel. *Chemosphere*, 59: 629-638.

Guibaud, G., Hullebusch, E., Bordas, F. (2006). Lead and cadmium biosorption by extracellular polymeric substances (EPS) extracted from activated sludges: pH-sorption edge tests and mathematical equilibrium modelling. *Chemosphere*, 64: 1955-1962.

Guibaud, G., Tixier, N., Bouju, A., Baudu, M. (2003). Relation between extracellular polymers, composition and its ability to complex Cd, Cu and Pb. *Chemosphere*, 52: 1701-1710.

Guo, H., Luo, S., Chen, L., Xiao, X., Xi, Q., Wei, W., Zeng, G., Liu, C., Wana, Y., Chen, J., He, Y. (2010). Bioremediation of heavy metals by growing hyper accumulator endophytic bacterium *Bacillus* sp. L14. *Bioresource Technology*, 101: 8599-8605.

Gupta, A., Whitton, B. A., Morby, A. P., Huckle, J. W., Robinson, N. J. (1992). Amplification and rearrangement of a prokaryotic metallothionein locus, *smt* in *Synechococcus* PCC 6301 selected for tolerance to cadmium. *Proc. Roy. Soc. B*, 248: 273-281.

Gupta, A., Morby, A.P., Turner, J.S., Whinon, B. A., Robinson, N. J. (1993). Deletion within the metallothionein locus of cadmium tolerant *Synechococcus* PCC 6301 involving a highly iterated palindrome (HIP1). *Mol. Microbiol*, 7: 189-195.

Ha, J., Ge'laber, A., Spormann, A. M., Brown Jr., G. E. (2010). Role of extracellular polymeric substances in metal ion complexation on *Shewanella oneidensis*: Batch uptake, thermodynamic modeling, ATR-FTIR, and EXAFS study. *Geochimica et Cosmochimica Acta*, 74: 1-15.

Haris, P. I., & Severcan, F. (1999). FTIR spectroscopic characterization of protein structure in aqueous and non-aqueous media. *Journal of Molecular Catalysis B: Enzymatic*, 7: 207-221.

Harrison, J. J., Ceri, H., Turner, R. J. (2007). Multimetal resistance and tolerance in microbial biofilms. *Nat. Rev. Microbiol.*, 5: 928-938.

Hassan, M., Lelie, D., Springael, D., Römling, U., Ahmed, N., Mergeay, M. (1999). Identification of a gene cluster, *czr*, involved in cadmium and zinc resistance in *Pseudomonas aeruginosa*. *Gene*, 238: 417-425.

Hassen, A., Saidi, N., Cherif, M., Boudabous, A. (1998). Resistance of environmental bacteria to heavy metals. *Bioresource Tenchnology*, 64: 7-15.

Helm, D., & Naumann, D. (1995). Identification of some bacterial cell components by FT-IR Spectroscopy. *FEMS Microbiology Letters*, 126: 75-80.

Helm, D., Labischinski, H., Challehand, G., Naumann, D. (1991). Classification and identification of bacteria by Fourier-transform infrared Spectroscopy. *Journal of General Microbiology*, 137: 69-79.

Helm, D., Labischinski, H., Naumann, D. (1991). Elaboration of a procedure for identification of bacteria using Fourier-Transform IR spectral libraries: a stepwise correlation approach. *Journal of Microbiological Methods*, 14: 127-142.

Hoostal, M. J., Bidart-Bouzat, M. G., Bouzat, J. L. (2008). Local adaptation of microbial communities to heavy metal stress in polluted sediments of Lake Erie. *FEMS Microbiology Ecology*, 65: 156-168.

Hori, R., & Sugiyama, J. (2003). A combined FT-IR microscopy and principal component analysis on softwood cell walls. *Carbohydrate Polymers*, 52: 449-453.

Howlett, N. G., & Avery, S. V. (1997). Induction of Lipid Peroxidation during Heavy Metal Stress in *Saccharomyces cerevisiae* and Influence of Plasma Membrane Fatty Acid Unsaturation. *Applied and Environmental Microbiology*, 63(8): 2971-2976.

Hynninen, A. (2010). Zinc, cadmium and lead resistance mechanisms in bacteria and their contribution to biosensing. Academic Dissertation in Microbiology, *Department of Food and Environmental Sciences Faculty of Agriculture and Forestry University of Helsinki*, Academic Dissertation in Microbiology.

Imlay, J. A., Chin, S. M., Linn, S. (1988). Toxic DNA damage by hydrogen peroxide through the Fenton reaction *in vivo* and *in vitro*. *Science*, 240: 640-642.

Iyer, A., Mody, K., Jha. B. (2005). Biosorption of heavy metals by a marine bacterium. *Marine Pollution Bulletin*, 50: 340-343.

Jarosláwiecka, A., & Piotrowska-Seget Z. (2014). Lead resistance in micro-organisms. *Microbiology*, 160: 12-25.

Jayanthi, B., Emenike, C. U., Auta, S. H., Agamuthu, P., Fauziah, S. H. (2016). Characterization of induced metal responses of bacteria isolates from active non-sanitary landfill in Malaysia. *International Biodeterioration & Biodegradation*, 1-9.

Ji. G., & Silver. S. (1995). Bacterial resistance mechanisms for heavy metals of environmental concern. *Journal of Industrial Microbiology*, 14: 61-75.

Jiménez-Galisteo, G, Fusté, E., Muñoz, E., Vinuesa, T., Villa, TG., Benz, R., Domínguez, A., Viñas, M. (2017). Identification and characterization of a cell wall

porin from *Gordonia jacobaea*. *J Gen Appl Microbiol.*, Advanced publication, Full paper: 1-8.

Joshi, P., & Juwarkar, A. (2009). In Vivo Studies to Elucidate the Role of Extracellular Polymeric Substances from *Azotobacter* in Immobilization of Heavy Metals. *Environ. Sci. Technol.*, 43: 5884-5889.

Kamnev, A. A. (2008). FTIR spectroscopic studies of bacterial cellular responses to environmental factors, plant-bacterial interactions, and signaling. *Spectroscopy*, 22: 83-95.

Kazarian, S. G., Chan, K. L. (2006). Applications of ATR-FTIR spectroscopic imaging to biomedical samples. *Biochim Biophys Acta*, 1758: 858-867.

Kermani, A. J. N., Ghasemi, M. F., Khosravan, A., Farahmand, A., Shakibaie, M. R. (2010). Cadmium bioremediation by metal-resistant mutated bacteria isolated from active sludge of industrial effluent. *Iran. J. Environ. Health. Sci. Eng.*, 7(4): 279-286.

Khan. S., Hesham. A., Qiao. M., Rehman. S., He. J-Z. (2010). Effects of Cd and Pb on soil microbial community structure and activities. *Environ Sci Pollut Res*, 17: 288-296.

Khan. Z., Nisar, M. A, Hussain, S. Z., Arshad, M. A., Rehman, A. (2015). Cadmium resistance mechanism in *Escherichia coli* P4 and its potential use to bioremediate environmental cadmium. *Appl Microbiol Biotechnol*, 99(24): 10745-10757.

Khan. Z., Rehman, A., Hussain. S. Z., Nisar, M. A., Zulfiqar, S., Shakoori, A. R. (2016). Cadmium resistance and uptake by bacterium, *Salmonella enterica* 43C, isolated from industrial effluent. *AMB Express*, 6(1): 54 1-16.

Klaassen, C. D., Liu, J., Diwan, B. A. (2009). Metallothionein protection of cadmium toxicity. *Toxicol Appl Pharmacol*, 238: 215-20.

Klauser, T., Pohlner, J., Meyer, T. F. (1990). Extracellular transport of cholera toxin B subunit using Neisseria IgA protease beta-domain: conformation-dependent outer membrane translocation. *The EMBO Journal*, 9(6): 1991-1999.

Kim, S., Reuhs, B. L., Mauer, L. J. (2005). Use of Fourier transform infrared spectra of crude bacterial lipopolysaccharides and chemometrics for differentiation of *Salmonella enterica* serotypes. *Journal of Applied Microbiology*, 99: 411-417.

Kniggendorf A., Gaul, T. W., Meinhardt-Wollweber, M. (2011). Hierarchical Cluster Analysis (HCA) of Microorganisms: An Assessment of Algorithms for Resonance Raman Spectra. *Applied Spectroscopy*, 65(2): 165-173.

Kumar, A., Bisht, B. S., Joshi, V. D. (2010). Biosorption of Heavy Metals by four acclimated microbial species, *Bacillus* spp., *Pseudomonas* spp., *Staphylococcus* spp. and *Aspergillus niger*. *J. Biol. Environ. Sci.*, 4 (12): 97-108.

Kumar, A., Bisht, B. S., Joshi, V. D. (2011). Bioremediation potential of three acclimated bacteria with reference to heavy metal removal from waste. *International Journal of Environmental Sciences*, 2 (2): 896-908.

Kuroda, K., Shibasaki, S., Ueda, M., Tanaka, A. (2001). Cell surface-engineered yeast displaying a histidine oligopeptide (hexa-His) has enhanced adsorption of and tolerance to heavy metal ions. *Appl. Microbiol Biotechnol*, 57: 697-701.

Lambert, P. A. (2002). Cellular impermeability and uptake of biocides and antibiotics in Gram-positive bacteria and mycobacteria. *Journal of Applied Microbiology Symposium Supplement*, 92: 46S-54S.

Lasch, P., Haensch, W., Naumann, D., Diem, M. (2004). Imaging of colorectal adenocarcinoma using FT-IR microspectroscopy and cluster analysis. *Biochimica et Biophysica Acta - Molecular Basis of Disease*, 1688: 176-186.

Lavine, B. K. (2000). Chemometrics. *Anal. Chem.*, 72 (12): 91-98.

Lemire, J. A., Harrison. J. J., Turner, R. J. (2013). Antimicrobial activity of metals: mechanisms, molecular targets and applications. *Nature Reviews: Microbiology*, 11: 371-384.

Liebert, C. A., Barkay, T., Turner, R. R. (1991). Acclimation of Aquatic Microbial Communities to Hg(II) and CH₃Hg⁺ in Polluted Freshwater Ponds. *Microb. Ecol.*, 21: 139-149.

Lin, M., Al-Holy, M., Al-Qadiri, H., Kang, D. H., Cavinato, A. G., Huang, Y., Rasco, B. A. (2004). Discrimination of intact and injured *Listeria monocytogenes* by Fourier transform infrared spectroscopy and principal component analysis. *J. Agric. Food Chem.*, 52: 5769-5777.

De Luca, M., Terouzi, W., Ioele, G., Kzaiber, F., Oussama, A., Oliverio, F., Tauler, R., Ragno, G. (2011). Derivative FTIR spectroscopy for cluster analysis and classification of morocco olive oils. *Food Chemistry*, 124: 1113-1118.

Madigan, M., Martinko, J., Bender, K., Buckley, D., Stahl, D. Brock Biology of Microorganisms (Global edition). *Pearson, Fourteenth edition*, pp: 200-201.

Marcelli, A., Cricenti, A., Kwiatek, W. M., Petibois, C. (2012). Biological applications of synchrotron radiation infrared spectromicroscopy (Research review paper). *Biotechnology Advances*, 30: 1390-1404.

Markowicz. A., Płociniczak. T., Piotrowska-Seget. Z. (2010). Response of Bacteria to Heavy Metals Measured as Changes in FAME Profiles. *Polish J. of Environ. Stud.*, 19 (5): 957-965.

Mariey, L., Signolle, J. P., Amiel, C., Travert, J. (2001). Discrimination, classification, identification of microorganisms using FTIR spectroscopy and chemometrics (Review). *Vibrational Spectroscopy*, 26: 151-159.

Maquelin, K., Kirschner, C., Choo-Smith, L.-P., van den Braak, N., Endtz, H.Ph., Naumann, D., Puppels, G. J. (2002). Identification of medically relevant microorganisms by vibrational spectroscopy. *Journal of Microbiological Methods*, 51: 255-271.

Masoudzadeha, N., Alidousta, L., Samiea, N., Hajfarajollaha, H., Sharafia, H., Modiria, S., Zahiria, H. S., Valib, H., Noghabia, K. A. (2014). Distinctive protein expression patterns of the strain *Brevundimonas* sp. ZF12 isolated from the aqueous zone containing high levels of radiation to cadmium-induced stress. *Journal of Biotechnology*, 186: 49-57.

Masoudzadeha, N., Zakeria, F., Lotfabada, T., Sharafia, H., Masoomia, F., Zahiria, H. S., Ahmadiana, G., Noghabia, K. A. (2011). Biosorption of cadmium by *Brevundimonas* sp. ZF12 strain, a novel biosorbent isolated from hot-spring waters in high background radiation areas. *Journal of Hazardous Materials*, 197: 190-198.

Mathe, I., Benedek, T., Tancsics, A., Palatinszky, M., Lanyi, S., Marialigeti, K. (2012). Diversity, activity, antibiotic and heavy metal resistance of bacteria from petroleum hydrocarbon contaminated soils located in Harghita County (Romania). *International Biodeterioration & Biodegradation*, 73: 41-49.

Matyar, F., Kaya, A., Dinçer, S. (2008). Antibacterial agents and heavy metal resistance in Gram-negative bacteria isolated from seawater, shrimp and sediment in Iskenderun Bay, Turkey. *Science of the Total Environment*, 407: 279-285.

Maynaud, G., Brunel, B., Yashiro, E., Mergeay, M., Cleyet-Marel, J-C., Le Que´re, A. (2014). CadA of *Mesorhizobium metallidurans* isolated from a zinc-rich mining soil is a PIB-2-type ATPase involved in cadmium and zinc resistance. *Research in Microbiology*, 165: 175-189.

Mecozzi, M., Pietroletti, M., Di Mento, R. (2007). Application of FTIR spectroscopy in ecotoxicological studies supported by multivariate analysis and 2D correlation spectroscopy. *Vibrational Spectroscopy*, 44: 228-235.

Mendelsohn, R. M. H. (1986). *Fourier transform infrared studies of lipidprotein interaction, Progress in Protein-Lipid Interactions* (vol 2). Netherlands: Elsevier Science Publishers.

Mergeay, M., Monchy, S., Vallaey, T., Auquier, V., Bentomane, A., Bertin, P., Taghavi, S., Dunn, J., van der Lelie, D., Wattiez, R. (2003). *Ralstonia metallidurans*, a bacterium specifically adapted to toxic metals: towards a catalogue of metal responsive genes. *FEMS Microbiol. Rev.*, 27: 385-410.

Mitra, R.S., Gray, R.H., Chin, B., and Bernstein, I.A. (1975). Molecular mechanisms of accommodation in *Escherichia coli* to toxic levels of Cd²⁺. *J Bacteriol*, 121: 1180-1188.

Morillo, J. A., Aguilera. M., Ramoz-Cormenzana, A., Monteoliva, S. M. (2006). Production of metal-binding exopolysaccharide by *Paenibacillus jamilae* using two-phase olive-mill waste as fermentation substrate. *Curr Microbiol*, 53: 189-193.

Movasaghi, Z., Rehman, S., Rehman, I. (2008) Fourier Transform Infrared (FTIR) Spectroscopy of Biological Tissues. *Applied Spectroscopy Reviews*, 43: 134-179.

Naik, M. M., Pandey, A., Dubey, S. K. (2012). Biological characterization of lead-enhanced exopolysaccharide produced by a lead resistant *Enterobacter cloacae* strain P2B. *Biodegradation*, 23: 775-783.

Naik, M. M., & Dubey, S. K. (2013). Lead resistant bacteria: Lead resistance mechanisms, their applications in lead bioremediation and biomonitoring. *Ecotoxicology and Environmental Safety*, 98: 1-7.

Naumann, D., Schultz, C., Helm, D. 1996. What can infrared spectroscopy tell us about the structure and composition of intact bacterial cells. In *Infrared Spectroscopy of Biomolecules* (H.H. Mantsch and D. Chapman, eds.), pp. 279–310, Wiley-Liss, New York, NY.

Naumann, D. (2000). Infrared Spectroscopy in Microbiology. *Encyclopedia of Analytical Chemistry*.

Naumann, D. (2001). FT-Infrared and FT-Raman spectroscopy in biomedical research. *Applied Spectroscopy Reviews*, 36(2&3): 239-298.

Naumann, D., Fijala, V., Labischinski, H., Giesbrech, P. (1988). The Rapid Differentiation and Identification of Pathogenic Bacteria Using Fourier Transform Infrared Spectroscopic and Multivariate Statistical Analysis. *Journal of Molecular Structure*, 174: 165-170.

Naumann, D., Keller, S., Helma, D., Schultz, C., Schrader, B. (1995). FT-IR Spectroscopy and FT-Raman Spectroscopy are powerful analytical tools for the non-invasive characterization of intact microbial cells. *Journal of Molecular Structure*, 347: 399-406.

Nedelkova, M., Merroun, M., L., Rossberg, A., Hennig, C., Selenska-Pobell, S. (2007). Microbacterium isolates from the vicinity of a radioactive waste depository and their interactions with uranium. *FEMS Microbiol Ecol*, 59: 694-705.

Nichols, P. D., Henson, J. M., Guckert, J. B., Nivens, D. E., White, D. C. (1985). Fourier transform-infrared spectroscopic methods for microbial ecology: analysis of bacteria, bacteria-polymer mixtures, and biofilms. *Journal of Microbiological Methods*, 4: 79-94.

Nies, D. H. (1992). Resistance to Cadmium, Cobalt, Zinc, and Nickel in Microbes. *Plasmid*, 27: 17-28.

Nies, D. H. & Silver, S. (1995). Ion efflux systems involved in bacterial metal resistance. *Journal of Industrial Microbiology*, 14: 186-199.

Nies, D. H. (1999). Microbial heavy-metal resistance. *Appl Microbiol Biotechnol*, 51: 730-750.

Nithya, C., Gnanalakshmi, B., Shunmugiah K. P. (2011). Assessment and characterization of heavy metal resistance in Palk Bay sediment bacteria. *Marine Environmental Research*, 71: 283-294.

Oust, A., Møretro, T., Kirschner, C., Narvhus, N. A., Kohler, A. (2004). Evaluation of the robustness of FT-IR spectra of lactobacilli towards changes in the bacterial growth conditions. *FEMS Microbiology Letters*, 239: 111-116.

Oust, A., Møretro, T., Kirschner, C., Narvhus, N. A., Kohler, A. (2004). FT-IR spectroscopy for identification of closely related lactobacilli. *Journal of Microbiological Methods*, 59: 149-162.

Ozaktas, T., Taskin, B., Gozen, A., G. (2012). High level multiple antibiotic resistance among fish surface associated bacterial populations in non-aquaculture freshwater environment. *Water Research*, 46: 6382-6390.

Ozek, N. S., Tuna, S., Erson-Bensan A. E., Severcan, F. (2010). Characterization of microRNA-125b expression in MCF7 breast cancer cells by ATR-FTIR spectroscopy. *Analyst*, 135: 3094-3102.

Ozek, N., Bal, B., Sara Y., Onur, R., Severcan, F. (2014). Structural and functional characterization of simvastatin-induced myotoxicity in different skeletal muscles. *Biochimica et Biophysica Acta*, 1840: 406-415.

Pagès, D., Sanchez, L., Conrod, S., Gidrol, X., Fekete, A., Schmitt-Kopplin, P., Heulin, T., Achouak, W. (2007). Exploration of intracolonial adaptation mechanisms of *Pseudomonas brassicacearum* facing cadmium toxicity. *Environmental Microbiology*, 9(11): 2820-2835.

Preisner, O., Lopes, J. A., Menezes, J. C. (2008). Uncertainty assessment in FT-IR spectroscopy based bacteria classification models. *Chemometrics and Intelligent Laboratory Systems*, 94: 33–42.

Preisner, O., Menezes J. C., Guiomar, R., Machado, J., Lopes, J. A. (2012). Discrimination of *Salmonella enterica* serotypes by Fourier transform infrared spectroscopy. *Food Research International*, 45: 1058-1064.

Principia, P., Villab, F., Bernasconib, M., Zanardinia, E. (2006). Metal toxicity in municipal wastewater activated sludge investigated by multivariate analysis and in situ hybridization. *Water Res*, 40: 99-106.

Popat, R., Harrison, F., McNally, L., Williams, P., Diggle, S. P. (2017). Environmental modification via a quorum sensing molecule influences the social landscape of siderophore production. *Proceedings of the Royal Society B, Biological Sciences*, 284(1852): 1-6.

Riddle, J. W., Kabler, P. W., Kenner, B. A., Bordner, R. H., Rockwood, S. W., Stevens, H. J. R. (1956). Bacterial identification by Infrared Spectrophotometry. *Journal of Bacteriology*, 72(5): 593-603.

Ringnér, M. (2008). What is principal component analysis? *Nature Biotechnology*, 26 (3): 303-304.

Rodriguez-Saona, L. E., Khambaty, F. M., Fry, F. S., Dubois, J., Calvey, E. M. (2004). Detection and Identification of Bacteria in a Juice Matrix with Fourier Transform–Near

Infrared Spectroscopy and Multivariate Analysis. *Journal of Food Protection*, 67(11): 2555-2559.

Roosa, S., Wattiez, R., Prygiel, E., Lesven, L., Billon, G., Gillan, D. C. (2014). Bacterial metal resistance genes and metal bioavailability in contaminated sediments *Environmental Pollution*, 189: 143-151.

Rouch, D. A., Lee, B. T. D., Morby, A. P. (1995). Understanding cellular responses to toxic agents: A model for mechanism choice in bacterial metal resistance. *Journal of Industrial Microbiology*, 14: 132-141.

Rusak, D. A., Brown, L. M., Martin, S. D. (2003). Classification of Vegetable Oils by Principal Component Analysis of FTIR Spectra. *Journal of chemical education*, 80 (5): 541-543.

Sabdon, A. (2011). Cadmium removal by a bio-reducing coral bacterium *Pseudoalteromonas* sp. strain CD15 isolated from the tissue of coral *Goniastrea aspera*, jepra water. *J Coastal Develop*, 13: 81-91.

Salehizadeh, H. & Shojaosadati, S. A. (2003). Removal of metal ions from aqueous solution by polysaccharide produced from *Bacillus firmus*. *Water Res*, 37: 4231-4235.

Sanchez-Castro, I., Amador-García, A., Moreno-Romero, C., Lopez-Fernandez, M., Phommavanh, V., Nos, J., Descostes, Merroun, M. M. (2016). Screening of bacterial strains isolated from uranium mill tailings porewaters for bioremediation purposes. *Journal of Environmental Radioactivity*, 1-12.

Schirawski, J., Hagens, W., Fitzgerald, G. F., van Sinderen, D. (2002). Molecular characterization of cadmium resistance in *Streptococcus thermophilus* strain 4134: an example of lateral gene transfer. *Appl Environ Microbiol*, 68: 5508-5516.

Schuster, K. C., Mertens, F., Gapes, J. R. (1999). FTIR spectroscopy applied to bacterial cells as a novel method for monitoring complex biotechnological processes. *Vibrational Spectroscopy*, 19: 467-477.

Severcan, F., Bozkurt, O., Gurbanov, R., Gorgulu, G. (2010). FT-IR spectroscopy in diagnosis of diabetes in rat animal model. *Journal of Biophotonics*, 3: 621-631.

Singh, R., Kumar, A., Kirrolia, A., Kumar, R., Yadav, N., Bishnoi, N. R., Lohchab, R. K. (2011). Removal of sulphate, COD and Cr(VI) in simulated and real wastewater by sulphate reducing bacteria enrichment in small bioreactor and FTIR study. *Bioresource Technology*, 102: 677-682.

Staley, C., Johnson, D., Gould, T. J., Wang, P., Phillips, P., James B. Cotner, J. B., Sadowsky, M. J. (2015). Frequencies of heavy metal resistance are associated with land cover type in the Upper Mississippi River. *Science of the Total Environment*, 511: 461-468.

Stuart, B., & Ando, D. J. (1997). *Biological applications of infrared spectroscopy*. Published on behalf of ACOL (University of Greenwich) by John Wiley.

Stuart, B. H. (2004). *Infrared Spectroscopy: Fundamentals and Applications*. J. Wiley.

Stintzi, A., Evans, K., Meyer J-M., Poole, K. (1998). Quorum-sensing and siderophore biosynthesis in *Pseudomonas aeruginosa*: *lasR/lasI* mutants exhibit reduced pyoverdine biosynthesis. *FEMS Microbiology Letters*, 166: 341-345.

Stohs, S. J., Bagchi, D. (1995). Oxidative mechanisms in the toxicity of metal ions. *Free Radic. Biol. Med*, 18: 321–336.

Tchounwou, P. B., Yedjou, C. G., Patlolla, A. K., Sutton, D. J. (2012). Heavy Metals Toxicity and the Environment. *Molecular, Clinical and Environmental Toxicology*, 101: 133-164.

Tzeng, D. & Berns, R. S. (2005). A Review of Principal Component Analysis and Its Applications to Color Technology. *Color research and application*, 30(2): 84-98.

Ullah, A., Heng, S., Munis, M. F. H., Fahad, S., Yang, X. (2015). Phytoremediation of heavy metals assisted by plant growth promoting (PGP) bacteria: A review. *Environmental and Experimental Botany*, 117: 28-40.

U.S. Pharmacopeia. Microbiological Best Laboratory Practices, <117>. USP 36-NF 31, 2013.

Valls, M., Lorenzo, V., Gonzalez-Duarte, R., Atrian, S. (2000). Engineering outer-membrane proteins in *Pseudomonas putida* for enhanced heavy-metal bioadsorption. *Journal of Inorganic Biochemistry*, 79: 219-223.

Valls, M. & Lorenzo, V. (2002). Exploiting the genetic and biochemical capacities of bacteria for the remediation of heavy metal pollution: Review. *FEMS Microbiology Reviews*, 26: 327-338.

Vega, L. M., Mathieu, J., Yang, Y., Pyle, B., McLean, R. J. C., Alvarez, P. J. J. (2014). Nickel and cadmium ions inhibit quorum sensing and biofilm formation without affecting viability in *Burkholderia multivorans*. *International Biodeterioration & Biodegradation*, 91: 82-87.

Wang, L., & Mizaikoff, B. (2008). Application of multivariate data-analysis techniques to biomedical diagnostics based on mid-infrared spectroscopy. *Analytical and Bioanalytical Chemistry*, 391: 1641-54.

Warnes, S. L., Caves, V., Keevil, C. W. (2012). Mechanism of copper surface toxicity in *Escherichia coli* O157:H7 and *Salmonella* involves immediate membrane depolarization followed by slower rate of DNA destruction which differs from that observed for Gram-positive bacteria. *Environ. Microbiol*, 14: 1730-1743.

Watcharamusika, A., Prapagdeea, B., Thavipokeb P., Boontanob, N. (2008). The Role of Exopolymers in Protection of *Ralstonia* sp., a Cadmium-resistant Bacterium, from Cadmium Toxicity. *Environment Asia*, 2: 37-42.

Wei, X., Fang, L., Cai, P., Huang, Q., Chen, H., Liang, W., Rong, X. (2011). Influence of extracellular polymeric substances (EPS) on Cd adsorption by bacteria. *Environmental Pollution*, 159: 1369-1374.

Wiegand, I., Hilpert, K., Hancock, R. E. W. (2008). Agar and broth dilution methods to determine the minimal inhibitory concentration (MIC) of antimicrobial substances. *Nature Protocols*, 3(2): 163-175.

Wenning, M., & Scherer, S. (2013). Identification of microorganisms by FTIR spectroscopy: perspectives and limitations of the method. *Appl Microbiol Biotechnol*, 97: 7111-7120.

Xie, P., Hao, X., Herzberg, M., Luo, Y., Nies, D. H., Wei, G. (2015). Genomic analyses of metal resistance genes in three plant growth promoting bacteria of legume plants in Northwest mine tailings, China. *Journal of Environmental Sciences*, 27: 179-187.

Xiong, W., Zeng, Z., Zhang, Y., Ding, X., Sun, Y. (2015). Fate of metal resistance genes in arable soil after manure application in a microcosm study. *Ecotoxicology and Environmental Safety*, 113: 59-63.

Xue, J., Lee, C., Wakeham, S. G., Armstrong, R. A. (2011). Using principal components analysis (PCA) with cluster analysis to study the organic geochemistry of sinking particles in the ocean. *Organic Geochemistry*, 42: 356-367.

Yoon, K. P. (2003). Construction and Characterization of Multiple Heavy Metal-Resistant Phenol-Degrading Pseudomonads Strains. *J. Microbiol. Biotechnol*, 13(6): 1001-1007.

Yue, Z-B., Li, Q., Li, C-C., Chen, T., Wang. J. (2015). Component analysis and heavy metal adsorption ability of extracellular polymeric substances (EPS) from sulfate reducing bacteria. *Bioresource Technology*, 194: 399-402.

YU. P. (2005). Applications of Hierarchical Cluster Analysis (CLA) and Principal Component Analysis (PCA) in Feed Structure and Feed Molecular Chemistry Research, Using Synchrotron-Based Fourier Transform Infrared (FTIR) Microspectroscopy *J. Agric. Food Chem.*, 53: 7115-7127.

Zeng, X., Tang, J., Liu, X., Jiang, P. (2012). Response of *P. aeruginosa* E1 gene expression to cadmium stress. *Curr Microbiol*, 65: 799-804.

Zhai, Q., Yin, R., Yu, L., Wang, G., Tian, F., Yu, R., Zhao, J., Liu, X., Chen, Y. Q., Zhang, H., Chen, W. (2015). Screening of lactic acid bacteria with potential protective effects against cadmium toxicity. *Food Control*, 54: 23-30.

APPENDIX A

IR spectra of Cd or Pb-acclimated (acute: A, gradual: G) and control groups of *Brevundimonas* sp. *Gordonia* sp., and *M. oxydans* in the 4000-650 cm^{-1} spectral region

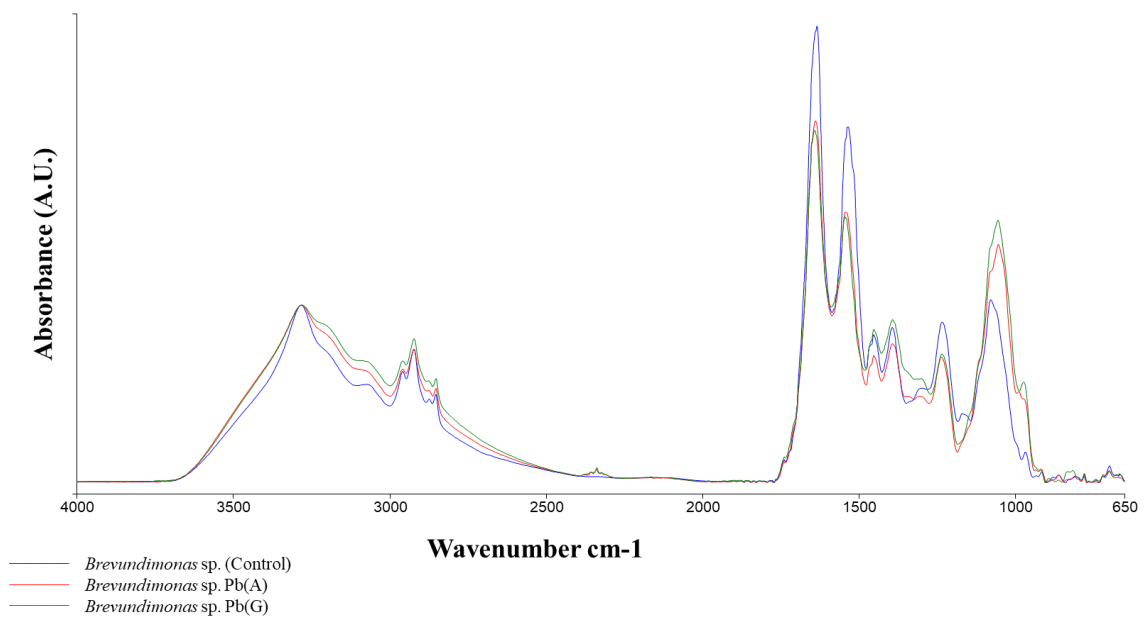


Figure A1. ATR-FTIR spectra of Pb-acclimated (acute: A, gradual: G) and control groups of *Brevundimonas* sp. in the 4000-650 cm^{-1} spectral region

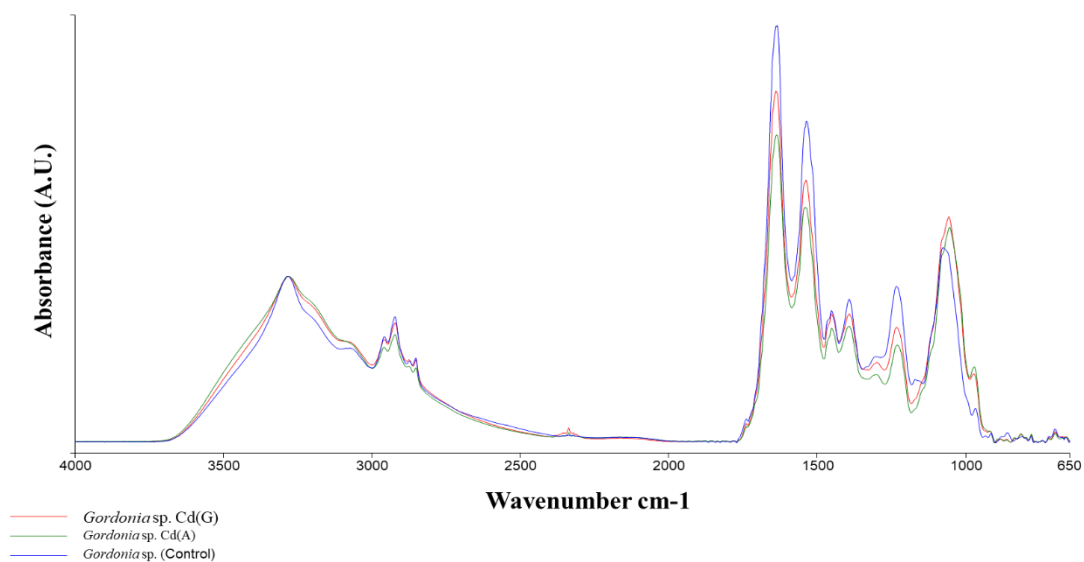


Figure A2. ATR-FTIR spectra of Cd-acclimated (acute: A, gradual: G) and control groups of *Gordonia* sp. in the 4000-650 cm⁻¹ spectral region

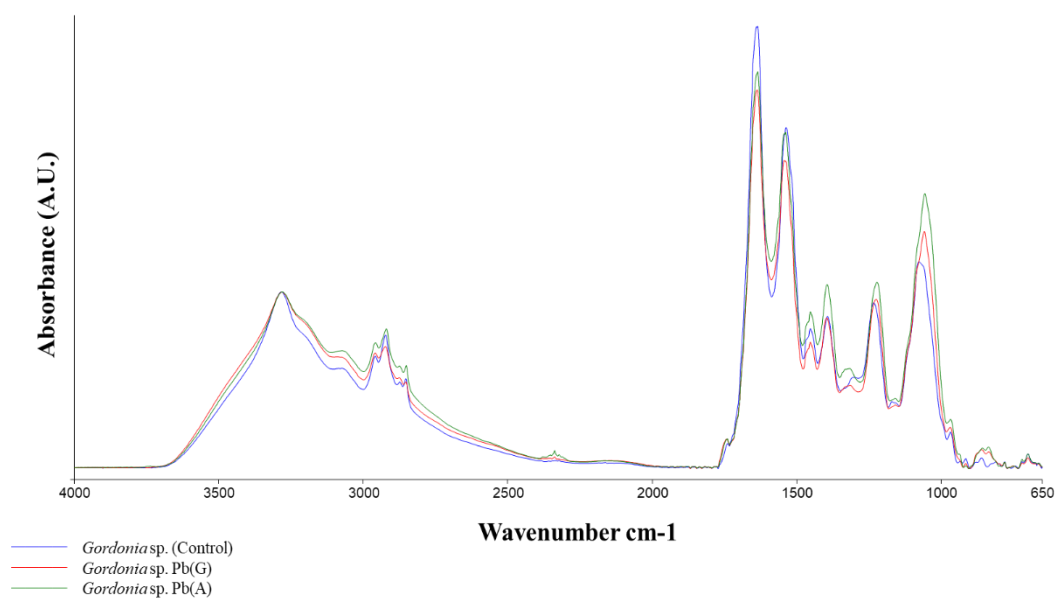


Figure A3. ATR-FTIR spectra of Pb-acclimated (acute: A, gradual: G) and control groups of *Gordonia* sp. in the 4000-650 cm⁻¹ spectral region

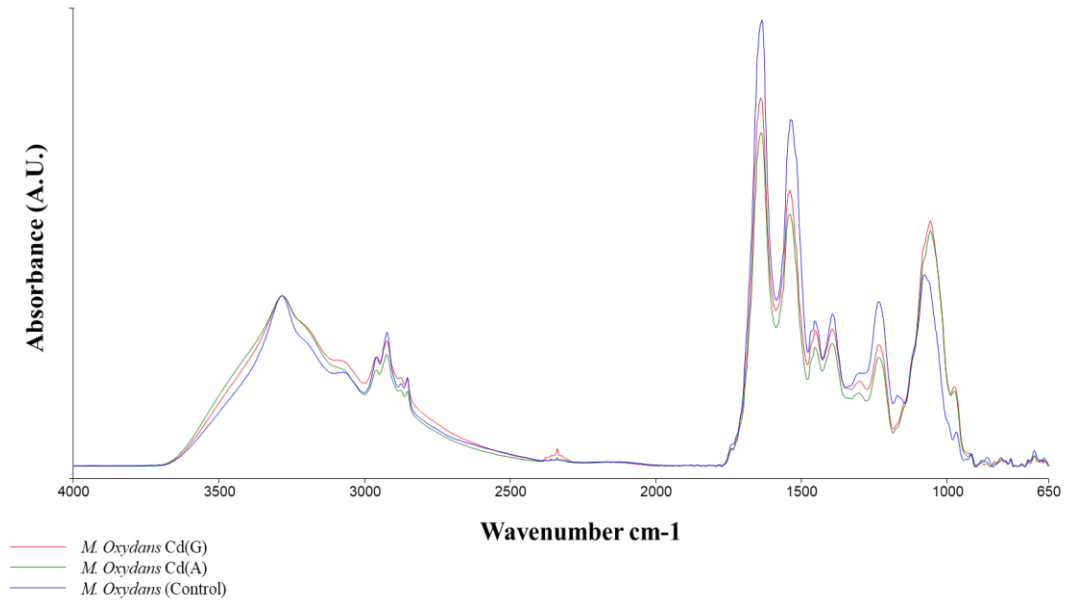


Figure A4. ATR-FTIR spectra of Cd-acclimated (acute: A, gradual: G) and control groups of *M. oxydans* in the 4000-650 cm^{-1} spectral region

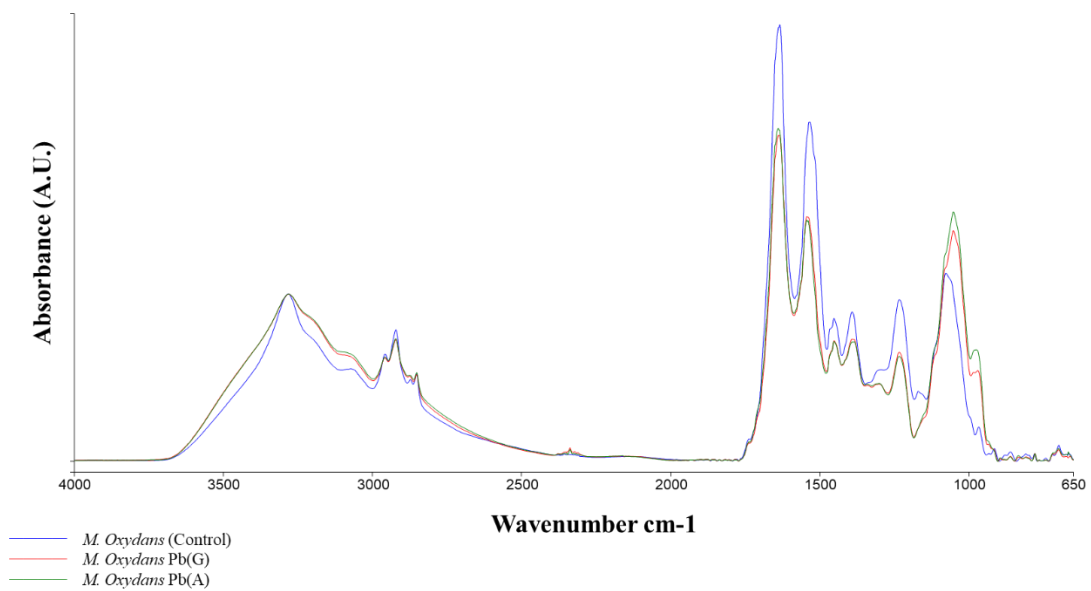
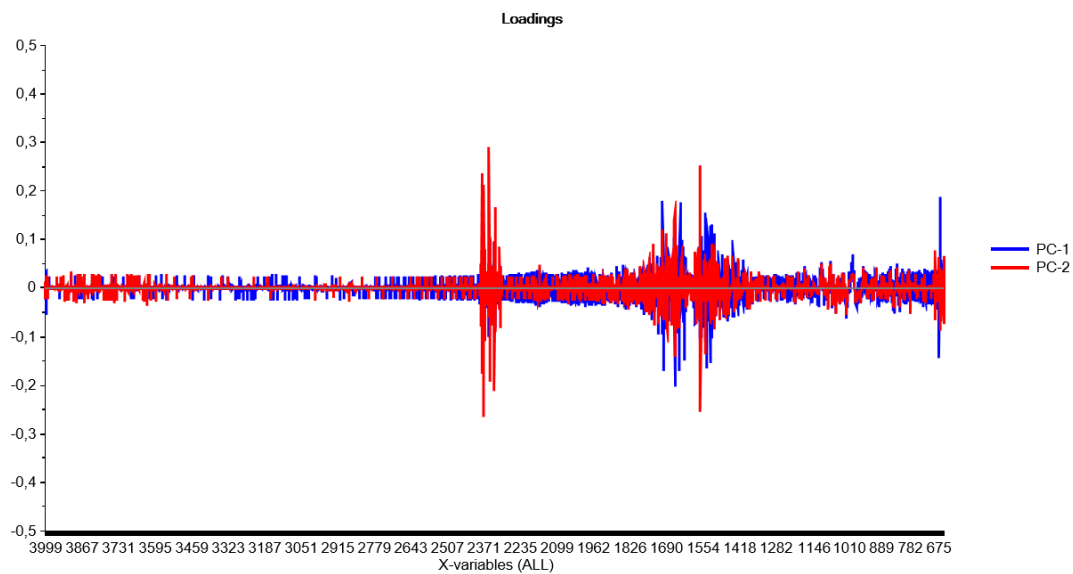


Figure A5. ATR-FTIR spectra of Pb-acclimated (acute: A, gradual: G) and control groups of *Gordonia* sp. in the 4000-650 cm^{-1} spectral region

APPENDIX B

PCA loading plots of cadmium or lead exposed (acute, gradual) and control *Brevundimonas* sp., *Gordonia* sp., and *M. oxydans*

A



B

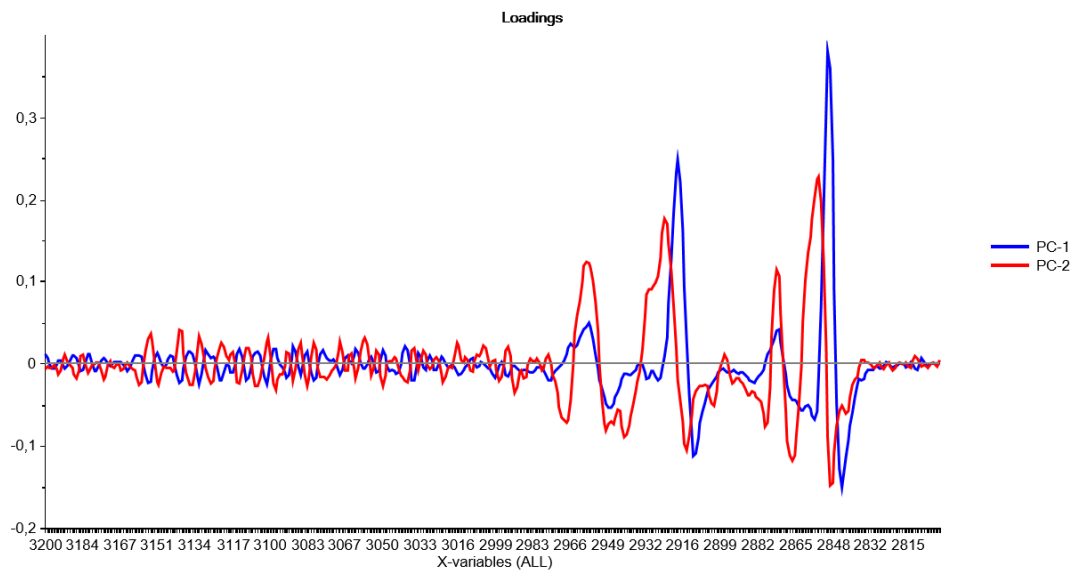
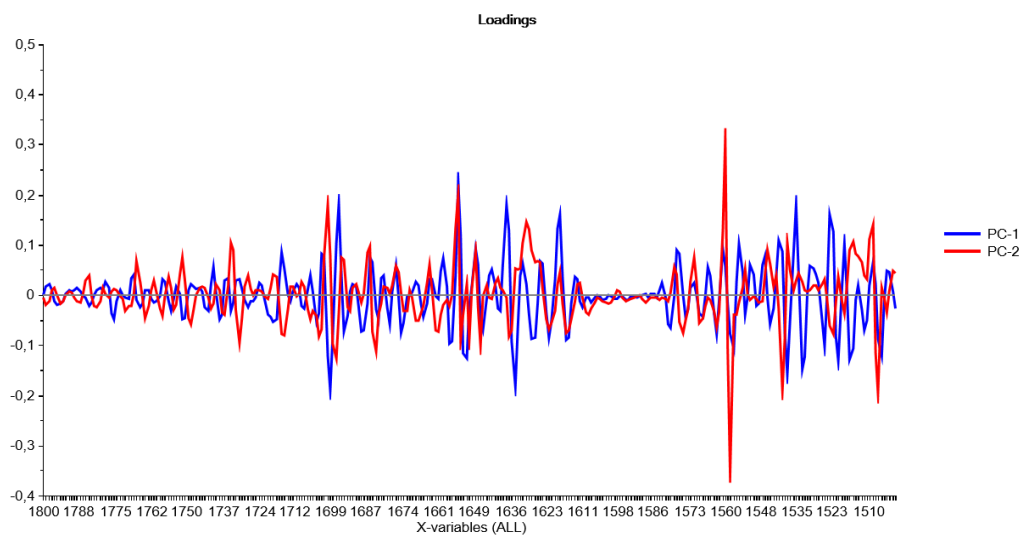


Figure B1. PCA loadings of cadmium exposed (acute, gradual) and control *Brevundimonas* sp. A- whole spectral region ($4000\text{-}650\text{ cm}^{-1}$), B- lipid region ($3200\text{-}2800\text{ cm}^{-1}$)

C



D

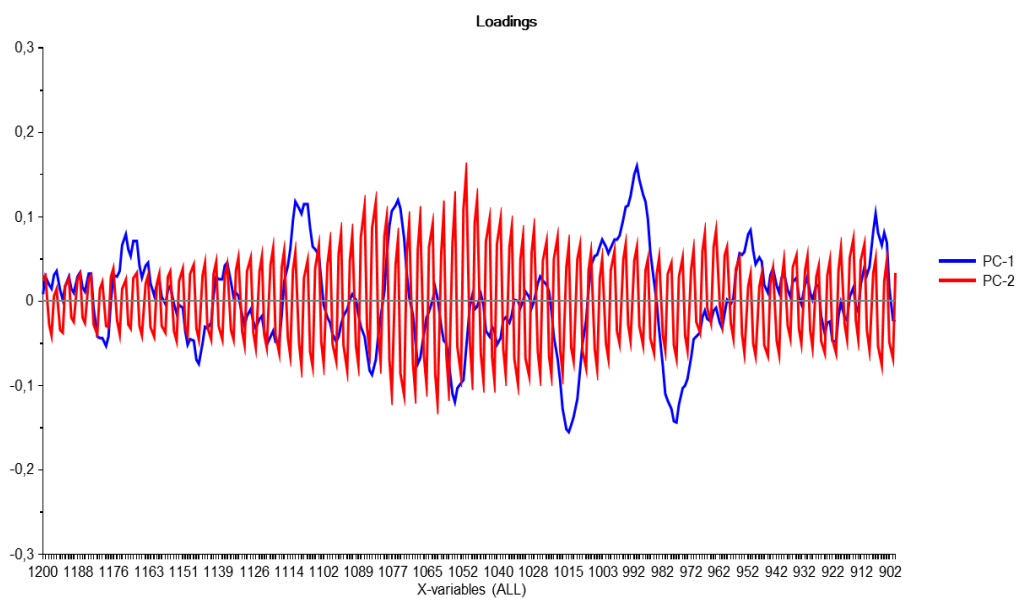


Figure B1 cont. PCA loadings of cadmium exposed (acute, gradual) and control *Brevundimonas* sp. A- protein region (1800-1500 cm^{-1}), B- carbohydrate region (1200-900 cm^{-1})

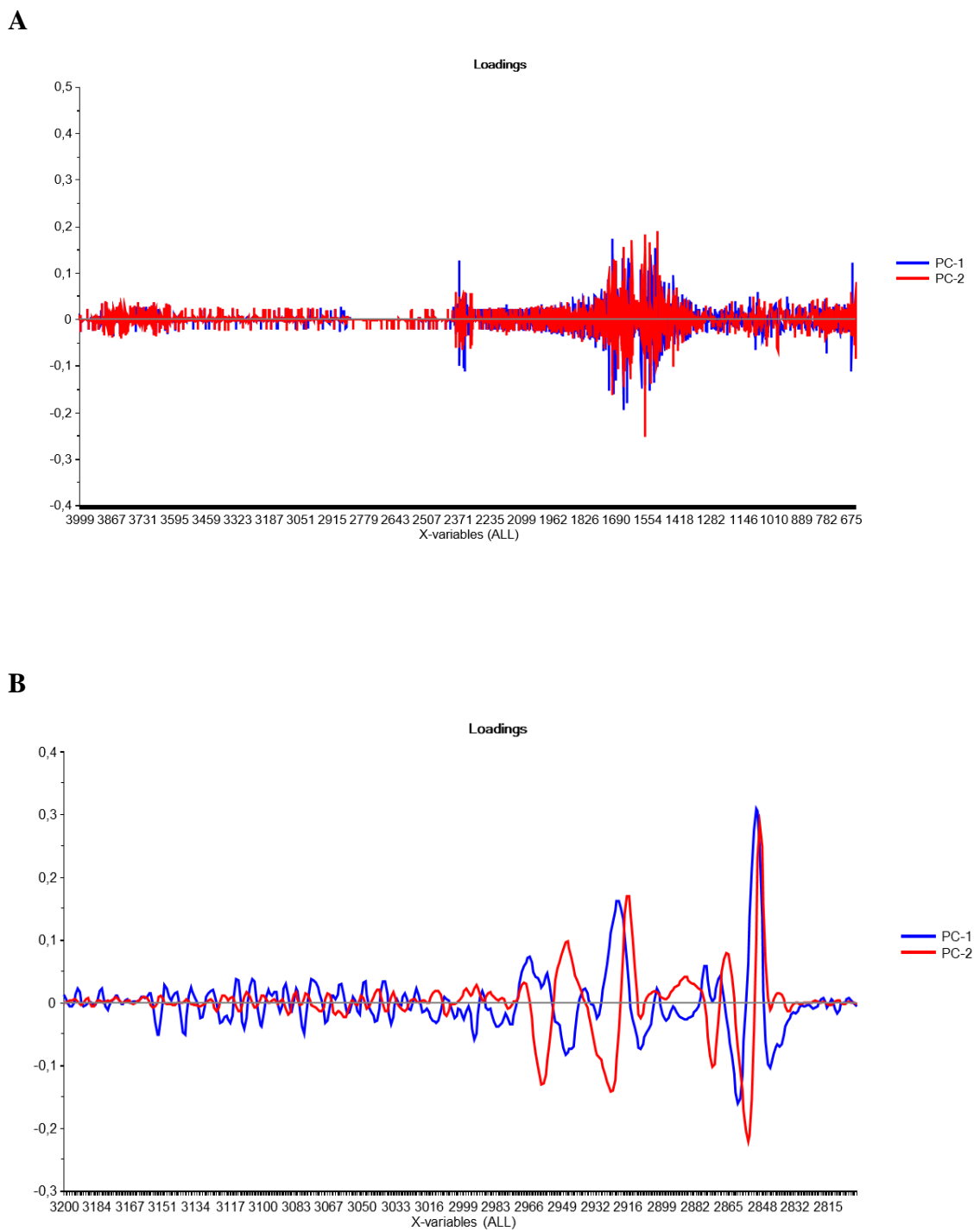
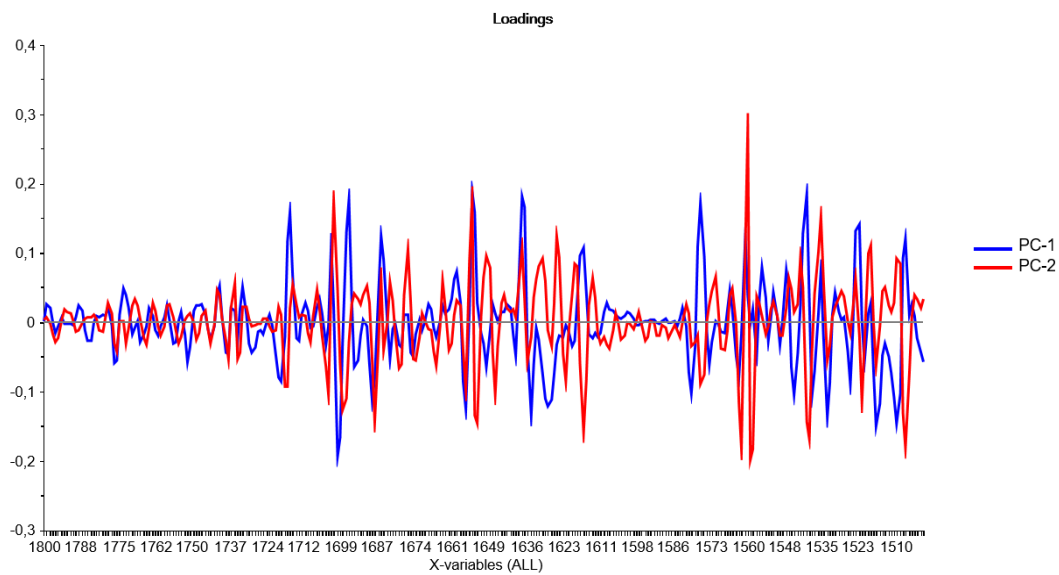


Figure B2. PCA loadings of lead exposed (acute, gradual) and control *Brevundimonas* sp. A- whole spectral region ($4000\text{-}650\text{ cm}^{-1}$), B- lipid region ($3200\text{-}2800\text{ cm}^{-1}$)

C



D

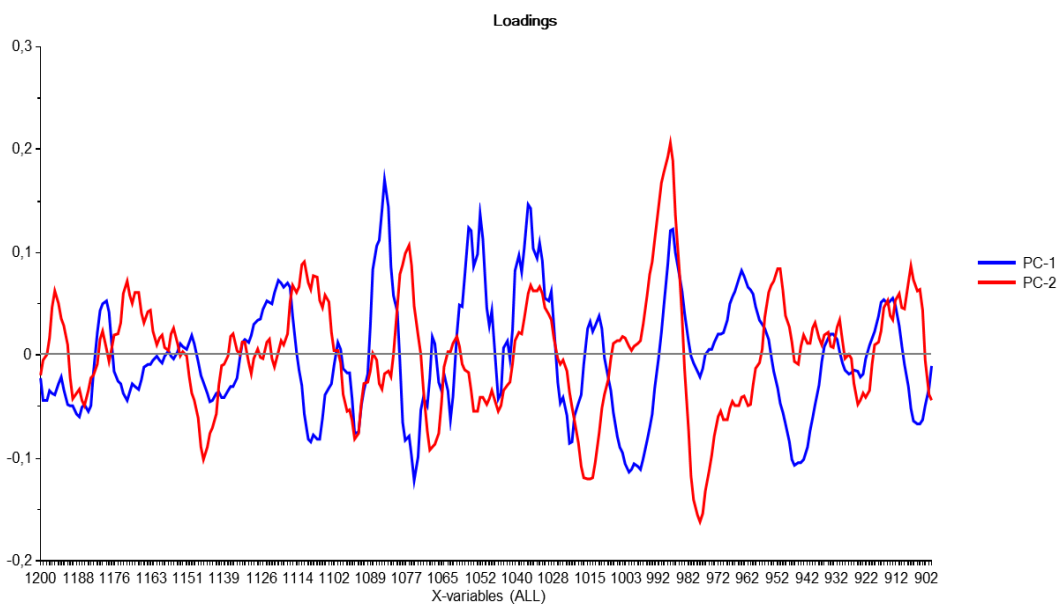
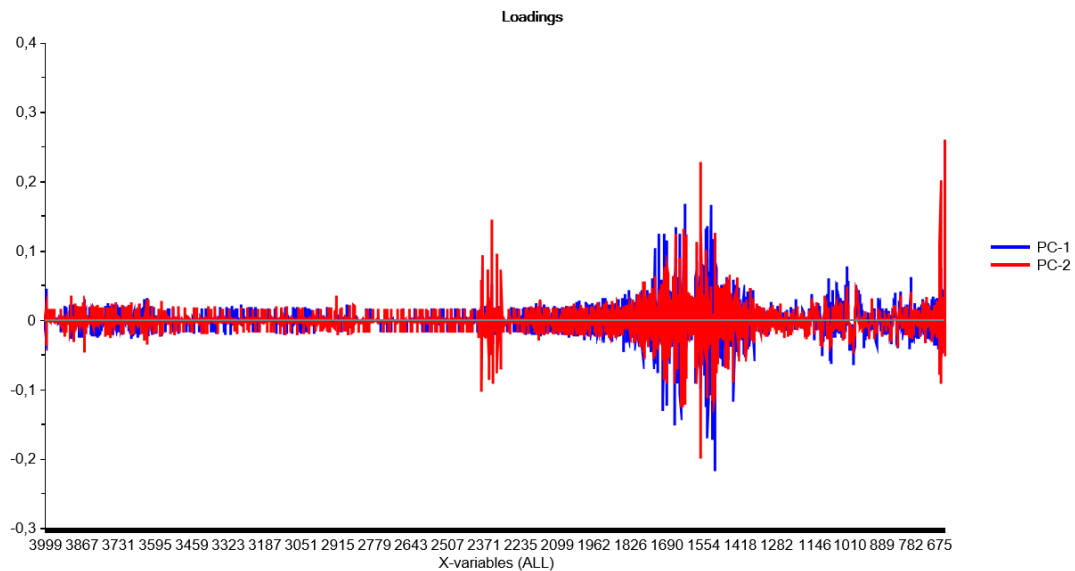


Figure B2 cont. PCA loadings of lead exposed (acute, gradual) and control *Brevundimonas* sp. C- protein region (1800-1500 cm^{-1}), D- carbohydrate region (1200-900 cm^{-1})

A



B

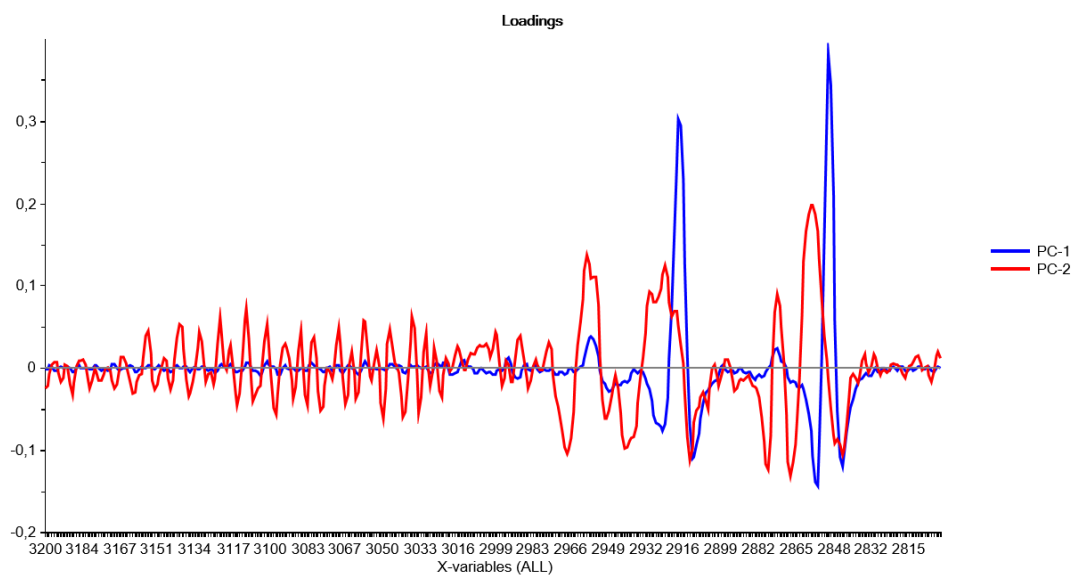
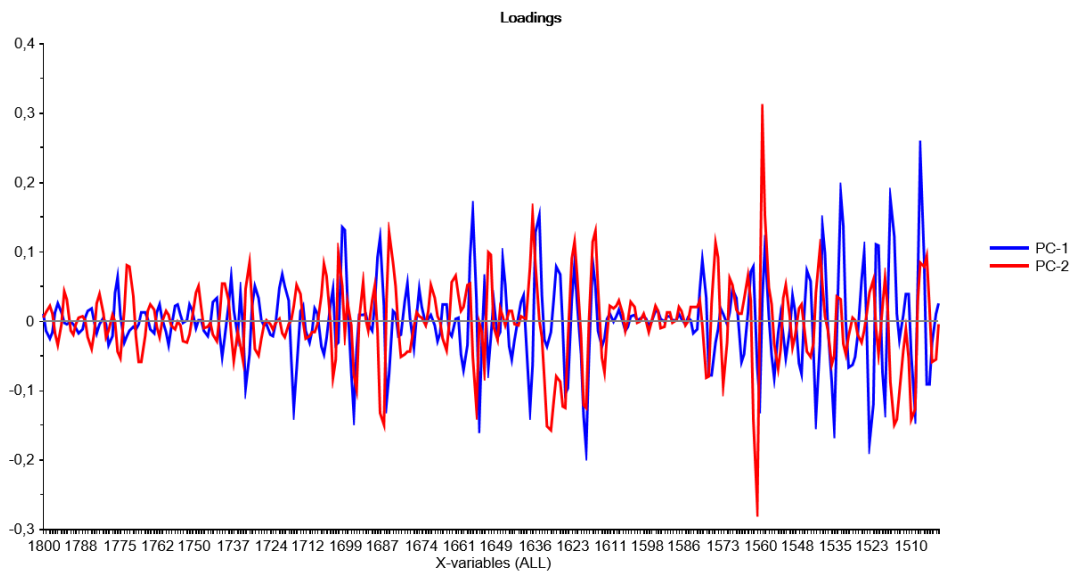


Figure B3. PCA loadings of cadmium exposed (acute, gradual) and control *Gordonia* sp. A- whole spectral region (4000-650 cm^{-1}), B- lipid region (3200-2800 cm^{-1})

C



D

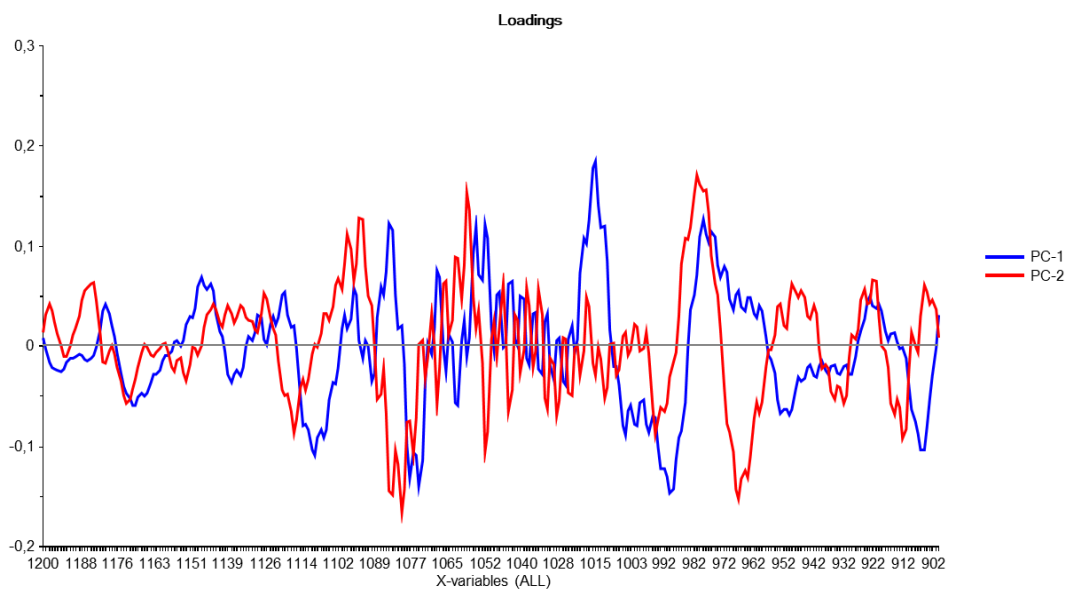
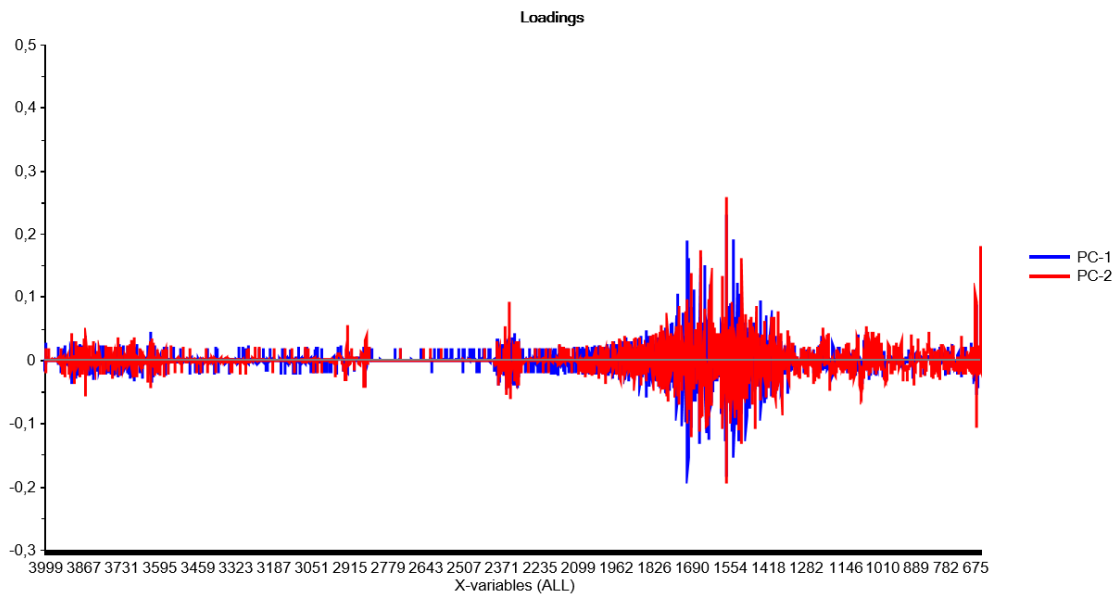


Figure B3 cont. PCA loadings of cadmium exposed (acute, gradual) and control *Gordonia* sp. C-protein region (1800-1500 cm^{-1}), D-carbohydrate region (1200-900 cm^{-1})

A



B

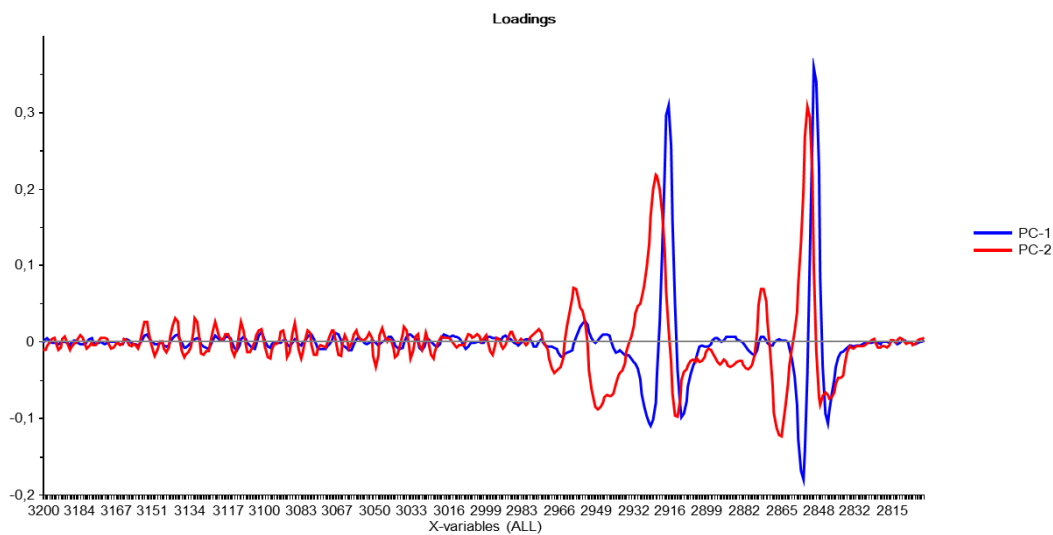


Figure B4. PCA loadings of lead exposed (acute, gradual) and control *Gordonia* sp. A- whole spectral region ($4000\text{-}650\text{ cm}^{-1}$), B- lipid region ($3200\text{-}2800\text{ cm}^{-1}$)

C

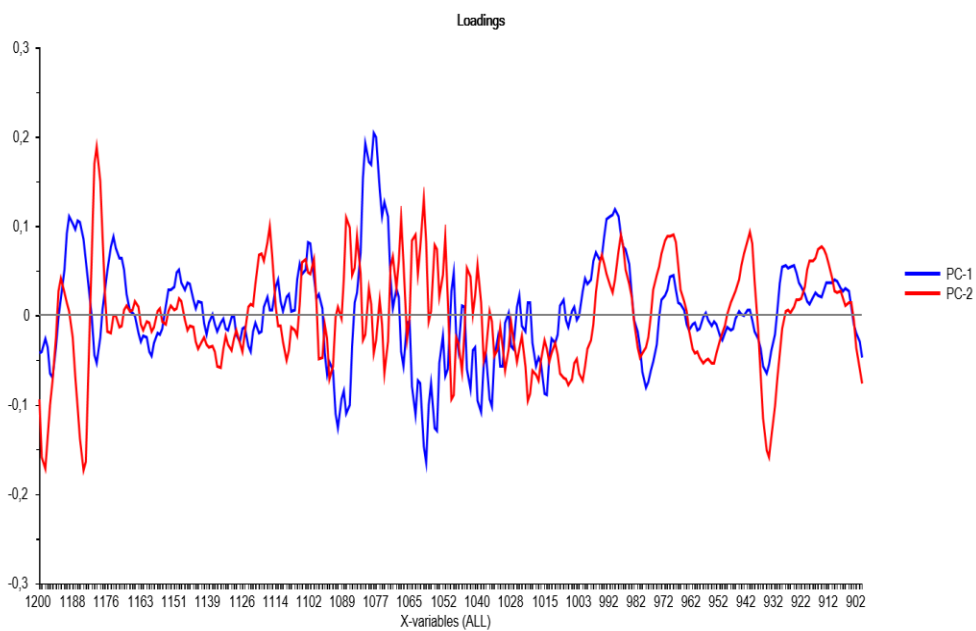
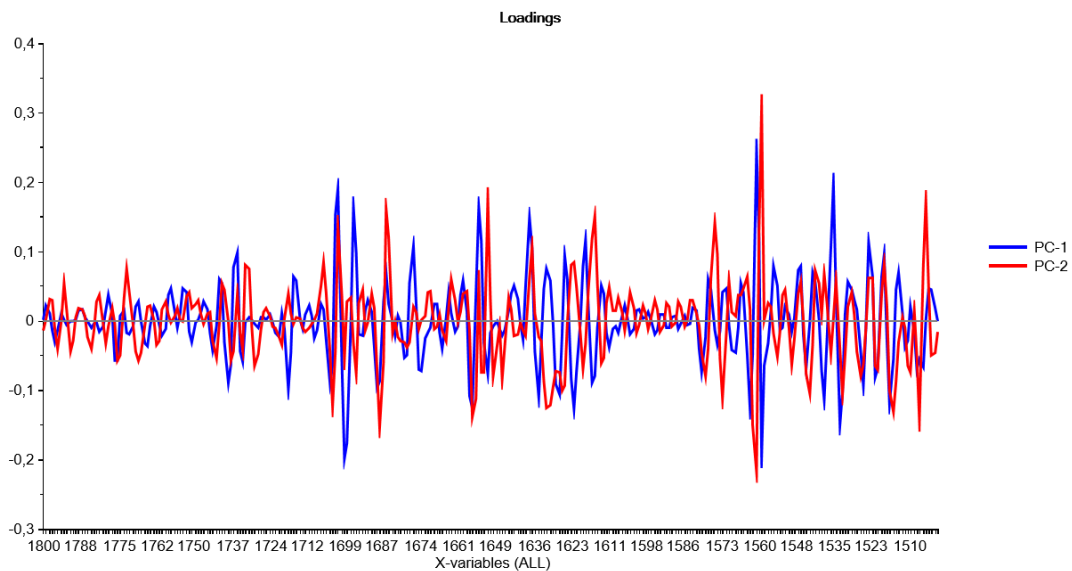


Figure B4 cont. PCA loadings of lead exposed (acute, gradual) and control *Gordonia* sp. C-protein region (1800-1500 cm^{-1}), D-carbohydrate region (1200-900 cm^{-1})

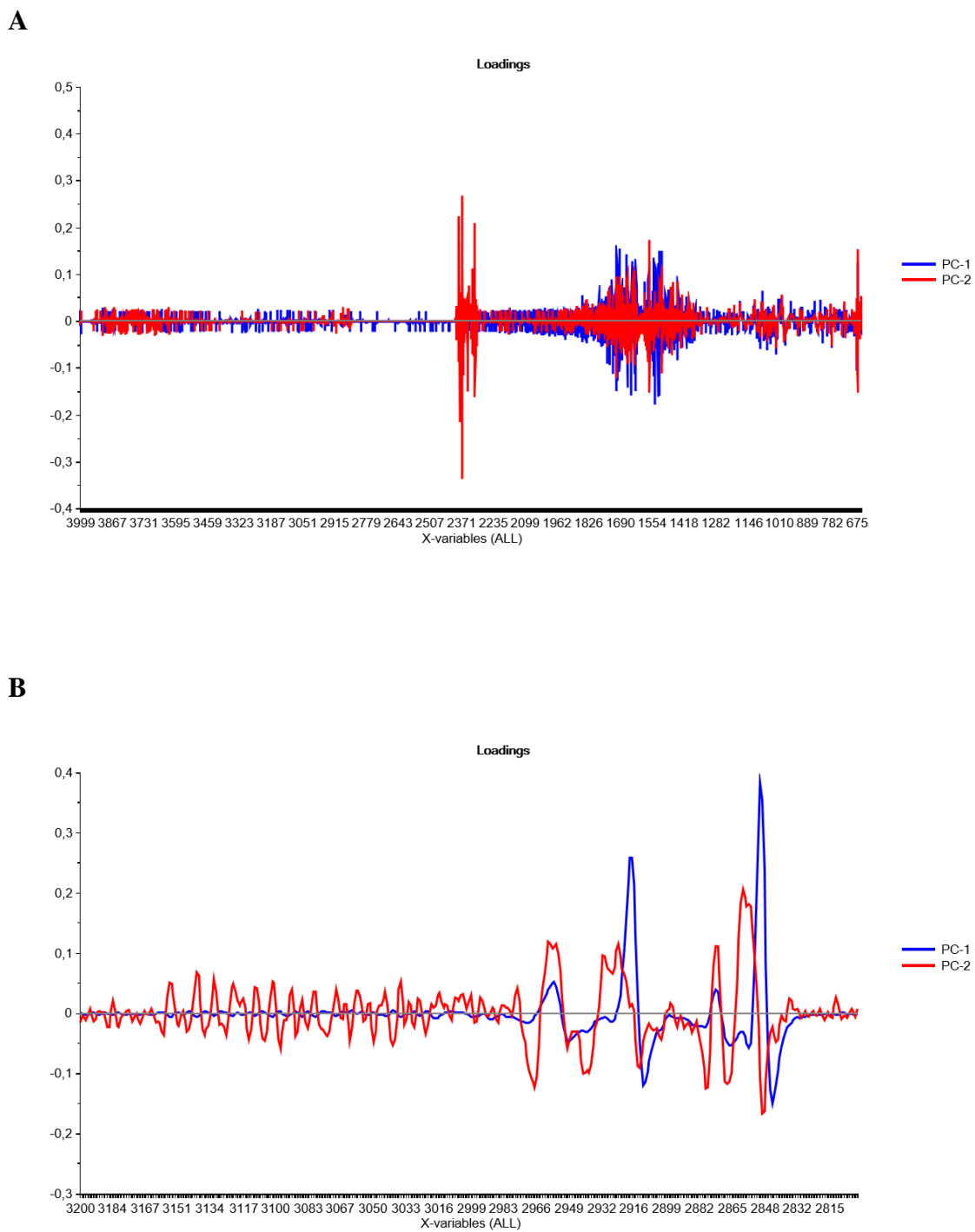
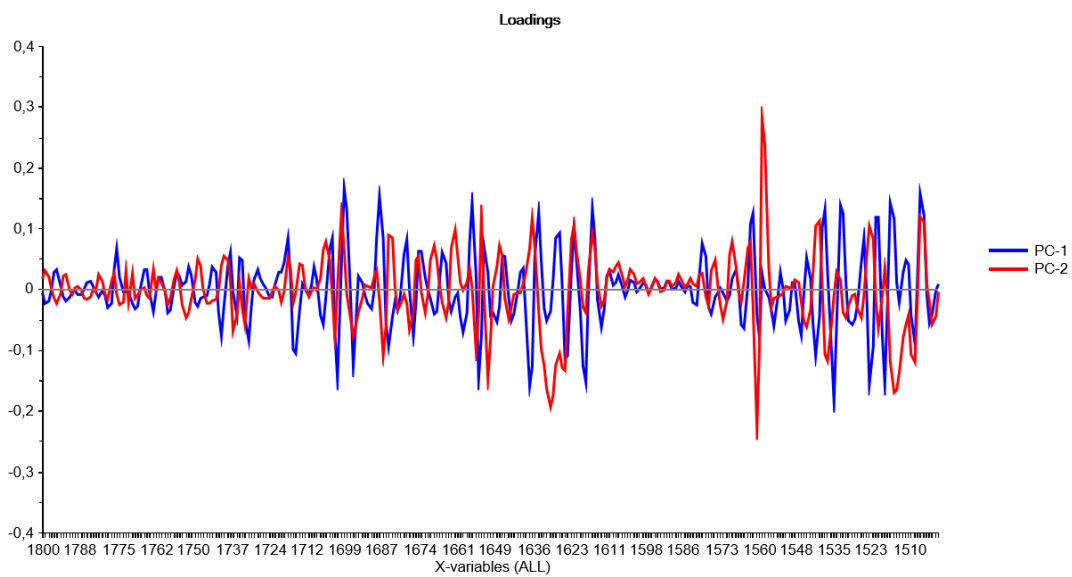


Figure B5. PCA loadings of cadmium exposed (acute, gradual) and control *M. oxydans* A- whole spectral region ($4000\text{-}650\text{ cm}^{-1}$), B- lipid region ($3200\text{-}2800\text{ cm}^{-1}$)

C



D

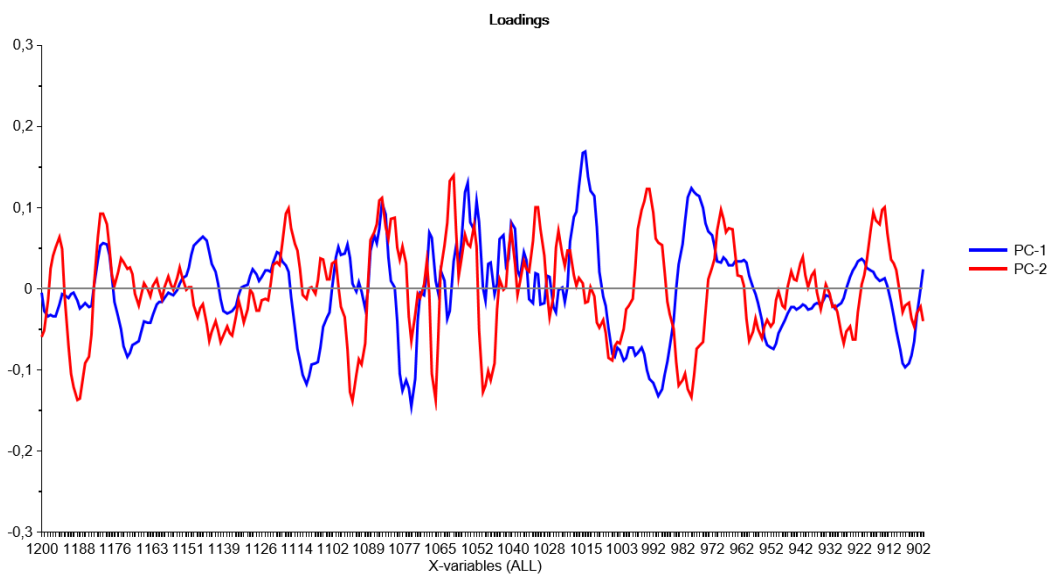
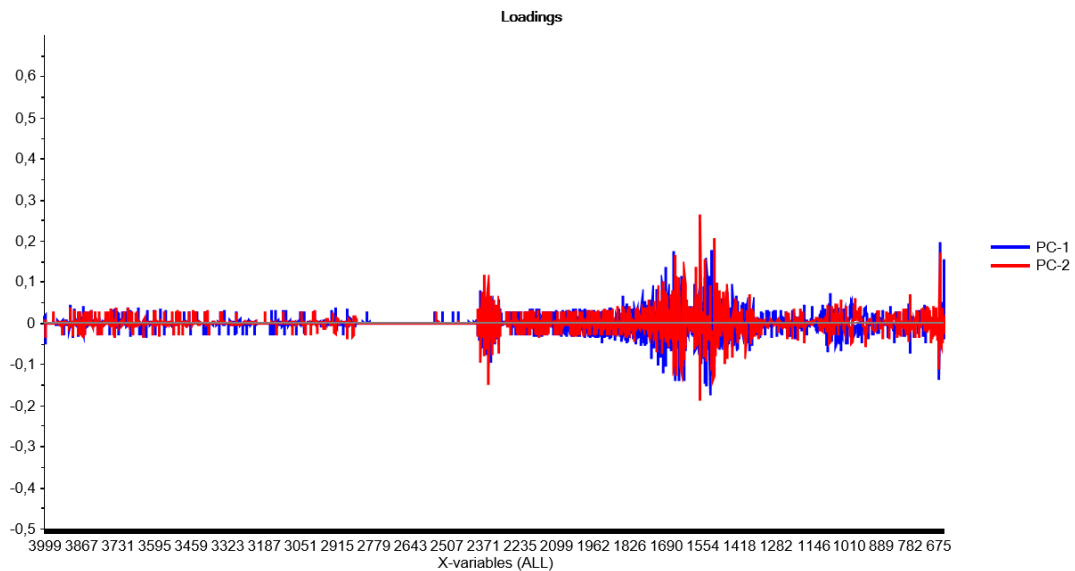


Figure A5 cont. PCA loadings of cadmium exposed (acute, gradual) and control *M. oxydans* C-protein region (1800-1500 cm^{-1}), D- carbohydrate region (1200-900 cm^{-1})

A



B

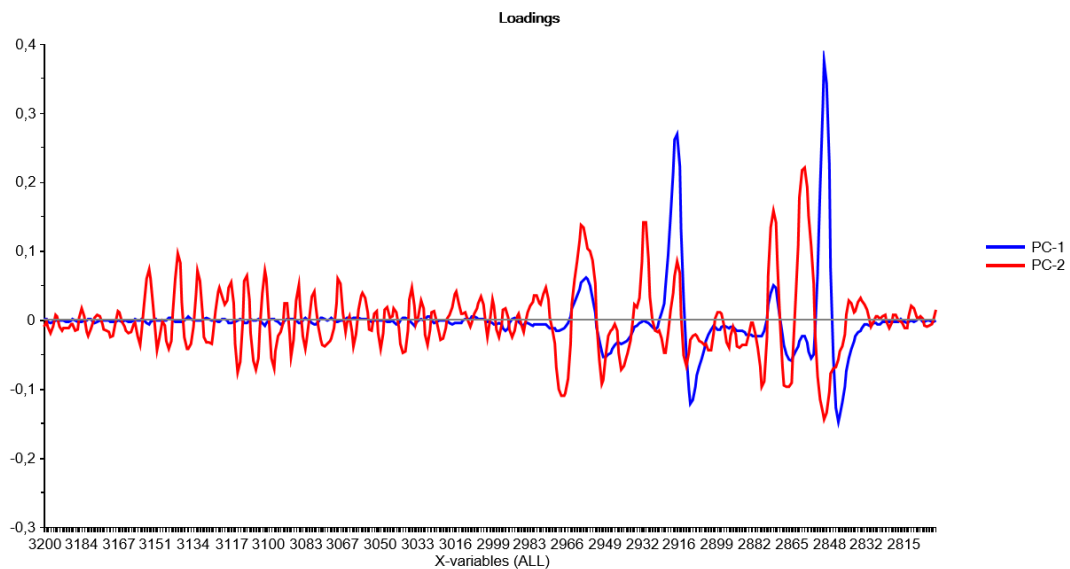
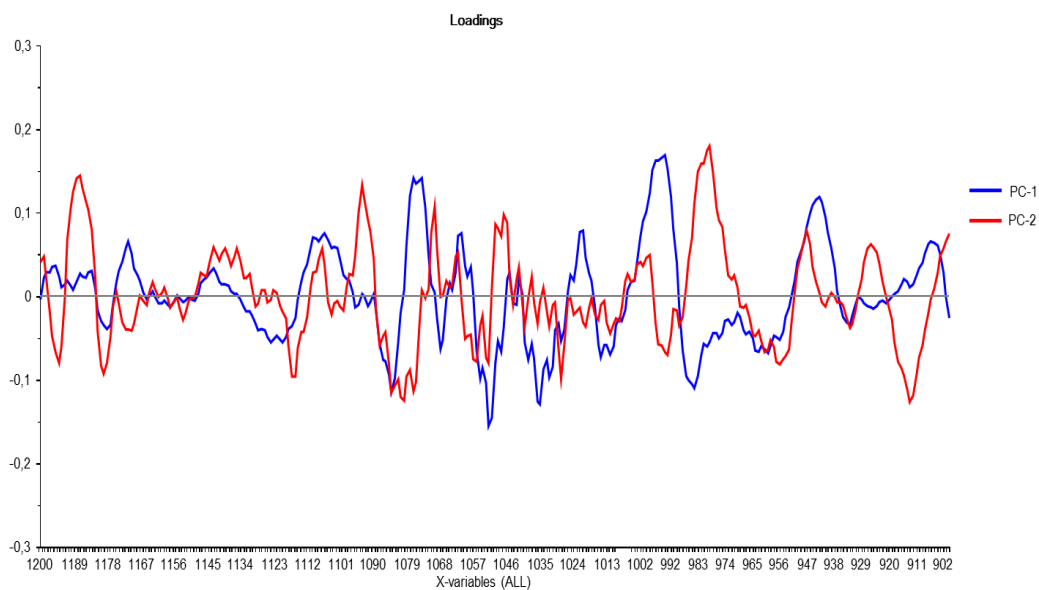
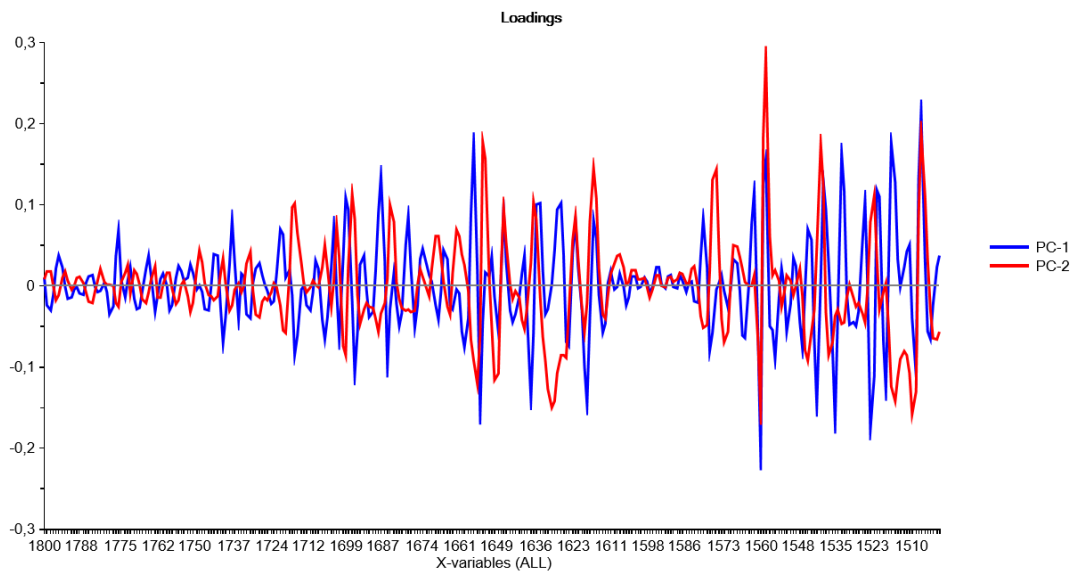


Figure B6. PCA loadings of lead exposed (acute, gradual) and control *M. oxydans* A- whole spectral region (4000-650 cm^{-1}), B- lipid region (3200-2800 cm^{-1})

C



D

Figure B6 cont. PCA loadings of lead exposed (acute, gradual) and control *M. oxydans* C- protein region (1800-1500 cm⁻¹), D- carbohydrate region (1200-900 cm⁻¹)

CURRICULUM VITAE

PERSONAL INFORMATION

Name/Surname : Eda Şeyma Kepenek
Address : Reşit Galip Cad. Hirfanlı Sok. Murat Apt. No: 18/9 GOP/ANKARA
Phone : Home: +90 312 437 36 21
Gsm : +90 532 504 22 15
e-mail : edaseymakepenek@gmail.com
Sex : Female
Marital Status : Single
Date of birth : 22 Agu 1976
Nationality : Turkish

EDUCATION

2012 – to date: (Doktorate Degree) Department of Biological Sciences – Middle East Technical University (METU), ANKARA

2004 - 2007: (MSc Degree) Department of Biological Sciences – Middle East Technical University (METU), ANKARA

2003 - 2004: Department of Basic English – Middle East Technical University (METU), ANKARA

1996 - 2003: (BSc Degree) Department of Biology (Environmental field)– Ankara University, ANKARA

1990 - 1993: (High School) Trabzon Affan Kitapçıoğlu Lisesi, Trabzon

PROJECT STUDIES

- **2014 Ap – 2016 Ap:** Method development for design and choice of bacteria in sustainable bioremediation of heavy metals (**TUBITAK**)
- **2011Sept - to date:** Molecular origin of physiological adaptation in Environmental species acclimated to high concentrations of lead and cadmium heavy metals (Phd thesis study)
- **2010 Sept– 2013 Sept:** Industrial production of high temperature enduring *Pyrococcus furiosus* alpha-amylase enzyme with *Pictia hiebia* pistoris (**KOSGEB**)
- **2005Ap – 2007 Nov:** Detection of Polymorphism of two milk proteins (PRL, DGAT1) and one disease (Complex Vertebral Malformation) related genes in native cattle breed of Turkey using molecular genetic techniques (Molecular Population Genetics) (**Master Thesis study**)

PAPERS

Unal. E. O., Kepenek. E. S., Dinc. H., Ozer. F., Sonmez. G., Togan. Z. I., Soysal. I. (2015). Growth hormone (GH), prolactin (PRL), Diacylglycerolacyl transferase (DGAT1) gene polymorphism in Turkish native cattle breeds. *Turkish Journal of Zoology*, 39(5): 734-748.

CONGRESS, SEMINARS AND TRAININGS

- IV International Congress of Molecular Biology Association of Turkey. November 27-29 METU/ANKARA. 2016.
- 5thNational Congress of molecular and diagnostic microbiology, June 24-28, 2008, Bilkent Hotel and Convention Centre, Ankara
- “Affymetrix GeneChip Microarray Systems and application fields”. Affymetrix Genechip mapping SNP 6.0 Cytotraining Santa Clara March 3rd to 7th 2008 San Francisco/USA (Microarray training)

- ESF workshop on ‘Population genetics modeling and habitat fragmentation: separating recent and ancient events for efficient.’ 2007
- 3rd Meeting of BALNIMALCON A Network of Universities and Research Institutes of Animal Science of the South Eastern European Countries, 10-12 February 2007 – Thessaloniki – Greece.
- 20th IUBMB International Congress of Biochemistry and Molecular Biology and 11th FAOBMB Congress held in KYOTO, JAPAN, June 18-23, 2006.

TECHNICAL SKILLS

DNA, RNA and Plasmid Isolation, PCR, Gel Electrophoresis (Agarose, PAGE), Western Blot Hybridization, RFLP, and Protein Electrophoresis Techniques (SDS and Native PAGE), Real-time PCR, FTIR(Fourier transmission infrared spectroscopy), DSC (Differential scanning calorimetry) Affymetrix Genechip Microarray applications (Expression, Mapping, Sequencing, Microbiology techniques

COMPUTER SKILLS

MS Office, Windows and Internet Applications, Nucleic acid and protein sequence data analysis programs- (Fasta Blast Database, Molecular Toolkit), OPUS, SPECTRUM data analysis programs. Molecular population genetics data analysis programs (Arlequin, NTSYS, Mat Lab), Microarray data analysis programs (PARTEK, Affymetrix Genechip Genotyping Console 2.0, Affymetrix Genechip Genotyping Console 2.1, Affymetrix Genechip Genotyping Console 3.0, Affymetrix Genechip Expression Console).

WORK EXPERIENCES

Nov2010 – Jan2015: Enzyme Biotechnology ltd.şti. (As Molecular Biologist)

Jan 2008- Jan2009: Affymetrix Genechip Mikroarray Systems (As Field Application Specialist (FAS) Ay-Ka Özel Sağlık Tesisleri, İlaç, Laboratuar Malz.ithalat, ihracat, Tic. Ve San. Ltd. Şti.

CERTIFICATES

2015May – 2015May: Certificate of Education of Accreditation and TS EN ISO/IEC 17025 general requirements for the competence of experiment and calibration laboratories standard (TÜRKAK).

2015May – 2015May: Certificate of Education of internal auditor belongs to TS EN ISO/IEC 17025 (TÜRKAK)

2015Jun – 2015Jun: Certificate of education of the traceability of measurements and the uncertainty of measurements experiments laboratories

06 March 2015: Occupational safety expertise (ÇSGB)

2010june – 2010Agust: EF Language School (Cambridge University)

PERSONAL SKILLS

Foreign Languages: English - spoken and written

Italian - basic